Chapter 10
Validating AIM-Based Instrumentation and Associated Measurement Techniques

Mark Copley, Jolyon P. Mitchell, Mårten Svensson, J. David Christopher, Jorge Quiroz, Geoffrey Daniels, Melanie Hamilton, and Dave Russell-Graham

Abstract The validation of the wide variety of equipment capable of making abbreviated impactor measurements is a key component providing proof that the AIM concept works in practice. This chapter provides a comprehensive collection of validation experiments that have been provided by a variety of different laboratories, mainly through the support of the Cascade Impactor sub-team of the European Pharmaceutical Aerosol Group (EPAG), who held a Workshop on the topic in December 2010. These studies have involved the whole range of OIP formats, thereby increasing confidence in the wide applicability of the approach. A series of

M. Copley (✉)
Copley Scientific Limited, Colwick Quays Business Park,
Private Road No. 2, Colwick, Nottingham NG4 2JY, UK
e-mail: M.Copley@copleyscientific.co.uk

J.P. Mitchell
Trudell Medical International, 725 Third Street, London, ON N5V 5G4, Canada
e-mail: jmitchell@trudellmed.com

M. Svensson
Emmace Consulting AB, Vinkelhaken 1D, Sodra Sandy 247 32, Sweden
e-mail: marten@emmace.se

J.D. Christopher
Nonclinical and Pharmaceutical Sciences Statistics, Merck Research Laboratories,
WP37C-305, 770 Sumneytown Pike, West Point, PA 19486-0004, USA
e-mail: j.david.christopher@merck.com

J. Quiroz
Novartis Pharmaceuticals Corporation, One Health Plaza,
Bldg. 438/2417B, East Hanover, NJ 07936, USA
e-mail: jorge.quiroz@novartis.com

G. Daniels
Inhaled Product & Device Technology, GlaxoSmithKline,
Park Road, Ware, Hertfordshire SG12 0DP, UK
e-mail: geoffrey.e.daniels@gsk.com

T.P. Tougas et al. (eds.), *Good Cascade Impactor Practices, AIM and EDA for Orally Inhaled Products*, DOI 10.1007/978-1-4614-6296-5_10,

"learnings" are summarized at the end of the chapter as guidance for those planning on implementing an AIM-based method.

10.1 Introduction

The introduction of AIM-based apparatuses into the mainstream of OIP inhaler performance testing is a highly desirable goal, as has been demonstrated in previous chapters. Not only can the methodology for acquiring aerodynamic size-related metrics be simplified, with the attendant prospect of reducing measurement variability, but the application of EDA principles may afford the prospect of better discrimination in terms of product quality than is possible with current methods that are based on grouped stages from full-resolution CI measurements or from a single performance measure by itself, such as fine particle mass. Validation of the wide variety of AIM-based apparatuses with all of the major OIP formats is a critical component of this process.

Experimental studies were recognized from the outset as being of crucial value to the development of the AIM concept, alongside detailed theoretical rationalization. The following is a brief synopsis of key events. Following proof-of-concept studies by Trudell Medical International with commercially available suspension and solution formulated MDIs undertaken in 2007–2008, a comparative precision experiment between abbreviated and full-resolution ACI systems was undertaken at the same location by the CI Working Group of IPAC-RS the following year. Subsequently, EPAG, through their Impactor sub-team, was responsible for initiating many follow-on investigations with a variety of inhaler types and abbreviated impactor configurations. Since 2010, experimental work has also been undertaken by several organizations outside these industry groups and is included in this chapter in order to demonstrate that the AIM-EDA concept is of interest and is gaining wider acceptance in the OIP manufacturing community. Included are studies carried out using the following abbreviated impactor systems: the C-FSA (Copley Scientific Ltd., Nottingham, UK); the FPD (Westech Instruments Services, Upper Stondon, Beds., UK); other generic abbreviated Andersen CI stacks, in particular, the Trudell (Medical) fast screening Andersen impactor (T-FSA); the FSI (MSP Corporation, St. Paul, MN, USA); and differently modified versions of the NGI. In combination, these initial results provide information to support use of the AIM concept with each type of OIP (DPI, pMDI, and nebulizers).

M. Hamilton
Inhaled Delivery Sciences, Inhaled Product & Device Technology,
GSK R&D Park Road, Ware, Herts SG12 0DP, UK
e-mail: Melanie.2.hamilton@gsk.com

D. Russell-Graham
Mylan Global Respiratory Group, Mylan Inc., Discovery Park, Sandwich CT13 9NJ, UK
e-mail: david.russell-graham@mylan.co.uk

Presentations covering much of the large amount of work undertaken by many groups in the past 5 years can be found on the websites of EPAG [1] and IPAC-RS [2, 3].

10.2 AIM-Based Apparatuses: Developments Before the Present Campaigns

The "Copley-Fisons" two-stage metal impactor [4] (Fig. 10.1) and the "Glaxo" Twin Impinger [5] (Fig. 10.2) can be considered as two of the earliest physical manifestations of the AIM concept. Both were listed as apparatuses A and B, respectively, in the European Pharmacopoeia up until the 4th edition published in 2002, after which apparatus B was withdrawn on the basis that it was no longer used.

The Twin Impinger (TI) is a glassware design based on the multistage liquid impinger (MSLI) [6]. The upper stage represents the throat, stage 1 and stage 2 of an MSLI, while the final stage corresponds to stages 3 and 4 and the filter. With both stages, particles are collected by impaction on liquid surfaces, an especially suitable method for both pMDI and DPI analysis. The reported d_{50} for the upper stage of the instrument is 6.3–6.4 µm at 60 L/min [7, 8]. This limit is likely to be viewed as too large by today's standards. However, it would not be too difficult to reduce the d_{50} value closer to 5µm by decreasing the tube diameter leading into the impingement vessel.

Both instruments separate the aerosol emitted by the inhaler into just two size fractions: an upper stage captures particles above a certain stage cut-off diameter

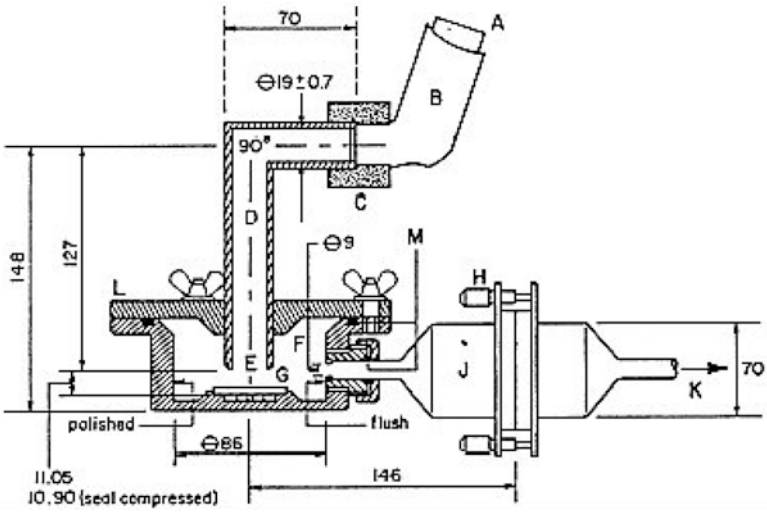

Fig. 10.1 "Copley-Fisons" two-stage metal impactor (*Courtesy of Copley Scientific Ltd., Nottingham, UK*)

Fig. 10.2 "Glaxo" twin impinger (TI) (*Courtesy of Copley Scientific Ltd., Nottingham, UK*)

and all remaining particles pass through to a final collection media. The upper stage of the Copley-Fisons impactor has a cut-off diameter of 9.8 μm d_{ae} at 60 L/min, so the boundary between fine-coarse particle size separation would again likely be viewed as higher than acceptable for present-day OIP applications.

The introduction of the TI was supported at the time by details of its experimental use, in that the value of the device was perceived as its ability for distinguishing between "good" and "poor" aerosols, in particular its application in the detection of agglomerating pMDI formulations, during product development [5]. The lack of sensitivity relative to fuller APSD measurement by the 4-stage multistage liquid impinger was, however, identified in the mid-1990s as a potential drawback for more discriminating investigation, especially for the comparison of generic with innovator OIPs [9]. Further studies confirmed initial claims about the insensitivity of Twin Impinger measurements to variability in operational parameters such as collecting fluid composition and volume and test flow rate [7]. The use of the TI at flow rates in excess of the design value of 60 L/min for low resistance DPI testing may, however, be a practical proposition [10]. Calibration with solid monodisperse aerosols has confirmed, that like other types of inertial impactor, its cut-off size for the upper stage decreases at sampling flow rates in excess of the routinely used 60 L/min [8], as predicted by the relationship:

$$d_{ae,50,1} = d_{ae,50,ref}\left[\frac{Q_{ref}}{Q_1}\right]^{1/2} \tag{10.1}$$

where Q_1 and Q_{ref} represent the calibration flow rate and reference flow rate of 60 L/min, respectively, and $d_{ae,50,1}$ and $d_{ae,50,ref}$ are the cut-off sizes at the calibration and reference flow rates, respectively.

In retrospect, it is clear that the study carried out by Miller et al. [7] fuelled uncertainty as to the ability of the TI to differentiate between OIP aerosols with markedly different APSDs, making the simplification that they are unimodal and lognormal, and therefore using *MMAD* and *GSD* to represent measures of central tendency and spread, respectively. By concluding that because the instrument only separated into two size fractions, and, moreover gave a broad rather than sharp separation, the impression was given that it could not distinguish between aerosols that fell within the same *MMAD/GSD* "family". It was possible that a discrete range of *MMAD/GSD* combinations would give the same results when analyzed using just two size fractions, and broad separation between fine/coarse size boundary and *MMAD* appeared to exacerbate the problem. Referring to the recent work by Tougas et al. [11], it is now clear that the sensitivity of this apparatus for APSD-related shifts will vary considerably according to the location of the *MMAD* of the product. The *MMAD* of many currently marketed pMDIs and DPIs is likely to be located in the region from 1 to 3 μm, and this separation is likely to be too far from the stage cut-off size for the unmodified TI, therefore potentially impairing its precision.

A further drawback of both the TI (and also the Copley-Fisons 2-stage metal impactor) is that, as they are currently supplied, neither instrument has an easily varied stage cut-off size. However, despite these disadvantages, in the near future as AIM research progresses, there may be cause to reexamine the potential role of this apparatus, possibly with a modified stage cut-off diameter, since the impinger design is attractive from the point of view of its ability to eliminate size-related bias caused by particle bounce and re-entrainment [12]. It would be a relatively easy modification to move the cut point for the TI to 5.0 μm aerodynamic diameter in the flow rate range from 30 to 100 L/min within which most OIPs are evaluated, by modifying the diameter of the tube entering the upper stage, in accordance with the relationship (Chap. 2):

$$\sqrt{C_{c,50}}\,d_{50} = \left[\frac{9\pi\eta W^3}{4\rho_0 Q}\right]^{1/2}\sqrt{St_{50}} \tag{10.2}$$

in which St_{50} is the dimensionless Stokes number at the size where the stage collection efficiency is 50%, W = tube diameter, d_{50} = stage cut size, Q = volumetric flow rate, η = air viscosity, ρ_0 = unit density (i.e., 1 kg/m^3), and $C_{c,50}$ is the Cunningham slip correction factor for a particle of size d_{50} [13]. However, the practicality of making this change so that this apparatus could be used at close to 30 L/min to evaluate pMDIs has not, to the authors' knowledge, yet been addressed.

The issue of flow rate sensitivity to stage d_{50} size with CIs, which is discussed in more detail in Chap. 2, highlights an important potential limitation to the AIM concept in the case of DPI testing. In contrast with MDI or nebulizer performance

assessments by the compendial methods in which the flow rate is maintained at a fixed value, development of DPI a product often involves testing at multiple flow rates. It is a relatively easy process with a full-resolution CI to interpolate the mass of API in particles finer than a fixed size limit, typically 5.0 μm aerodynamic diameter, from the cumulative mass-weighted APSD obtained at each required flow rate, even though the individual stage d_{50} values change. In contrast, since interpolation is not possible when using an AIM-based CI, as an APSD is not generated, a different upper stage would be needed for testing at each required flow rate in order to maintain a stage d_{50} fixed at the appropriate value.

At this point then it is fair to say that while the AIM concept, in the physical form of the Twin Impinger, was seen as a convenient and efficient analytical tool for relatively coarse differentiation, doubts remained about its sensitivity. The theoretical work by Tougas et al. [11] on the development of EDA metrics that is described in detail in Chaps. 7 and 8, followed some time after these initial practical studies. In summary, EDA points the way to achieve better measurement precision in association with OIP APSD-related data by the following approaches: adoption of a ratio of *LPM* to *SPM* rather than individual mass fractions, simultaneous use of ISM, and the selection of an optimal boundary value for *LPM/SPM* on the basis of *MMAD* value.

Limited interest in AIM precursor concepts continued through the 1990s, a decade marked at its closing by the development of the full-resolution NGI on the basis of the very latest understanding of inertial impaction [14]. In the context of AIM-based equipment, during the mid-1990s, Van Oort and Downey [15] and Van Oort and Roberts [16] returned to the issue of reducing the analytical burden by cutting the number of size fractions, this time by simply reducing the number of stages used in an Andersen CI stack (see Chap. 5). In these works, for the first time, there was recognition of the importance of tailoring the boundary between the two size fractions used for EDA to suit the product under test. Based on full-resolution data gathered using an ACI (or NGI), analysis was focused on the stages where most of the drug collects to give size fractions that could more precisely and successfully capture changes in OIP APSD.

Unfortunately, at that time and up until the early part of the next decade, the suggestion of an abbreviated way of working failed to gain traction with the regulators [17], who favored full-resolution APSD measurements, diminishing interest in continued development of simplified systems. However, since then much has changed. In particular, the regulatory landscape has altered dramatically with the introduction of new concepts, perhaps most importantly Quality by Design, an approach designed to promote product and process development on the basis of thorough and secure knowledge [18]. Nevertheless, there are legitimate concerns that this new way of working will significantly increase the analytical burden. Hence, both the pharmaceutical industry and regulatory agencies alike have become more receptive to new approaches, based on sound science, which may help reduce the amount of testing required. Interest in the use of AIM systems based on both the ACI and NGI has therefore been renewed.

10.3 Proof-of-Concept Experiments Undertaken at Trudell Medical International: Assessing the Performance of Systems Based on the Nonviable 8-Stage ACI

In practical terms, abbreviating measurement with the vertical stack design of the ACI is relatively straightforward, as the early work by Van Oort and colleagues indicated, being simply a matter of configuring the stack with fewer stages and adjusting the length of the retaining springs to compensate for the shorter configuration. However, the issue of aerodynamic performance is a critical one; reduced stacks potentially may exhibit changed air flow patterns that can significantly affect inertial impaction behavior. Particle bounce, the re-entrainment, the distribution of active losses to internal surfaces, and the effect of impactor dead volume have all been shown to be important considerations [19, 20]. Furthermore, identifying optimal stage cut-off diameter values for product QC and also for the potential support of human respiratory tract (pHRT)-pertinent studies to develop in vitro–in vivo relationships (the latter being the focus of Chap. 12) are also topics for practical AIM implementation with this system as well as other designs of full-resolution CI [21].

In 2008, two proof-of-concept studies were undertaken by the group at Trudell Medical International (TMI) in order to validate the performance of two abbreviated systems for the purpose of improving productivity in testing add-on devices (spacers and valved holding chambers) used with pMDIs. Their work was based on the full-resolution 8-stage nonviable ACI, the C-FSA and the T-FSA abbreviated systems also based on the nonviable ACI operating principle [19, 20].

The C-FSA is a commercially available (Copley Scientific, UK) two-stage pHRT-based abbreviated stack, based on the Andersen *nonviable* CI that divides the incoming dose into coarse, fine, and extra-fine fractions (*CPF*, *FPF*, and *EPF*), respectively (Fig. 10.3a, b). In its commercially available formats, a range of stages enables configuration to give stage cut-off diameters (d_{50} values) of 4.7 and 1.1 μm at 28.3, 60, or 90 L/min, or alternatively 5.0 and 1.0 μm at 28.3 L/min, depending on the specific application.

Similar in design to the C-FSA, the T-FSA was also developed from research into AIM-based methods at TMI with MDIs delivering "dry particles" of salbutamol (albuterol) following propellant evaporation (Fig. 10.4a). The T-FSA was a hybrid C-FSA, which had an upper stage cut-off size of 4.7 μm so that data from this stage could therefore be directly compared with mass deposition of API on stage 2 of the full-resolution ACI. The d_{50} size of the lower stage was 1.0 μm, rather than 1.1 μm.

In a later modification, the T-FSA also included a non-operable (collection surface removed) ACI stage 0 to provide functional dead space before the first size separating stage, enabling closer mimicry of this potentially important aspect of the full-resolution ACI.

Two discrete investigations were carried out, each focusing on pMDI-produced aerosols, one involving dry particles (after HFA-134a propellant evaporation), the other containing low-volatile liquid ethanol excipient that was associated with the aerosol particles entering the measurement equipment. In the first study, dry fluticasone propionate (FP) particles were produced using a commercially available

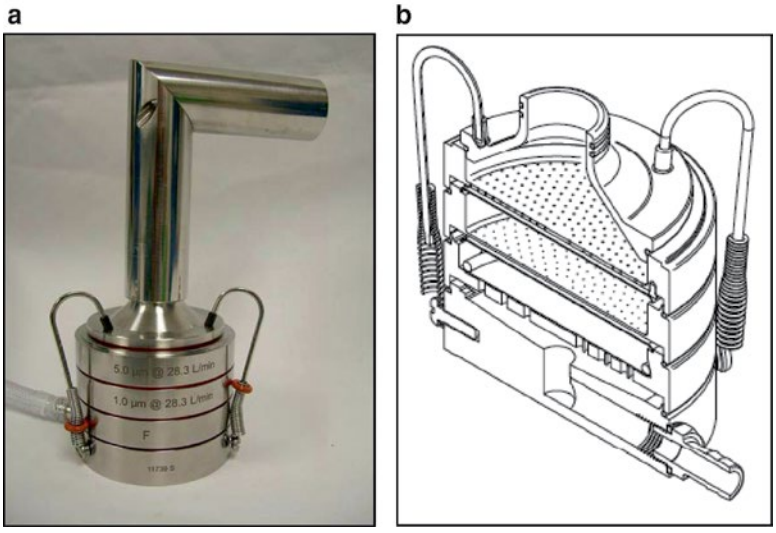

Fig. 10.3 The standard Copley C-FSA with cut-point sizes of 1.0- and 5.0-µm aerodynamic diameter—other cut-point sizes are also available. (**a**) External view showing CI with Ph. Eur./USP induction port. (**b**) Internal cross-section of CI without induction port (*Courtesy of Copley Scientific Ltd., Nottingham, UK*)

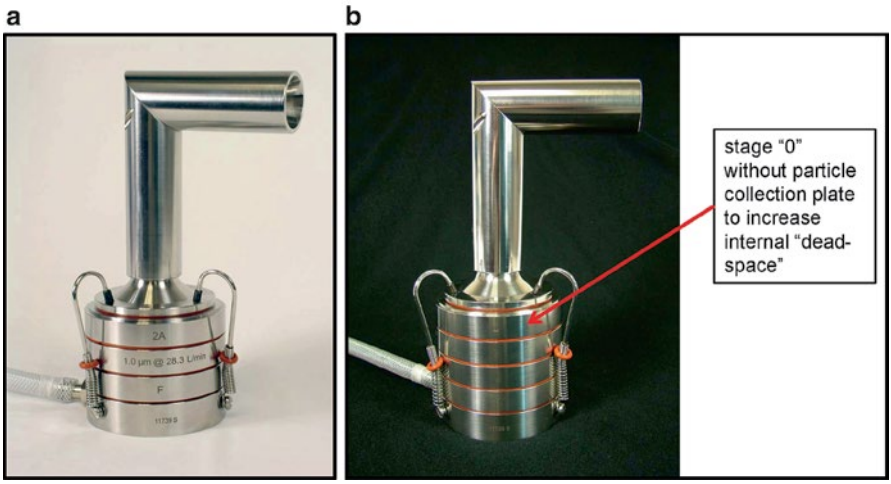

Fig. 10.4 The T-FSA system with Ph. Eur./USP inlet. (**a**) Basic T-FSA for initial experiments with "dry" aerosol particles containing salbutamol (albuterol). (**b**) Modified T-FSA containing an additional stage "0" without collection plate to increase dead space before first impaction stage to be more comparable with that in the full-resolution ACI when sampling "wet" beclomethasone dipropionate aerosol particles from formulations containing ethanol as cosolvent (*Courtesy of Trudell Medical International, London, Canada*)

Table 10.1 Cumulative mass-weighted data for Flovent®-110 measured by modified C-FSA[a] ($n = 5$ replicates) with coating on collection plates (*From* [19]—*used with permission*)

				Number of actuations per determination			
				1	2	5	10
Location in C-FSA	Size range (μm)	Upper size limit (μm)	Size fraction	Cumulative mass % < stated upper size limit (mean ± SD)			
Induction port	Undefined	Undefined	$CPF_{>4.7\mu m}$	60.8 ± 4.2	60.8 ± 3.3	60.1 ± 1.2	61.4 ± 2.5
Upper stage 2A	>4.7[a]						
Lower stage	1.0–4.7	4.7	$FPF_{<4.7\mu m}$	39.2 ± 4.2	39.2 ± 3.3	39.9 ± 1.2	37.9 ± 3.0
Back-up filter	<1.0	1.0	$EPF_{<1.0\mu m}$	3.1 ± 0.6	3.5 ± 0.3	3.5 ± 0.4	3.3 ± 0.2

[a] Upper stage cut size was 4.7 μm rather than 5.0 μm aerodynamic diameter

pMDI, Flovent®-HFA (GSK plc, UK); 110 μg/actuation ex-actuator mouthpiece. APSD measurements were made using the T-FSA and C-FSA with uncoated collection surfaces, and then with collection surfaces coated with polyoxyethylene lauryl ether (Brij-35) surfactant. These data were compared with analogous results generated using a full-resolution ACI (Table 10.1).

In this and other tables in this Chapter, unless otherwise stated, $CPF_{>4.7\mu m}$, $FPF_{<4.7\mu m}$, and $EPF_{<1.0\mu m}$ represent coarse, fine, and extra-fine mass fractions with the subscripts indicating the pertinent size limit. The cut-point sizes are based on the manufacturer's nominal values with Q at 28.3 L/min, and the numbering in the left-most column is based on the stage numbering sequence of the full-resolution ACI, with the "A" indicating that stage 2 was not the standard C-FSA stage with 5.0 μm cut-point size.

The impact of the number of actuations used during testing was directly investigated. In all the experiments, the mass recovery with each system was found to be broadly equivalent and well within the specification set down by the FDA [22] (±15% label claim/actuation). Furthermore, with the abbreviated systems, the mass of fine particles recovered per actuation was acceptable even with a single actuation. This is an important result since the FDA recommends minimizing the number of actuations to the clinical dose (typically 2-actuations), within the constraint of reaching a detectable limit on each stage, to improve impactor performance.

With uncoated collection surfaces (Table 10.2), the amount of material in the extra-fine fraction decreased with increasing number of actuations; from 9.4 ± 0.7 μg with a single actuation to 5.3 ± 0.4 μg with ten actuations (modified C-FSA data). This is consistent with previously reported observations suggesting that the deposition of material on an uncoated collection surface makes it progressively "stickier," potentially reducing the extent of particle bounce [23–25]. The use of surfactant-coated collection plates removed this dependence on actuation number and improved accuracy for both the T-FSA and C-FSA relative to the benchmark results generated with the full-resolution ACI (Table 10.3 and Fig. 10.5).

These measurements with either of the reduced impactors with collection surface coating were found to be substantially equivalent to the full-resolution ACI (Table 10.3). This outcome occurred despite the fact that relative API mass deposition per stage in the AIM-based systems was higher than in the full-resolution

Table 10.2 Cumulative mass-weighted data for Flovent®-110 measured by modified C-FSA[a] ($n = 5$ replicates) without coating on collection plates (*From* [19]—*used with permission*)

				Number of actuations per determination			
				1	2	5	10
Location in C-FSA	Size range (μm)	Upper size limit (μm)	Size fraction	Cumulative mass % < stated upper size limit (mean ± SD)			
Induction port Upper stage 2A	Undefined >4.7	Undefined	$CPF_{>4.7\mu m}$	59.3 ± 2.3	61.7 ± 2.6	60.5 ± 1.7	61.1 ± 3.4
Lower stage	1.0–4.7	4.7	$FPF_{<4.7\mu m}$	40.7 ± 2.3	38.3 ± 2.6	39.5 ± 1.7	37.8 ± 4.0
Back-up filter	<1.0	1.0	$EPF_{<1.0\mu m}$	9.4 ± 0.7	7.5 ± 0.6	6.4 ± 0.4	5.3 ± 0.4

[a] First stage cut size was 4.7 $_{\mu m}$ rather than 5.0 μm aerodynamic diameter

Table 10.3 Key size fraction metrics determined for 5-actuations of Flovent®-110 into the T-FSA ($n = 5$ replicates/CI system): comparison with equivalent data from a modified[a] C-FSA and ACI (*From* [19]—*used with permission*)

				Cumulative mass % < stated upper size limit (mean ± SD)		
Location	Size range (μm)	Upper size limit (μm)	Size fraction	T-FSA	C-FSA	ACI
Induction port	Undefined	Undefined	$CPF_{>4.7\mu m}$	57.6 ± 3.5	60.1 ± 1.2	57.7 ± 2.2
Upper stage[a]: 2A—C-FSA; 2—T-FSA	>4.7					
Lower stage	1.0–4.7: C-FSA; 1.1–4.7: T-FSA, ACI	4.7	$FPF_{<4.7\mu m}$	42.4 ± 3.5	39.9 ± 1.2	42.3 ± 2.2
Back-up filter	<1.0: C-FSA; <1.1: T-FSA, ACI	1.0: C-FSA; 1.1: T-FSA, ACI	$EPF_{<1.0\mu m}$	3.8 ± 0.5	3.5 ± 0.4	1.2 ± 0.2

[a] First stage cut size of modified C-FSA was 4.7 μm rather than 5.0 μm aerodynamic diameter

CI for the same number of actuations of the inhaler, resulting in the potential for earlier overloading of stages. Interestingly, the small but measurable wall losses associated with those stages in the full ACI that were removed to create the abbreviated designs were believed to have been transferred to the lower stage in the abbreviated systems. Fortunately this resulted in an increase in extra-fine particle mass of only ca. 2%.

It is perhaps to be expected that collection surface coating will be especially critical in abbreviated systems since any tendency toward non-ideal behavior is magnified as a consequence of the increased inertia of particles that would otherwise be collected by previous stages in the full-resolution configuration.

In the follow-on investigation [20], measurements were made with a formulation containing 8% w/v ethanol as cosolvent (Qvar™; 80 μg/actuation beclomethasone dipropionate (BDP) ex-actuator mouthpiece), using surfactant-coated collection surfaces with both the C-FSA and T-FSA. Tests with liquid ethanol-sensitive paper confirmed that the ethanol evaporated inside the impactor during measurement, penetrating only to the first stage (Fig. 10.6a, b).

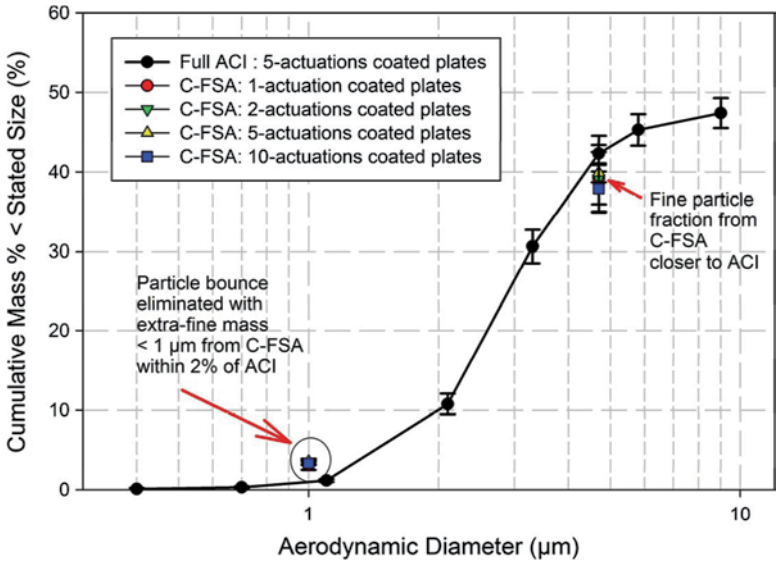

Fig. 10.5 Effect of number of actuations of Flovent-110® on C-FSA-measured data when used with surfactant-coated collection plates (*From* [19]—*used with permission*)

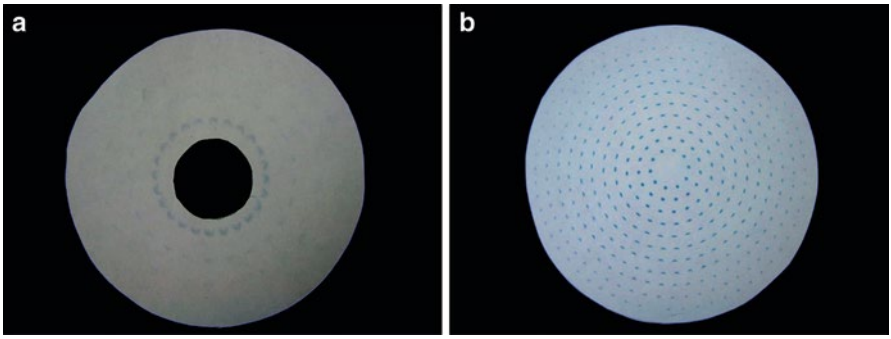

Fig. 10.6 Use of liquid ethanol-sensitive paper to diagnose presence of liquid droplets within the upper stages of the C-FSA. (**a**) Traces confirming liquid ethanol presence with incoming aerosol to C-FSA from sampling 10-actuations of Qvar™-80, using liquid ethanol-sensitive filter paper located on collection plate below stage. (**b**) Traces confirming liquid ethanol presence with incoming aerosol to C-FSA from sampling 10-actuations of Qvar™-80, using liquid ethanol-sensitive filter paper located on collection plate below stage 1 (*From* [20]—*used with permission*)

The introduction of additional dead space in the T-FSA, compared with the C-FSA, was found to improve agreement with the ACI in terms of fine particle mass, a result attributed to the provision of more similar conditions for ethanol evaporation within the former configuration (Fig. 10.7). Overall, the difference between the data using the slightly modified C-FSA and T-FSA was so small that

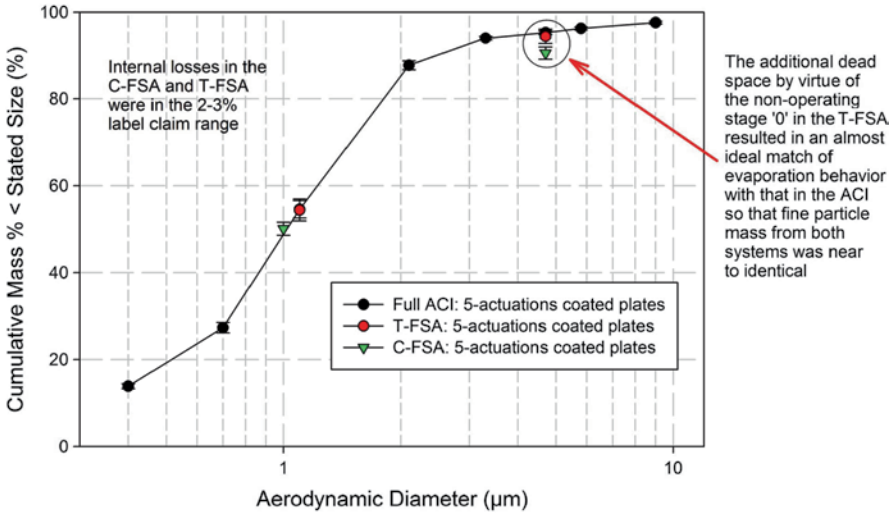

Fig. 10.7 Comparative 5-actuations per measurement data for the T-FSA, C-FSA, and ACI with Qvar™-80 (*From* [20]—*used with permission*)

for almost all practical purposes, either of these abbreviated systems could be used for this particular formulation. However, care would need to be taken to reevaluate the situation for formulations containing higher levels of low-volatile cosolvent.

10.4 The IPAC-RS Impactor Precision Comparison: Comparing the Performance of an AIM ACI-Based System Configured for pHRT Studies with a Similar System Tailored to QC Applications

One of the central issues for AIM implementation is setting the boundary value(s) for size-related metrics appropriately given the limited number of size fractions produced by abbreviated systems. To a large extent, in the OIP QC environment, this decision will likely be taken on a product-by-product basis, depending upon the product APSD obtained in early development (see Chap. 6).

Outside of the product QC environment, an alternative strategy is to set boundaries to reflect areas of potential clinical interest—the sub-5 µm fraction being an obvious target for *FPF*, being the size limit defined for the fine particle dose in the European Pharmacopoeia [4]. The stage cut-off diameter of stage 2 of the full-resolution Andersen CI instrument is slightly finer at 4.7 µm aerodynamic diameter at 28.3 L/min, and as a result, this size is often used as the limiting value for convenience during the assessment of pMDIs. In addition to the differentiation between

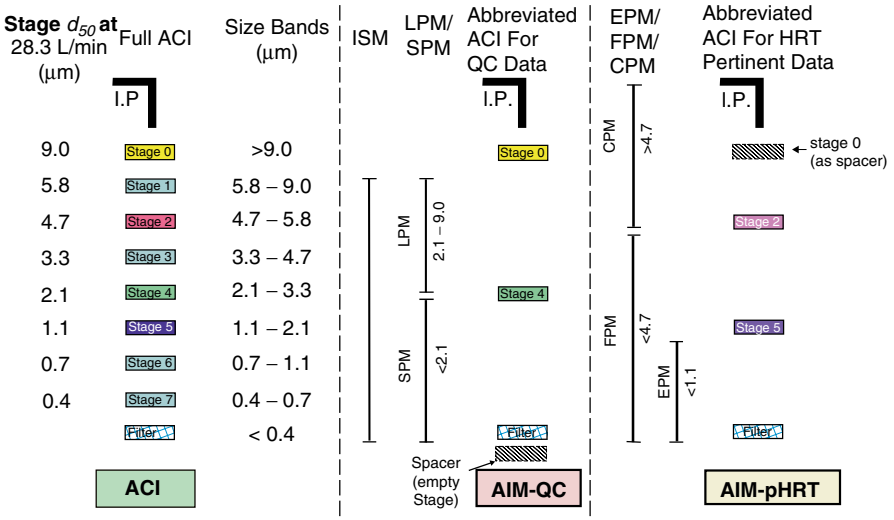

Fig. 10.8 CI configurations used in the IPAC-RS AIM precision experiment; the additional "spacer" stage used after filter stage for the AIM-QC system has no measurement function and does not interfere with analysis (*From* [26]—*used with permission*)

fine and coarse mass fractions, there may be a need to evaluate the portion of the emitted dose from some OIPs, particularly pMDI solution formulations such as Qvar™ and Alvesco® in terms of extra-fine fraction < ca. 1 μm, comprising a sub-fraction of the fine particle mass. In such instances, a second impaction stage provides added flexibility to the abbreviated impactor, with cut-off size exactly at this limit or in the case of systems derived by removing stages from a full-resolution nonviable ACI, retaining stage 5, whose cut-off size is 1.1 μm at 28.3 L/min. This was the rationale underlying the development of the so-called potential-HRT configuration, referred to from now onward as the "AIM-pHRT"-abbreviated impactor that was evaluated in the IPAC-RS precision comparison study at Trudell Medical International in 2009 [26]. This apparatus is included here for the sake of completeness, as it formed one arm of the precision comparison study. However, the underlying reasons for the development of AIM-pHRT configurations are explored in more detail in Chap. 12. Like the T-FSA described earlier, the "pHRT-FSA" configuration had a non-operable stage 0 inserted prior to the first separation stage to give dead space equivalence to the full-resolution impactor. The "pHRT-FSA" system was evaluated together with a so-called AIM-QC configuration having a single stage with cut-off size at 2.1 μm (stage 4 from the full-resolution ACI operated at 28.3 L/min) chosen to be close to the MMAD of the product used in the evaluation (AIM-QC apparatus).

The two abbreviated configurations compared with that of the benchmark full-resolution system are illustrated schematically in Fig. 10.8. C1, C2, and C3 are the configurations for the full-resolution nonviable ACI, AIM-QC, and AIM-pHRT

Table 10.4 Experiment design with three cascade impactor configurations, six inhalers, three dosing sets by inhalers, and three replicates of the same inhalers; the values in square parentheses indicate the order of test on a particular day (*From* [26]—*used with permission*)

Inhaler	Replicate	Cascade impactor configuration [dosing set]		
1	1	ACI [1]	AIM-QC [2]	AIM-pHRT [3]
	2	AIM-pHRT [5]	ACI [6]	AIM-QC [4]
	3	AIM-QC [9]	AIM-pHRT [7]	ACI [8]
2	1	AIM-QC [2]	ACI [1]	AIM-pHRT [3]
	2	ACI [4]	AIM-pHRT [6]	AIM-QC [5]
	3	AIM-pHRT [9]	AIM-QC [8]	ACI [7]
3	1	ACI [1]	AIM-pHRT [3]	AIM-QC [2]
	2	AIM-pHRT [6]	AIM-QC [5]	ACI [4]
	3	AIM-QC [8]	ACI [7]	AIM-pHRT [9]
4	1	AIM-QC [3]	AIM-pHRT [1]	ACI [2]
	2	AIM-pHRT [5]	ACI [6]	AIM-QC [4]
	3	ACI [7]	AIM-QC [8]	AIM-pHRT [9]
5	1	ACI [1]	AIM-pHRT [3]	AIM-QC [2]
	2	AIM-QC [5]	ACI [4]	AIM-pHRT [6]
	3	AIM-pHRT [9]	AIM-QC [8]	ACI [7]
6	1	AIM-pHRT [2]	ACI [3]	AIM-QC [1]
	2	ACI [4]	AIM-QC [5]	AIM-pHRT [6]
	3	AIM-QC [9]	AIM-pHRT [7]	ACI [8]

systems, respectively. A commercially available HFA-salbutamol pMDI was used as the test product, and careful attention was made to the design of the experiment to minimize the influence of possible confounding sources of error (e.g., operator, environment, inhaler, etc.).

The experiment was conducted using a design with the three impactor configurations already described, six inhalers, with three measurements made per inhaler per impactor configuration (Table 10.4). The specific objective of the study was to assess the repeatability of the impactor configurations (not to assess inhaler product performance); consequently, the experiment was conducted so that the following sources of variability were reasonably controlled:

1. Inhaler-to-inhaler variability over manufacturing run of OIP evaluated
2. Through-life trends of pMDI canister
3. Inter-operator variability
4. Inter-impactor system variability

Another feature of the study design was the inclusion of recurrent testing of each of the six inhalers on all three impactors. These precautions were taken to enable estimation of the intrinsic variability (precision) of each impactor system in isolation from other potentially confounding effects.

The statistical analysis estimated and compared the repeatability of three impactor configurations side-by-side, based on first quantifying the following

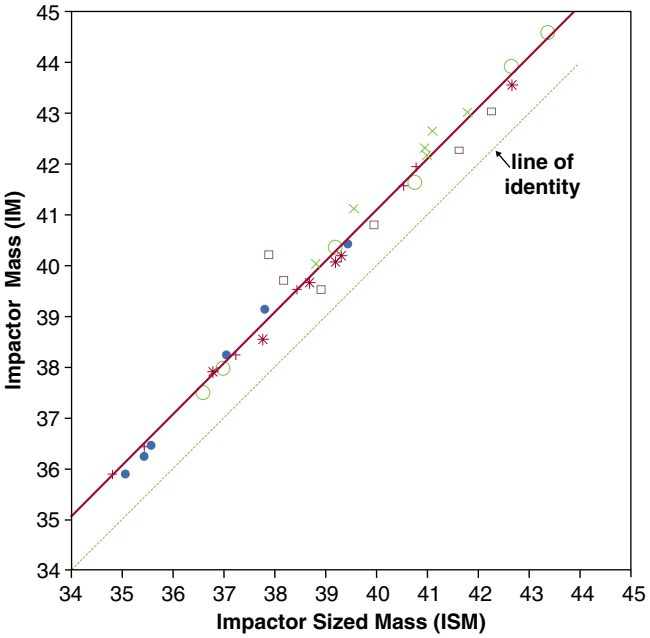

Fig. 10.9 Relationship between *IM* versus *ISM*, showing measurements with a different symbol for each of the six inhalers evaluated (*From* [26]—*used with permission*)

three principal metrics related to the total mass of salbutamol emitted from the inhaler, normalized on a per actuation basis:

1. Impactor mass (*IM*), defined as the total mass of API recovered from all components of the measurement system downstream of the induction port (i.e., mass on all stages including stage 0 for the full-resolution Andersen CI).
2. Ex-actuator mass (*Ex-ActM*), defined as the total mass of API recovered from all components of the measurement system including the induction port.
3. Ex-metering valve mass (*Ex-MVM*), defined as the total mass of API recovered from the measurement system together with that from the actuator mouthpiece of the inhaler.

Values of the subfractions of the mass/actuation were subsequently established and the relationship between *IM* (capable of being measured by all systems) and impactor-sized mass (*ISM*), determined only by the AIM-QC and full-resolution ACI, quantified (Fig. 10.9).

The consistent ca. 1 μg/actuation offset between *IM* and *ISM*, representing a fixed mass of API retained by stage 0 of the full-resolution ACI, enabled the precision comparison to take place between the two abbreviated configurations and the full-resolution CI, based on IM (Fig. 10.10).

On this basis, both abbreviated impactors had comparable precision with that of the ACI (Table 10.5).

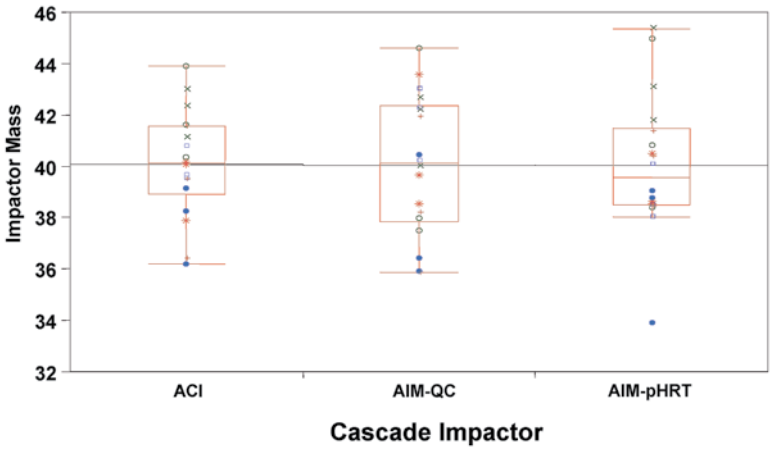

Fig. 10.10 Box-whisker plots of impactor mass by inhaler and cascade impactor configuration. The mean is represented by the tick mark at the center of the line (*From* [26]—*used with permission*)

Table 10.5 Summary statistics and 95% confidence intervals on ratio of standard deviations of abbreviated to full configurations for metrics related to inhaler APSD (*From* [26]—*used with permission*)

Metric	Impactor configuration	Mean (μg)	SD [repeatability] (μg)	Coefficient of variation (%)	95% CI[a] on ratio of SDs of abbreviated to full configuration
ISM	ACI	38.97	1.57	4.07	–
	AIM-QC	38.96	2.68	6.87	[0.93; 3.05]
LPM/SPM	ACI	2.70	0.28	9.98	–
	AIM-QC	2.69	0.35	12.83	[0.68; 2.24]

[a]Inclusion of 1.00 in confidence interval (CI) indicates no statistically significant difference

Separate estimates of variability were made for each metric (*ISM*, *LPM/SPM* with the AIM-QC and full-resolution ACI) and *FPM* (identical with *CPM* in terms of precision) for the AIM-pHRT and ACI. The estimates of precision associated with all these metrics obtained by the appropriate abbreviated impactor were substantially equivalent to the corresponding metrics with the full-resolution system (Fig. 10.11 and Tables 10.5 and 10.6).

Interestingly, all these metrics consistently tracked minor differences between the six inhalers that were used in the investigation (Fig. 10.11b, d, f). When the size fractions from either abbreviated impactor were compared with the corresponding cumulative mass-weighted APSD data from the ACI (Fig. 10.12), excellent agreement was apparent in almost all instances. However, an unexpected outcome was the magnitude of the positive bias associated with *EPF* measured by the AIM-pHRT system, which was almost 8% greater than the corresponding full-resolution data (Table 10.6), illustrated in the comparison of this metric with the expected value from the ACI (Fig. 10.12).

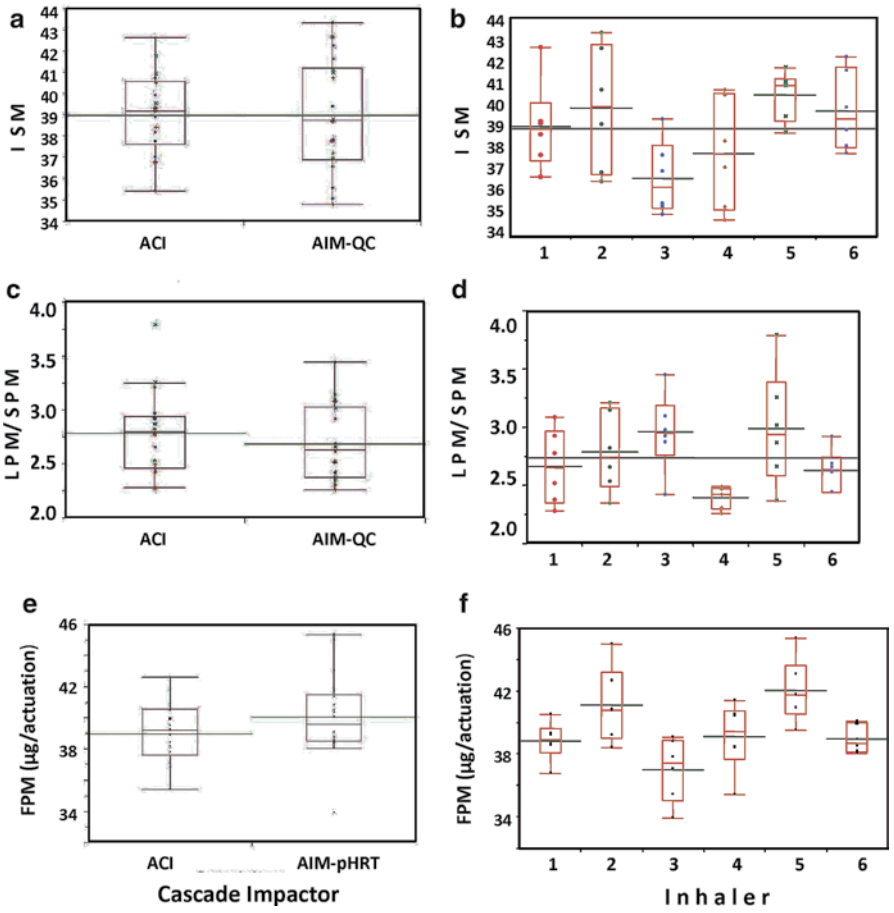

Fig. 10.11 Comparison of performance metrics in precision study: (**a**) ISM by impactor type; (**b**) *ISM* by inhaler number; (**c**) ratio LPM/SPM by impactor type; (**d**) *LPM/SPM* by inhaler number; (**e**) *FPM* by impactor type; and (**f**) *FPM* by inhaler number (*From* [26]—*used with permission*)

Table 10.6 Summary statistics and 95% Confidence Intervals (CIs) on ratio of standard deviations of AIM-pHRT system to nonviable ACI for metrics relating to inhaler APSD (*From* [26]—*used with permission*)

Metric	Impactor configuration	Mean (µg)	SD [repeatability] (µg)	Coefficient of variation (%)	95% CI on ratio of SDs of abbreviated to full configuration
CPM	ACI	44.08	2.87	6.52	[0.57; 1.89]
	AIM-pHRT	45.17	3.00	6.64	
FPM	ACI	35.43	1.40	3.88	[0.69; 2.25]
	AIM-pHRT	35.00	1.74	4.97	
EPM	ACI	2.21	0.74	33.72	[0.73; 2.40]
	AIM-pHRT	7.93	0.99	12.44	

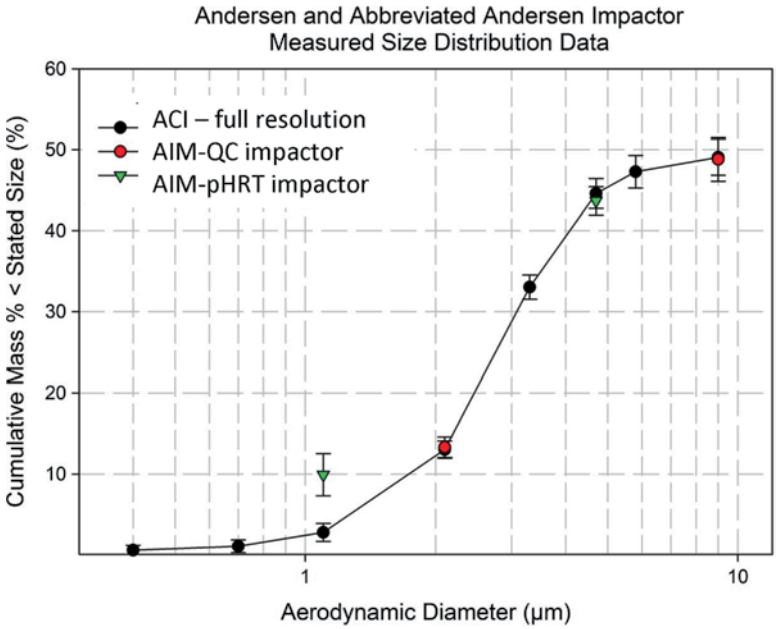

Fig. 10.12 Comparative measures of impactor-sized subfractions by AIM-QC and AIM-pHRT abbreviated systems with ACI (original AIM-pHRT data set) (*From* [26]—*used with permission*)

This observation prompted a follow-on investigation to eliminate the cause of the bias [27]. Microscopic inspection of the coated surface below the second stage (cut-off diameter 1.1 µm) revealed depressions in the coating directly beneath the nozzles, where impaction of particles would be expected (Fig. 10.13).

Interestingly, no other collection surfaces, in either of the abbreviated systems, exhibited the same problem. It was concluded therefore that the relatively high Reynolds number associated with flow through the nozzles of this lower stage ($Re_f = 292$ at 28.3 L/min) leads to displacement of the coating surface, inhibiting its ability to trap particles effectively. Particle bounce is therefore relatively high, re-entrainment carrying over material that should be efficiently collected into the *EPM*.

This problem was successfully resolved by floating a filter coated in surfactant on top of the collection plate (Fig. 10.14) that provided a surface that was both energy absorbent but at the same time resisted relocation by the incoming flow (Fig. 10.15). This unexpected outcome adds weight to the argument for a very careful consideration of particle bounce for all abbreviated systems, regardless of OIP class.

Rather surprisingly, increased precision, one of the potential benefits initially claimed for AIM systems by virtue of eliminating variability arising from stages that collected API close to the lower limit of detection, was not observed with either abbreviated system. In explanation, it was hypothesized that precision gains achieved by eliminating the analysis of material from stages where little sample collects are offset by other factors, possibly related to the flow of aerosol in the

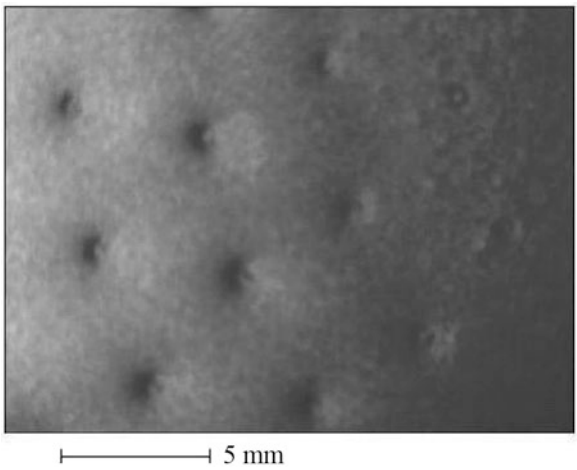

Fig. 10.13 Photomicrograph of displaced Brij 35 surfactant on collection plate for the second impaction stage of the AIM-pHRT impactor (*From* [27]—*used with permission*)

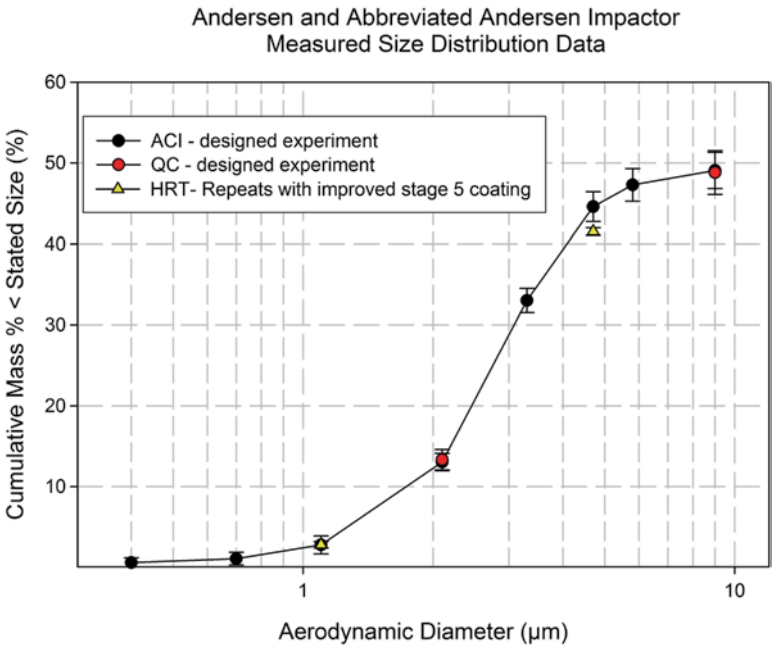

Fig. 10.14 Comparative measures of impactor-sized subfractions by ACI with measures of CPF, FPF, and EPF after modifying second impaction stage of AIM-pHRT CI with Brij-35-soaked filter (*From* [27]—*used with permission*)

reduced systems. Despite this finding, measurement time gains were found to be significant; analysis with the abbreviated systems taking around 30% of the time consumed using the ACI. This finding of more rapid determinations is a consistent trend across other reported studies to be discussed later in this chapter.

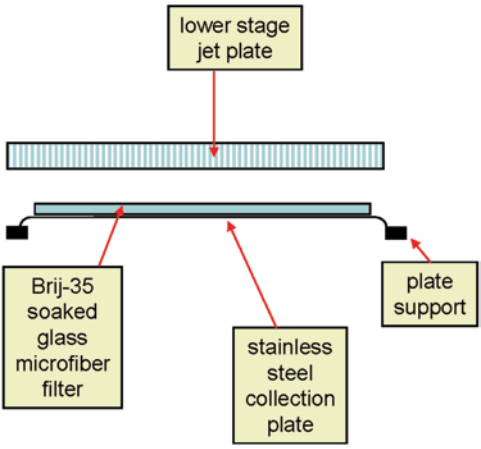

Fig. 10.15 Schematic of Brij-35-soaked glass microfiber filter, showing filter located on top of stainless steel collection plate (*From* [27]—*used with permission*)

10.5 Other Studies with ACI-Based AIM Systems

More recently, the commercialized version of the abbreviated ACI (FSA, Copley Scientific Ltd.) has been extensively evaluated by Keegan and Lewis in connection with the rapid screening of prototype pMDI actuators in early-stage product development [28, 29]. In a rapid prototyping environment, it is often desirable to optimize a device or system based upon the delivered mass and fine particle mass (≤5 μm) that are obtained through the cascade impactor method. A number of prototypes with slightly altered configurations may be screened to provide an optimized embodiment.

In their first study [28], MDIs containing beclomethasone dipropionate (BDP) (100 μg/50 μL) with 13% w/w ethanol cosolvent in HFA134a propellant were manufactured for use as the model product, equipped with a Bespak 630 series actuator with a 0.22 mm orifice diameter (Bespak, UK). A standard FSA with cut-point sizes of <5 μm and <1 μm d_{ae} was evaluated as the abbreviated CI configuration. BDP was recovered only from the impaction plates in the so-called rapid (rFSA) procedure, whereas this API was recovered from all CI surfaces following the standard method (FSA). The rFSA method therefore permitted as few as three separate actuations from each prototype formulation to be analyzed in terms of $FPM_{<5.0}$μm, compared with 4-actuations that were required to achieve the required sensitivity with the standard (FSA) procedure. The impaction plates were coated after FSA assembly (using either method) using aerosolized 1% w/w glycerol delivered in HFA134a propellant by a proprietary process. The recovery solvent was an 85:15 methanol–water mixture.

Following each actuation into the FSA, samples were collected from the USP/Ph. Eur. induction port and impaction plates (including back-up filter), but interstage drug loss was not determined. The stack was then reassembled with clean components. Following the final actuation, a sample was collected from the actuator and an average deposition over the appropriate number of pMDI actuations was reported.

Table 10.7 Comparison of particle distribution metrics for BDP (100 μg per actuation/50 μL metered volume) using three impactor methods (*From* [28]—*used with permission*). $n = 3$; mean ± SD

	TEM (μg)		$FPM_{<5.0\mu m}$ (μg)		$EFM_{<1.0\mu m}$ (μg)	
Method	Mean	SD	Mean	SD	Mean	SD
ACI	88.2	2.5	50.8	3.1	18.4	1.1
FSA	88.2	3.3	45.9	3.7	20.9	1.9
rFSA	85.9	3.2	46.0	0.5	21.3	1.4
p-Value[a]	*0.59*		*0.13*		*0.12*	

[a]One-way ANOVA

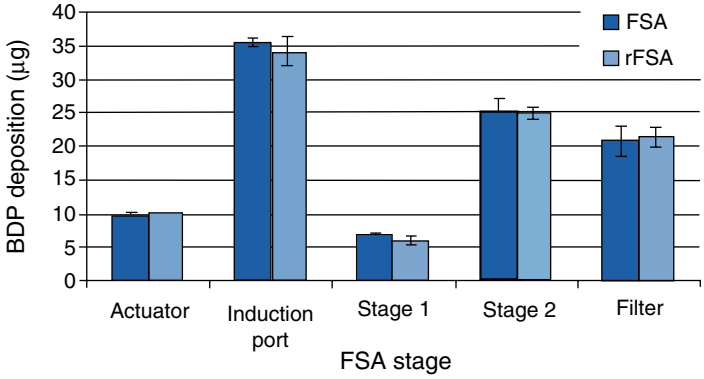

Fig. 10.16 Deposition profiles for BDP (100 μg per actuation/50 μL metered volume) within the abbreviated impactor both with (FSA) and without (rFSA) recovery of interstage drug loss ($n = 3$; mean ± SD for each data series) (*From* [28]—*used with permission*)

Assay for BDP was undertaken by UPLC-MS in both standard FSA and rFSA procedures.

In addition to the abbreviated CI-based measurements, benchmark full-resolution APSD determinations based upon two actuations of the model product were made using the ACI with collection plates coated using 1% w/w glycerol and also equipped with the same induction port. All measurements were undertaken at a flow rate of 28.3 L/min.

Comparison of the key metrics, *TEM*, $FPM_{<5.0\mu m}$, and $EPM_{<1.0\mu m}$, are summarized in Table 10.7. Note that in this work, delivered dose is equivalent to *TEM*.

No statistical difference ($p > 0.05$; ANOVA) between the reported metrics was evident. However, both FSA methods showed a tendency to slightly underestimate $FPM_{<5.0\mu m}$ and marginally overestimate $EPM_{<1.0\mu m}$, when compared to equivalent measures derived from the benchmark ACI. This finding is consistent with that discussed earlier for pMDIs containing ethanol as low-volatile cosolvent [20]. Importantly, this study showed no significant differences ($p > 0.05$; ANOVA) between either rFSA or FSA methods, despite the omission of the interstage drug deposition in the latter (Fig. 10.16).

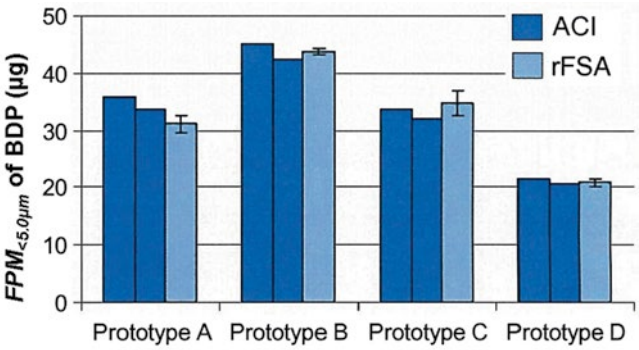

Fig. 10.17 Comparison of values of $FPM_{<5.0\mu m}$ achieved by aerosolizing BDP (100 μg per actuation/50 μL metered volume) with novel prototype actuators A–D: series 1 and 2 refers to the two ACI measurements ($n=2$) shown separately: series 3 refers to the rFSA measurements ($n=3$), in which mean ± SD is illustrated for group (*From* [28]—*used with permission*)

In the second phase of their investigation, four prototype actuators were assessed using a standard procedure ($n=2$; ACI) and rFSA method ($n=3$) in order to determine the screening capability of the rapid method. The trend in $FPM_{<5.0\mu m}$ observed between prototypes A–D was found to be independent of the impactor method, with prototype B delivering the optimal dose (Fig. 10.17).

Keegan and Lewis observed that their rFSA method reduced the time taken to obtain replicate ACI measurements by 50%. This time saving was in addition to other reported benefits such as reduced solvent consumption, analysis time, and data processing. They concluded that their AIM-based methodology represents a sufficiently precise method for determining key particle distribution metrics such as $FPM_{<5.0\mu m}$ for the purpose of screening and design optimization studies.

In their second investigation [29], Keegan and Lewis turned their attention to the use of their FSA as a tool for the rapid screening of solution pMDIs containing increasing concentrations of ethanol. The effect of adding 1.3% w/v glycerol was also investigated with the preparation containing 13% ethanol. The general test procedure used by Keegan and Lewis was similar to that for the full FSA method described in their first study [28].

An additional spacing stage was included above the first impaction stage in the FSA, as recommended by Mitchell et al. (see Fig. 10.4) [20] for some measurements. In this modified FSA (mFSA) configuration, more time was allowed for ethanol to evaporate, with the aim of achieving closer agreement with full-resolution benchmark ACI measurements for these MDI products. However, this annular spacer stage differed from the approach adopted by Mitchell et al., in that it consisted of a metal ring without the nozzle plate (Fig. 10.18).

The MDIs, again containing BDP as API (100 μg per actuation/50 μL metered volume), were manufactured containing 8%, 13%, and 26% w/w ethanol in HFA134a propellant. Each MDI was equipped with the same actuator as used in their first study. Values of $CPM_{>5.0\mu m}$, $FPM_{<5.0\mu m}$, and $EPM_{<1.0\mu m}$ obtained from each of the

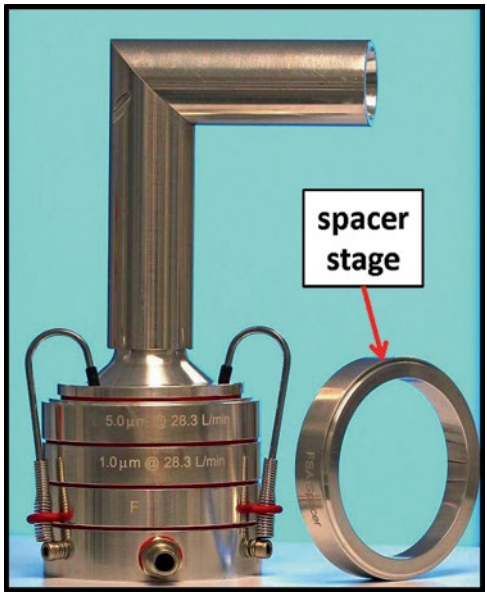

Fig. 10.18 FSA with annular spacer stage (mFSA) used by Keegan and Lewis (*From* [29]—*used with permission*)

impactor configurations are summarized in Fig. 10.19. There was no difference between the reported values for the glycerol-containing formulation regardless of the impactor used ($p > 0.05$). The addition of glycerol to a solution pMDI formulation modulates the MMAD, increasing it from 1.3 µm (13% ethanol) to 2.8 µm. This effect may reduce impaction due to incomplete ethanol evaporation since the residual droplets are larger. Significant differences ($p < 0.01$) in the metrics obtained when the ethanol concentration was at its highest (26%w/w) became evident between the impactor systems.

The difference between the average BDP masses at each particle size fraction for the ethanol-containing MDIs is reported in Table 10.8. The residual values in this table represent the absolute magnitude of the difference between FSA- and ACI-measured values of each metric, expressed as a percentage and in micrograms. Keegan and Lewis observed a consistent increase in the magnitude of the difference between the FSA value and that calculated from ACI stage deposition as the ethanol concentration in the formulation increased. Importantly, however, the inclusion of the additional "spacer" stage in the FSA attenuated these divergence between FSA and ACI-measured values of both $CPM_{>5.0\mu m}$ and $FPM_{<5.0\mu m}$, as would be expected from the earlier observations of Mitchell et al. [20]. However, this behavior was offset by increases in divergence with values of $EPM_{<1.0\mu m}$ when the "spacer" stage was included.

Figure 10.20 shows the effect of the "spacer" stage on deposition of BDP on the collection plate of the first FSA stage in comparison with the calculated equivalent from the full-resolution ACI (impaction stage mass less $FPM_{<5.0\mu m}$).

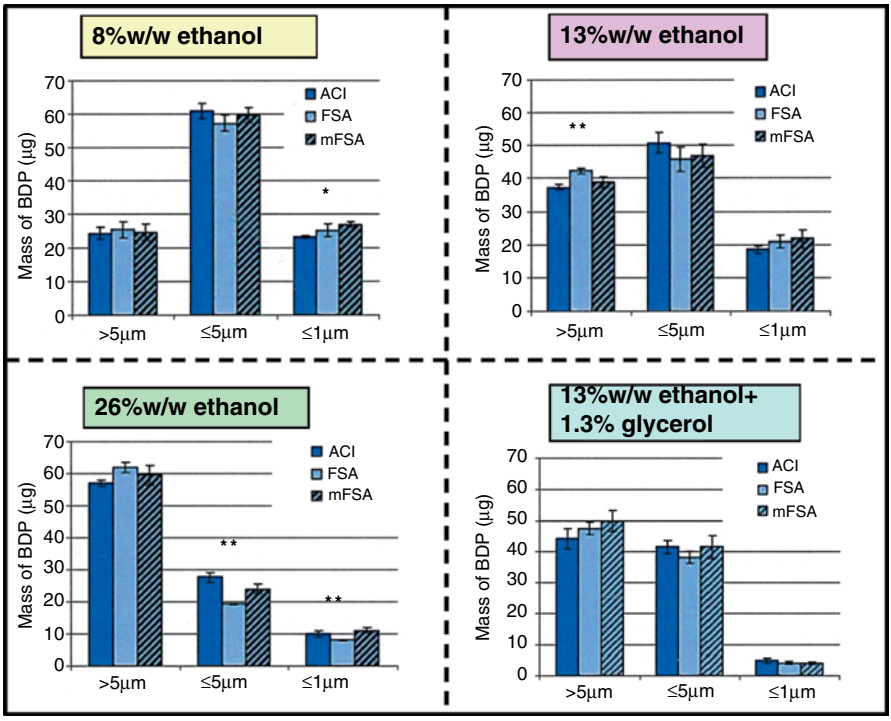

Fig. 10.19 Comparison of impactor size fractions (ANOVA; $*p<0.05$; $**p<0.01$) from solution formulations containing 100 µg BDP per 50 µL dose ($n=3$; ±SD). *mFSA* modified FSA as described above (*From* [28]—*used with permission*)

Table 10.8 Residual FSA-measured particle dose values relative to associated ACI values[a] (*From* [28]—*used with permission*)

		Ethanol content (%w/w)					
		8%		13%		26%	
Metric	FSA type	µg	%	µg	%	µg	%
$CPM_{>5.0\mu m}$	FSA	−1.1	4.5	−4.9	**13.1**	−4.8	8.4
	mFSA	−0.3	1.2	−1.4	4.1	−2.5	4.4
$FPM_{<5.0\mu m}$	FSA	3.8	6.2	4.9	9.6	8.4	**30.4**
	mFSA	1.3	2.0	3.8	7.5	3.6	**13.0**
$EPM_{<1.0\mu m}$	FSA	−2.0	8.6	−2.4	**13.0**	2.3	**22.8**
	mFSA	−3.6	**15.5**	−3.2	**17.3**	−0.9	8.9

[a]Bold typeface indicates a difference of >10% of the ACI reported value

The outcome depicted confirms the previously reported observation of impaction of partially evaporated droplets from solution MDI formulations containing ethanol [20]. However, Keegan and Lewis noted that the addition of the "spacer" stage to the FSA did not make any significant difference to the BDP deposition observed for

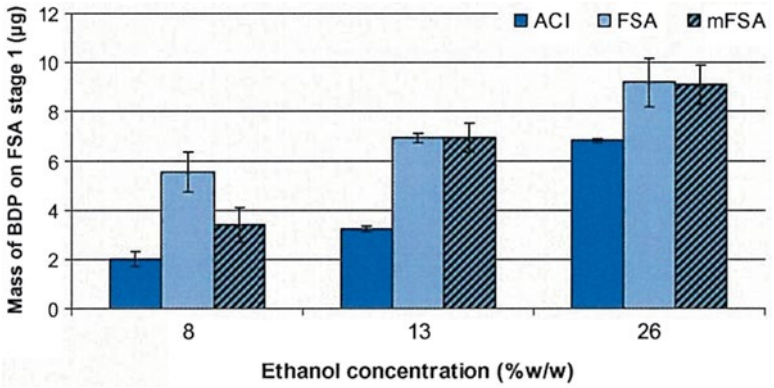

Fig. 10.20 Mass BDP deposited on stage 1 of the FSA configurations compared with the equivalent mass deposited in the ACI ($n = 3$; ±SD). *mFSA* modified FSA as described above (*From* [28]—*used with permission*)

formulations with ethanol concentrations >8% w/w. They suggested that the inclusion of a "spacer" stage may help to attenuate some differences between the FSA and ACI. However, it is likely that the magnitude of the effect will be formulation/device specific.

Keegan and Lewis concluded that, in general, the FSA may provide representative values for key particle metrics that are not significantly different from the full-resolution ACI for solution pMDI formulations. If it can be used, this abbreviated impactor offers a tool that eliminates the need for post-analysis data processing to obtain key metrics when screening formulations.

The outcomes from all of the work reported in this section reinforce the recommendation that the implementation of an AIM-based method should always be preceded by some form of validation study with the particular products of interest, using an appropriate full-resolution CI as the benchmark technique.

10.6 Assessing the Performance of AIM Systems Based on the Andersen Viable Cascade Impactor

The Andersen viable cascade impactor (AVCI) is the earliest version of the Andersen multistage CIs to be developed [30]. It is similar in operating principle to the nonviable ACI, with the important exception that the stage wells are larger so that they can each accommodate a Petri dish instead of a collection plate [31]. The Westech fine particle dose impactor (Westech Instrument Services, Upper Stondon, Beds., UK) was designed as a simple two-impaction stage and filter sampler for the rapid determination of fine particle mass from pMDIs at 28.3 L/min (Smurthwaite MJ (2012) Westech instrument services, UK, personal communication). The design is based on an abbreviated AVCI (Fig. 10.21) but incorporates some new design features

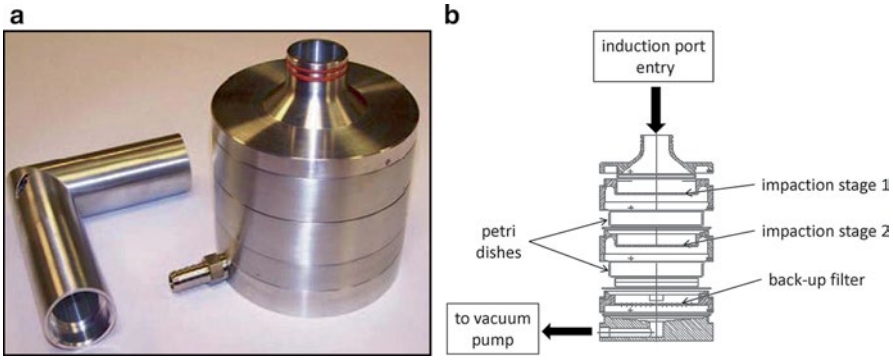

Fig. 10.21 Westech Instrument Services fine particle dose impactor (FPD–AVCI). (**a**) External appearance. (**b**) Cross-section through interior (*Courtesy of Westech Instrument Services Ltd.*)

to improve ease of use, notably a bayonet fixing between stages to allow rapid assembly/disassembly of the CI. The replacement of the standard ACI collection plates with glass or metal Petri dishes facilitates in situ recovery of API. The size-separation stages themselves are based on stages 2 and 6 of the AVCI, having nominal jet diameters of 0.914 mm and 0.254 mm, respectively, with corresponding cut points of 4.7 and 1.1 μm aerodynamic diameter.

In 2010, Chambers and colleagues at AstraZeneca (AZ), UK undertook a performance evaluation study of the FPD apparatus, comparing it against a 6-stage nonviable ACI, and also a 2-stage abbreviated nonviable ACI (sACI) that utilized ACI stages 2 and 5 with a blank stage 0 present (and was therefore equivalent to the T-FSA/AIM-pHRT design), as benchmark systems [32]. Here the prefix "s" stands for standard (i.e., nonviable ACI) components. The performance of the CIs was assessed against the following metrics:

1. Total mass [dose collected by impactor equivalent to impactor mass (*IM*)]
2. Mass of API collected by induction port (USP/Ph. Eur.) [equivalent to nonimpactor-sized mass (*NISM*)]
3. Coarse particle mass >4.7 μm aerodynamic diameter ($CPM_{>4.7\mu m}$)
4. Fine particle mass <4.7 μm aerodynamic diameter ($FPM_{<4.7\mu m}$)
5. Extra-fine mass collected on back-up filter ($EPM_{<1.1\mu m}$)

Three pMDIs containing a single component API were used to evaluate the performance of the FPD–AVCI and sACI relative to data generated from the 6-stage ACI. The collection plates of the 6-stage ACI were uncoated in accordance with normal practice for working with this class of OIP. However, the respective plates and Petri dishes of the sACI and FPD–AVCI were coated with a Brij 35-coating solution based on the findings from the earlier work reported in Sect. 10.3.

An additional experiment was carried out in order to investigate the extent of possible particle re-entrainment whereby Brij-coated Westech filter papers were placed on the plates and Petri dishes of both stages of the sACI and FPD–AVCI,

Table 10.9 Experiment order in the AstraZeneca (UK) 2011 FPD–AVCI evaluation study

Experiment	pMDI no.	pMDI actuation numbers	Impactor
6-Stage ACI (control)	1	1–6	A
	2		B
	3		C
sACI with Brij-coated plates	1	9–11	A
	2		C
	3		B
FPD–AVCI with Brij-coated petri dishes	1	14–16	A
	2		B
	3		C
FPD–AVCI with Brij-coated filter on petri dishes	1	19–21	B
	2		A
	3		C
sACI with Brij-coated filter on plates	1	24–26	C
	2		A
	3		B

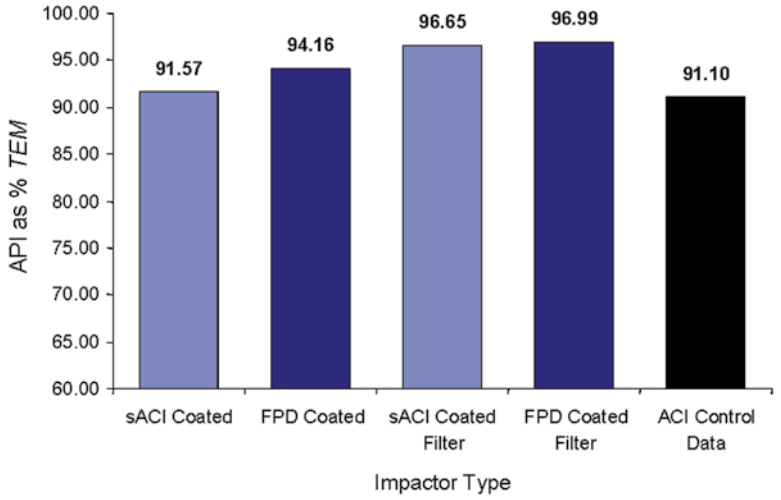

Fig. 10.22 Impactor mass (*IM*) of API expressed as % of nominal dose recovered from the various systems evaluated by Chambers et al. (*From* [32]—*used with permission*)

following the practice described in Sect. 10.4 for the second stage of the AIM-pHRT system evaluated at TMI [27]. Three impactors of each type were evaluated, but in order to guard against systematic bias in the different experiments, the impactor order was swapped between experiments (Table 10.9). The measurement of *IM* as percentage of the nominal dose by sACI with Brij-coated Petri dishes was in closest agreement with that obtained from the control ACI (Fig. 10.22).

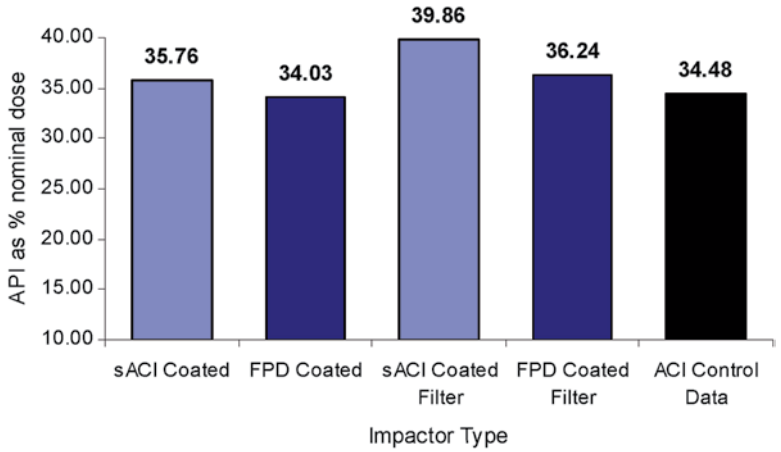

Fig. 10.23 $FPM_{<4.7\mu m}$ as percentage of *TEM* (mass/actuation) ex-MDI for the various systems evaluated by Chambers et al. (*From* [32]—*used with permission*)

IM, determined by the FPD–AVCI, was greater than with the control ACI by +3.4% for the surfactant (Brij)-coated FPD–AVCI, and +6.5% for the same CI when Brij-coated filters were used. Importantly, the addition of Brij-coated filters to the sACI resulted in a similar increase in *IM* relative to the ACI, in this instance being +6.7%.

These data are suggestive of decreased internal losses when the Brij-soaked filters were used to mitigate particle bounce further than could be achieved by simply coating the collection plates with the same surfactant. The measure of agreement between sACI with coated plates and the ACI control is probably to be expected, given the similarity in internal geometry and dead space.

All abbreviated systems were closely correlated to the 6-stage ACI in terms of either $CPM_{>4.7\mu m}$ or $FPM_{<4.7\mu m}$ (Fig. 10.23). The sACI slightly underestimated $CPM_{>4.7\mu m}$ relative to that measured with the reference ACI, but that introduction of the Brij-coated filter papers on the sACI stages resulted in an increase in $CPM_{>4.70\mu m}$, providing additional support for an argument that bounce and re-entrainment were not entirely eliminated when the plates were coated with surfactant, without the means to stabilize the coating when flow passed through these CIs.

$FPM_{<4.7\mu m}$ determined by the Brij-coated sACI and the FPD data both agreed closely with the same measure obtained using the reference ACI. The addition of Brij-coated filters increased $FPM_{<4.7\mu m}$ in line with similar effects associated with both $CPM_{>4.7\mu m}$ and *IM*.

When both $FPM_{<4.7\mu m}$ and $CPM_{>4.7\mu m}$ were calculated as a percentage of *IM* (Fig. 10.24), this form of data presentation highlighted more clearly that both abbreviated CIs correlated well with the ACI; although, $CPM_{>4.7\mu m}$ was slightly underestimated by the sACI. The increase in upper stage deposition with this formulation was confirmed by the addition of Brij-coated filters paper to the sACI. However, these observed differences are slight and comparable with true variability associated with the product itself.

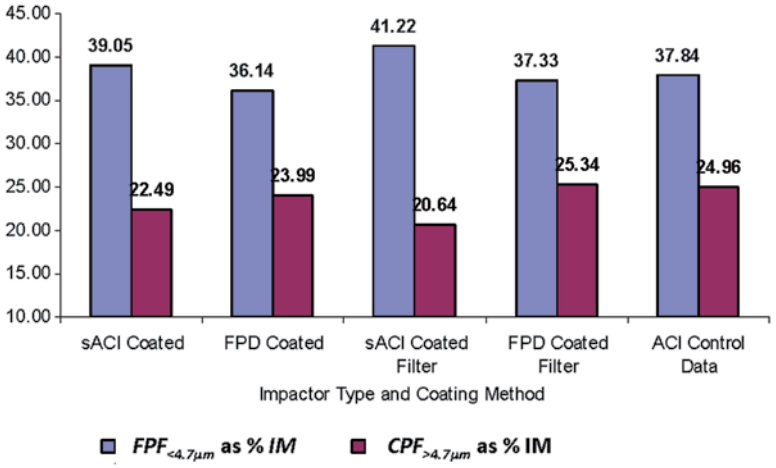

Fig. 10.24 $FPF_{<4.7\mu m}$ and $CPF_{>4.7\mu m}$ as a percentage of *IM* for the various systems evaluated by Chambers et al. (*From* [32]—*used with permission*)

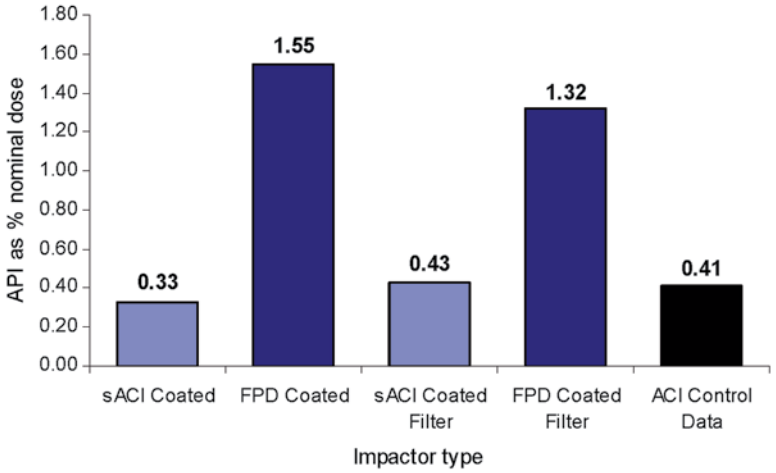

Fig. 10.25 Measures of $EPM_{<1.1\mu m}$ as percentage of *TEM* (mass/actuation) ex-MDI for the various systems evaluated by Chambers et al. (*From* [32]—*used with permission*)

The largest discrepancy seen between the impactors (Fig. 10.25) was in filter deposition ($EPM_{<1.1\mu m}$), where the magnitude obtained with the FPD–AVCI (1.55% of nominal dose with Brij-coated surfaces; 1.32% with added Brij-coated filters) was more than three times greater than equivalent values obtained using either the sACI (0.33% Brij-coated plates; 0.43% with added Brij-coated filters) or the ACI control (0.41%).

Table 10.10 pMDI products evaluated by Guo et al. with the FPD–AVCI [33]

Product name	API	Propellant	Excipients	Formulation type
Aerobid®	Flunisolide	CFC	Sorbitan trioleate	Suspension
Combivent®	Salbutamol (AS)/ipratropium bromide (IB)	CFC	Soya lecithin	Suspension
MaxAir™	Pirbuterol	CFC	Sorbitan trioleate	Suspension
Advair®	Fluticasone propionate (FP)/ salmeterol xinafoate (SX)	HFA	None	Suspension
Flovent-110®	Fluticasone propionate	HFA	None	Suspension
Proair®	Salbutamol	HFA	Ethanol	Suspension
Proventil™	Salbutamol	HFA	Oleic acid, ethanol	Suspension
Atrovent®	Ipratropium bromide	HFA	Water, citric acid, ethanol	Solution

This pattern of divergence between the various abbreviated options was comparable in absolute terms with the behavior observed with measures of $FPM_{<4.7\mu m}$. The fact that the addition of Brij-coated filters to the collection dishes of the FPD–AVCI only slightly reduced $EPM_{<1.1\mu m}$ suggests that particle re-entrainment is an unlikely cause.

However, it should be emphasized that these differences between the abbreviated systems with or without surfactant-saturated filters to control particle bounce and re-entrainment and the control ACI were small, and therefore unlikely to prevent any of these options being used as an abbreviated impactor of choice with this particular formulation. This type of detailed study illustrates well the approach that should be taken when validating a potential AIM-based system for any OIP.

Guo et al. have also recently presented measurements undertaken with the Westech FPD–AVCI impactor, evaluating eight different suspension and solution pMDIs (Table 10.10) [33]. $CPF_{>5.0\mu m}$, $FPF_{<5.0\mu m}$, and $EPF_{<1.0\mu m}$ determined by the FPD–AVCI were compared to the same metrics obtained by means of an 8-stage nonviable ACI. Ten actuations from the pMDI-on-test were delivered into the FPD–AVCI or ACI, and API recovery proceeded afterward by validated quantitative chemical analysis. Since the ACI does not have stages with cut-off diameters precisely at 5 μm and 1 μm, the three measures of interest were interpolated from the cumulative APSD data obtained with the full-resolution CI.

Equivalent total API recovery was observed for all pMDI products between FPD and ACI (Fig. 10.26). Although agreement between FPD–AVCI and ACI data was generally good, Guo et al. found small but significant differences in all three subfractions with some of the formulations, especially with $CPF_{>5.0\mu m}$, with the values obtained using the FPD–AVCI higher than their ACI-determined counterparts (Fig. 10.27).

Guo et al. concluded that, whether or not the pMDI is a solution or suspension, formulation was not the only deciding factor on whether or not there is a divergence between abbreviated and full-resolution data [33].

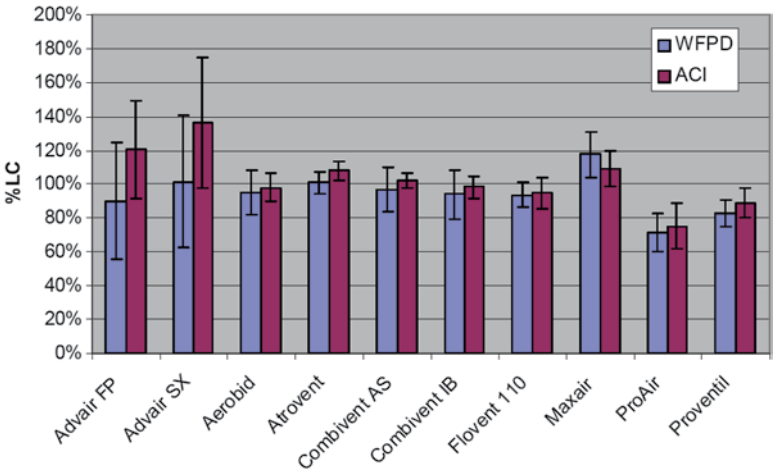

Fig. 10.26 Total API recovery for eight different pMDI products comparing FPD–AVCI and nonviable 8-stage ACI. *%LC* percent label claim (*From* [33]—*courtesy of W. Doub*)

In retrospect, the internal dead space associated with the FPD–AVCI is significantly greater than that for the abbreviated nonviable ACI systems, due to the need to accommodate the three dimensional structure of the Petri dish rather than near-to-flat collection plates associated with the nonviable ACI internal configuration (compare Fig. 10.28a, b). The extra dead space in the FPD–AVCI might therefore be expected to result in increased $FPF_{<5.0\mu m}$ through increased time for particle shrinkage due to cosolvent evaporation. However, this outcome was not seen to a marked extent with formulations containing cosolvent except with Proventil™.

Furthermore, cosolvent evaporation would not explain the observed bias toward larger values of $CPF_{>5.0\mu m}$, that was apparent with almost all the products, whether or not cosolvent was present in the formulation. It therefore appears that another explanation is needed to explain these results in a more satisfying way. One possibility could be the potential for increased impaction of coarse particulate at the first stage of the FPD–AVCI, again brought about by differences in internal geometry between this abbreviated impactor and the nonviable ACI.

Further investigation is therefore warranted, this time, ideally using both AVCI and nonviable ACI as control impactors, given the similarity of this impactor to the interior of the FPD–AVCI (compare Fig. 10.16 with Fig. 10.28a).

10.7 Assessing the Performance of AIM Systems Based on the Fast Screening Impactor

Up until this section, the focus has been on abbreviated impactors that are based on either the nonviable or viable ACI internal configurations. Such systems were the first to be evaluated, as in the case of abbreviated nonviable ACI systems, they can be

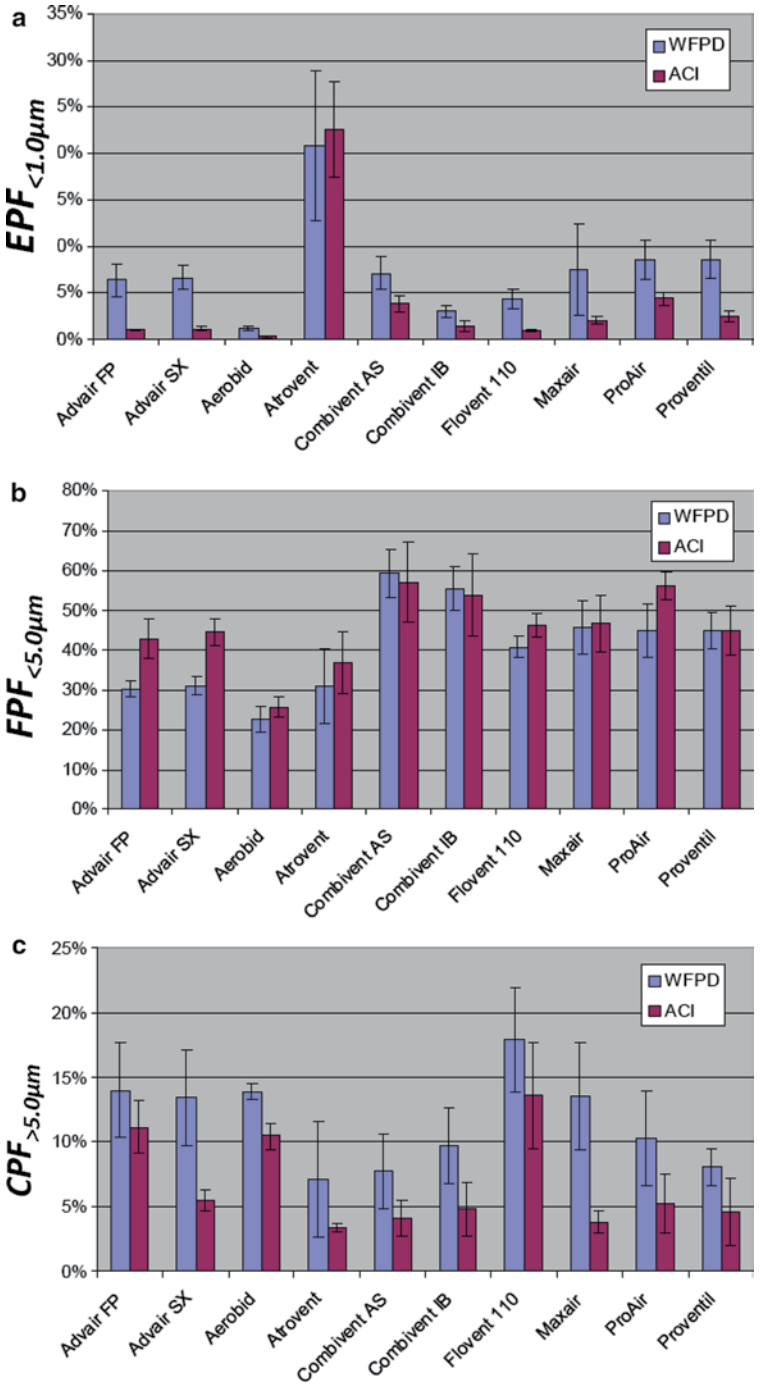

Fig. 10.27 Comparisons of measures of $CPF_{>5.0\mu m}$, $FPF_{<5.0\mu m}$, and $EPF_{<1.0\mu m}$ for 8-different pMDI products comparing FPD–AVCI and nonviable 8-stage ACI. *%LC* percent label claim (*From* [33]—*courtesy of W. Doub*)

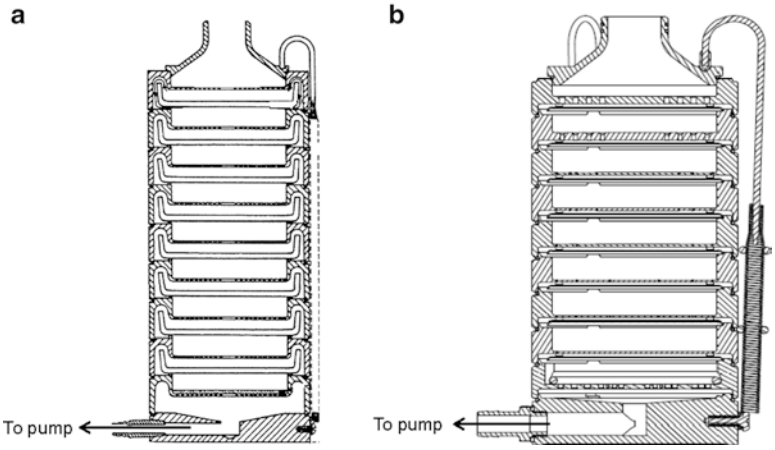

Fig. 10.28 Andersen 8-stage impactors (**a**) viable (AVCI); (**b**) nonviable (ACI) [*Courtesy of Westech Instrument Services Ltd. (**a**) and Copley Scientific Ltd. (**b**)*]

constructed easily from existing components of the full-resolution system. In the past 10 years since commercialization, the NGI has become increasingly used to characterize OIPs, especially since its acceptance as a pharmacopeial apparatus for APSD determinations (Apparatus 5 and 6 in Chap. 601 of the US Pharmacopeia, and apparatus E in Chap. 2.9.18 of the European Pharmacopoeia—see Chap. 2). Abbreviated systems based on this impactor are either newly introduced units or involve modification of a full-resolution impactor, which is discussed later in this chapter.

The fast screening impactor (FSI) is a newly introduced one-stage impactor (Fig. 10.29), importantly with no "parent" full-resolution apparatus; although its design is based on a modified NGI pre-separator [34]. With this abbreviated impactor, large non-inhalable liquid boluses from nebulizing systems and powder boluses in the case of DPIs are captured in a liquid trap, and the sample is then separated by a fine-cut impaction stage whose d_{50} is 5.0 µm. A filter collector below the pre-separator body collects the fine fraction.

The stage collection efficiency characteristics of four slightly different designs of FSI insert having a nominal cut point of 5 µm aerodynamic diameter have been reported by Roberts and Romay [34] (Table 10.11), permitting the FSI to be operated in the flow rate range from 30 to 90 L/min, and therefore making it suitable for DPI aerosol characterization, as well as with the other forms of OIP.

The sharpness of cut, given by the closeness of the geometric standard deviation (GSD_{stage}) to unity (see Chap. 2), was excellent in all the cases for which data were presented (the GSD_{stage} of the insert developed to operate at 35 L/min was subsequently also confirmed to be close to 1.10). These values compare with values of GSD_{stage} in the range 1.1–1.4 for the NGI [35, 36] intentionally designed to have optimum performance in terms of size-fractionation and resolution capability [14]. There are now inserts manufactured with 5 µm cut point for use at 5 L/min intervals

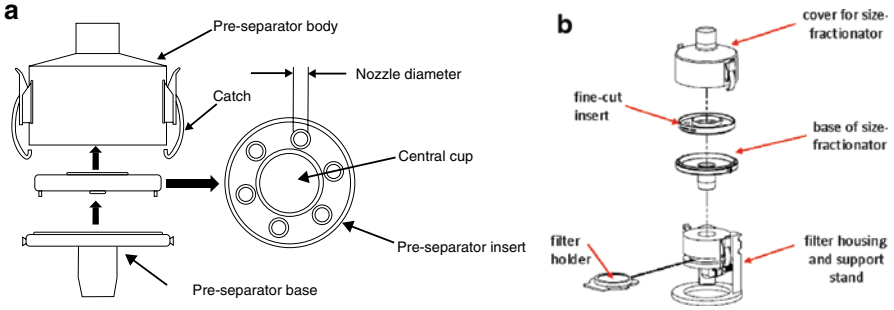

Fig. 10.29 Fast screening impactor (FSI). (**a**) Components. (**b**) Assembly (*Courtesy of MSP Corp., St. Paul, MN*)

Table 10.11 Design and calibration data for the FSI at different flow rates with inserts having a nominal stage d_{50} of 5.0 $_{\mu m}$ (*From* [34]—*courtesy of D.L. Roberts*)

Flow rate (L/min)	Number of nozzles	Size of nozzles (mm)	Nozzle-to-nozzle circumferential distance/nozzle diameter (dimensionless)	$STK^{1/2}$ (critical Stokes number for impaction)	GSD_{stage}
30	6	4.08	11.0	0.49	1.07
35	7	4.08	9.4	0.49	1.10[a]
60	12	3.94	5.7	0.51	1.12
90	9	5.00	5.9	0.51	1.12

[a]Measured subsequent to publication of [34]

from 30 to 100 L/min [37], primarily for DPI testing in accordance with the method given in monograph 2.9.18 of the Ph. Eur.

If greater control of cut point is required and the sampling flow rate from the inhaler can be varied, the use of a fixed insert at different volumetric flow rates (Q) can allow fine adjustment of the boundary for the coarse/fine fraction, as cut-off diameters (d_{50}) shift in accordance with Marple-Liu theory [Eq. (10.2)]. Other inserts can therefore be manufactured to order, providing any desired cut point in the range 1.0–10 µm aerodynamic diameter for measurements at a given flow rate (Roberts DL (2012) MSP Corporation, St. Paul, MN, USA, personal communication).

The first reports issued in late 2009 by a group from Pfizer (Sandwich, UK) [38, 39] described the use of an FSI for DPI studies. To begin with, a commercially available DPI was measured at 70 L/min using a FSI with a 5 µm insert. The NGI APSD measurements were made in accordance with the compendial DPI methodology, which was adapted, in the case of the FSI evaluation, to reflect the simplified information obtainable from this abbreviated system. Results were gathered for the uncoated FSI and again following collection surface coating with a very fine layer of silicone fluid applied as a 1% v/v solution in cyclohexane. Their metrics, $CPF_{>5.0\mu m}$, $FPF_{<5.0\mu m,}$ and total impactor recovery (equivalent to IM) were compared with data from a full-resolution NGI, with data from the full-resolution APSD

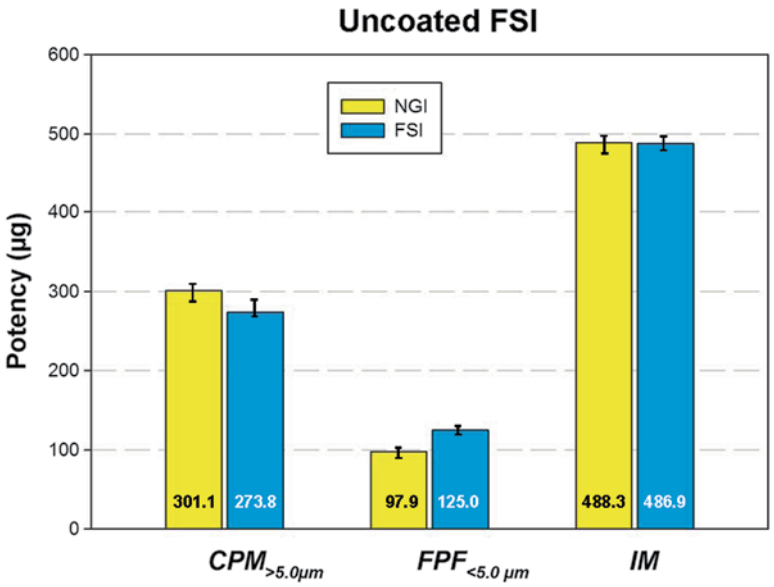

Fig. 10.30 Size-related metrics from FSI with uncoated collection surfaces with equivalent NGI-generated metrics (*From* [38]—*courtesy of D. Russell-Graham*)

interpolated to give an equivalent $FPF_{<5.0\mu m}$ assuming a unimodal and lognormal APSD; since the NGI has no stage with a cut-off diameter located at precisely 5.0 µm aerodynamic diameter. Their metrics obtained with the particle collection surfaces of the FSI uncoated were in reasonably close agreement with those measured using their full-resolution NGI (Fig. 10.30), but there was a small but systemic bias toward higher values of $FPF_{<5.0\mu m}$ with the FSI.

These findings are consistent with particle bounce and re-entrainment and were largely eliminated, using the silicone fluid coating (Fig. 10.31).

Similar trials were carried out with other DPIs at flow rates determined via the standard pharmacopeial method for DPI testing, using an appropriate insert to maintain the 5 µm stage cut-off at each flow rate. These results confirm the initial conclusion that a coated FSI produced $FPF_{<5.0\mu m}$ values that were closely comparable to those obtained using the full-resolution NGI. However, the magnitude of minor discrepancies between the NGI and FSI varied from product to product, serving to highlight the necessity of justifying the use of AIM techniques through suitable method development and comparative testing against a full-resolution instrument, for each inhaler product.

A further study was investigated by this group to assess the value of AIM as a screening tool during early-stage formulation screening [38]. This investigation was structured to simulate a Design of Experiments (DoE) of the type routinely applied during early-stage product development. Here, the goal was to investigate the ability of the FSI to correctly identify trends in FPF resulting from changes in percentage

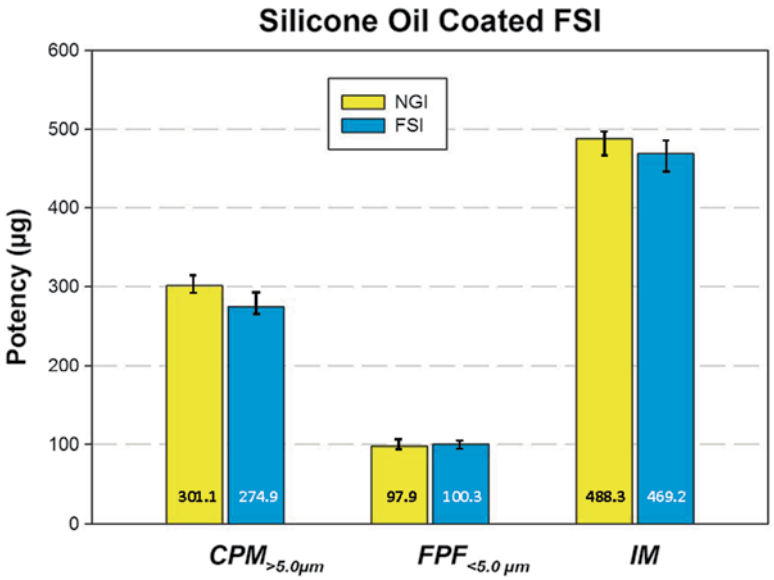

Fig. 10.31 Size-related metrics from FSI with silicone-oil-coated collection surfaces with equivalent NGI-generated metrics (*From* [38]—*courtesy of D. Russell-Graham*)

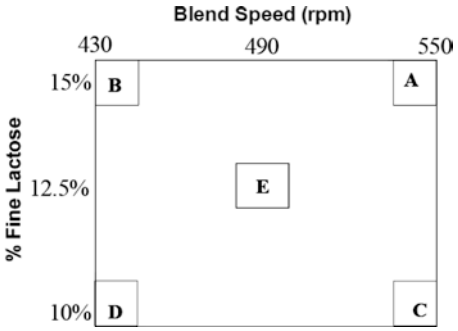

Fig. 10.32 DoE for dry powder blending parameters investigated by FSI (*From* [38]—*courtesy of D. Russell-Graham*)

fine lactose content and blend speed. Five DPI formulations were prepared: A, B, C, and D mark the four extremes of the experimental range defined by high (15%) and low (10%) fine lactose content and high (550 rpm) and low (430 rpm) blend speed, while E lies in the center of the defined space (Fig. 10.32). Theoretically, $FPM_{<5.0\mu m}$ would be expected to increase with increasing fine lactose content and increasing blend speed, excipient content being the dominating effect, giving a ranking for the formulations of A, B, E, C, and D, with A expected to deliver superior performance.

The FSI results correctly identified the influence of excipient fine content (Table 10.12) but failed to indicate any statistical difference between formulations

Table 10.12 Comparison between FSI and NGI for screening of DPI lactose blends based on $FPM_{<5\mu m}$ (*From* [38]—*courtesy of D. Russell-Graham*)

	NGI		FSI	
Blend	Mean (μg)	RSD (%)	Mean (μg)	RSD (%)
A	58.4	4.9	66.6	3.8
B	59.2	4.5	66.2	4.0
C	50.4	13.4	60.9	3.1
D	55.4	3.7	60.6	3.6
E	63.2	6.8	62.8	6.0

produced at different blend speeds. The values of FSI-determined $FPM_{<5.0\mu m}$ for the blends were as expected, according to the predicted order in relation to percentage of fine lactose in each blend.

However, surprisingly, blend speed appeared to have had no effect on this metric. In contrast, corresponding values of $FPM_{<5.0\mu m}$ determined by NGI showed the anticipated differentiation between both blend speed and % lactose fines, except for a higher than expected value of $FPM_{<5.0\mu m}$ for blend E.

In a supplementary study, a commercial DPI device was loaded with capsules of different fill weights to investigate in greater detail the tracking capability of the FSI over a wider variation in fine particle mass ($FPM_{<5.0\mu m}$) than was evident in the preceding study. The tracking ability for this metric was assessed over a far greater magnitude (~90 μg) than expected in product development. A new marketed DPI was filled with capsules of four different fill weights—and therefore different values of $FPM_{<5.0\mu m}$—using a different formulation to that evaluated in the previous studies. Three actuations of each fill weight were delivered into each CI system in accordance with the compendial methodology as previously described.

This head-on comparison for $FPM_{<5.0\mu m}$ by both measurement techniques revealed a near 99% correlation within a wide range of potency (Fig. 10.33). On that basis, it appears that if precautions are taken to eliminate bias from particle bounce, the FSI can track changes in this performance metric as well as the NGI. However, these authors acknowledged at the time that more work would need to be done to compare the tracking ability of their FSI compared with that for the NGI in cases where differences in blend performance are as small as typically found in product development. While $FPM_{<5.0\mu m}$ tracking between the FSI and NGI was the main objective of this study, such an approach would also be useful to test a new inhaler and drug blend in early product development using also $CPF_{>5.0\mu m}$ and total impactor recovery (*TIR*) of API as a supplementary performance metric and system suitability check, respectively.

Aside from the technical contribution made by the Pfizer work, their investigations also provided useful practical information relating to the potential time savings associated with AIM (Table 10.13).

The total time quoted for six FSI measurements was estimated to be about one-third that required for six equivalent analyses with a fully optimized NGI set-up utilizing multiple sets of equipment and analysts. Given that FSI techniques were

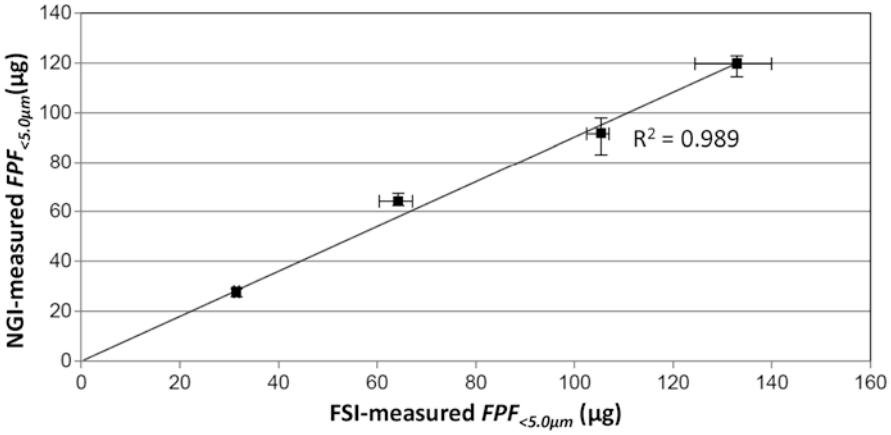

Fig. 10.33 $FPF_{<5.0\mu m}$ comparison by NGI and FSI from supplementary study investigating effect of dry powder blending properties (*From* [38]—*courtesy of D. Russell-Graham*)

Table 10.13 Comparative measurement times (h) between FSI and NGI use in aerosol assessment from 6-DPI replicate measurements (*From* [38]—*courtesy of D. Russell-Graham*)

Impactor	Experimental	Analysis	Data processing	Total
FSI	2.0	0.67	0.33	3.0
NGI	6.0	2.5	0.5	9.0

not yet fully optimized during this assessment, these findings would suggest that, conservatively, time savings of more than 50% are easily achievable using abbreviated systems, a potentially massive gain in productivity.

This group has since extended their investigation of the FSI by comparing it with the NGI across a range of drug products dispensed from different DPIs, exploring the potential impact of differences in pressure drop profile experienced by the device on the data obtained from the abbreviated and full-resolution impactors [40]. The following conditions were evaluated:

1. Product (1) contained two dosage strengths of the same API, each evaluated at 60 L/min (Fig. 10.34a).
2. Products (2) and (3) were each two-component combination DPIs, tested at 60 and 70 L/min, respectively (Fig. 10.34b, c).
3. Product (4) was a DPI having a greater flow rate dependency on API APSD, evaluated at 60 L/min by FSI and at 60 and 90 L/min by NGI (Fig. 10.34d).

It was postulated that the difference in internal volume between the FSI and NGI could cause differences in the pressure drop profile experienced by the product, by varying the characteristics of the time-dependent flow which passes through the impactor when the flow is initiated at the controller. The internal volume of the FSI (estimated to be approx. 960 mL) is substantially smaller than that of the NGI which is close to 1,940 mL, when the pre-separator is included [41].

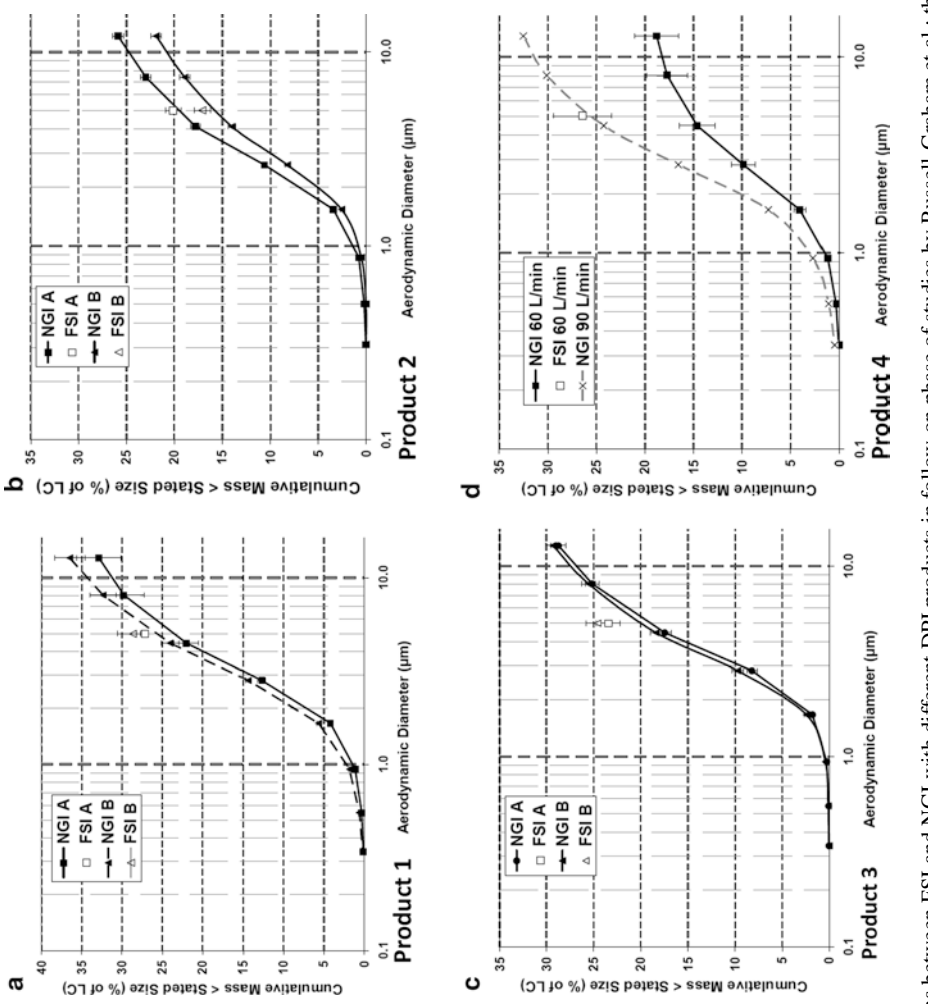

Fig. 10.34 Comparisons between FSI and NGI with different DPI products in follow-on phase of studies by Russell-Graham et al.; the terms A and B in the legends for each plot refer to different (undisclosed) dosage strengths of API (*From* [40]—*courtesy of D. Russell-Graham*)

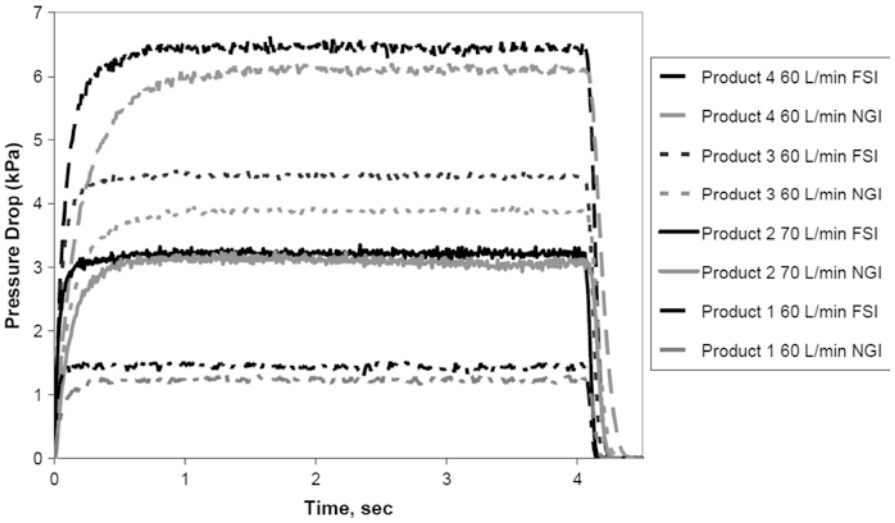

Fig. 10.35 Pressure drop-elapsed time profiles for DPI combinations studied by Russell-Graham et al. (*From* [40]—*courtesy of D. Russell-Graham*)

Their start-up kinetics for each DPI, shown by the time-dependent variation in pressure drop at the mouthpiece for each device-impactor combination (Fig. 10.35), show that the set flow (as measured via pressure drop) is not experienced instantaneously by the product and that the pressure drop profile varied depending on both the device resistance and choice of abbreviated or full-resolution impactor.

The plateau (equilibrium) pressure drop attained, which would be expected to depend on the device resistance, was also observed to differ between the two measurement apparatuses, particularly for Product 3. This was an unexpected observation, but was not thought to be large enough to account for the differences in FPF observed, particularly for Products 1–3 which are not known to be highly flow dependent. An alternative explanation provided by this group involved the observation that the initial acceleration of the pressure drop experienced by each DPI product varied substantially comparing abbreviated with full-resolution apparatus (Fig. 10.36).

In the initial 0.1–0.2 s period, which may be critical for the de-agglomeration of the powder to generate the fine particle fraction delivered from the DPI, the pressure drop measured with the FSI was almost double that measured with the NGI. This effect appeared most pronounced for the product with the highest device resistance (Product 4) which was, perhaps coincidentally, the most flow dependent of the group of devices. This work lends support to the hypothesis that the different internal volume of the FSI may be significant in considering its comparability to the NGI for the testing of DPI products, but further work, including the introduction of additional extra-impactor volume to the FSI apparatus, needs to be done to provide confirmatory data.

More recently, Pantelides et al. have reported further assessments of pressure drop-elapsed time profiles for the FSI, exploring the influence of dead space, systematically increasing the internal volume of the FSI in 500 mL steps by the addition of glass vessels of varying volume and shape configurations (Fig. 10.37), in

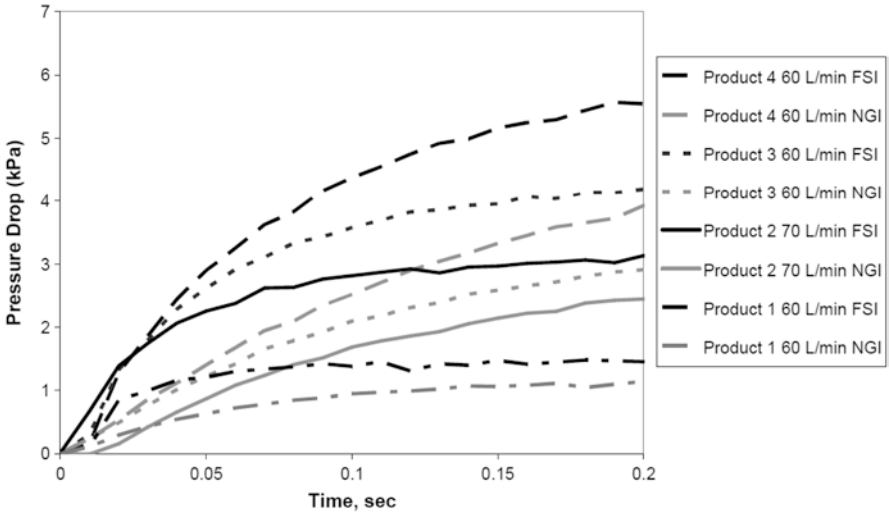

Fig. 10.36 Expanded pressure drop time profiles at the start of measurement for DPI combinations studied by Russell-Graham et al. (*From* [40]—*courtesy of D. Russell-Graham*)

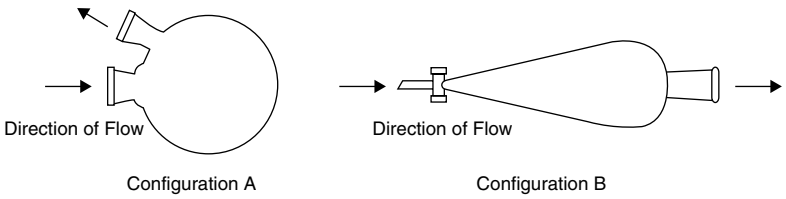

Fig. 10.37 Dead volume configurations used by Pantelides et al.: (A) rapid expansion of flow and (B) more gradual expansion of flow (*From* [42]—*used with permission*)

order to simulate rapid expansion of flow (configuration A) and more gradual expansion (configuration B) [42]. These vessels were located between the FSI and switching valve (Fig. 10.38).

Additionally, the FSI was tested locating a standard NGI pre-separator prior to the modified fine-cut pre-separator stage. Pressure drop profiles were recorded via a pressure tap at the DPI mouthpiece using an inhalation profile recorder similar to the method described by Burnell et al. [43].

The base of the coarse particle collector of the FSI was coated with silicone oil to mitigate particle bounce and re-entrainment as described previously for the work performed with the FSI by this group. The pressure drop profiles for the NGI, FSI, and modified FSI configurations are shown in Fig. 10.39.

The flow initiation portions are superficially similar to those illustrated in Fig. 10.35, taken from the previous study by this Pfizer (UK) group. The new data showed a consistent trend of slowed pressure ramp (acceleration) rate with increasing impactor dead volume in the order FSI (1,045 mL with USP/Ph. Eur. induction port), FSI +500 mL Configuration A, NGI (2,025 mL with pre-separator and USP/

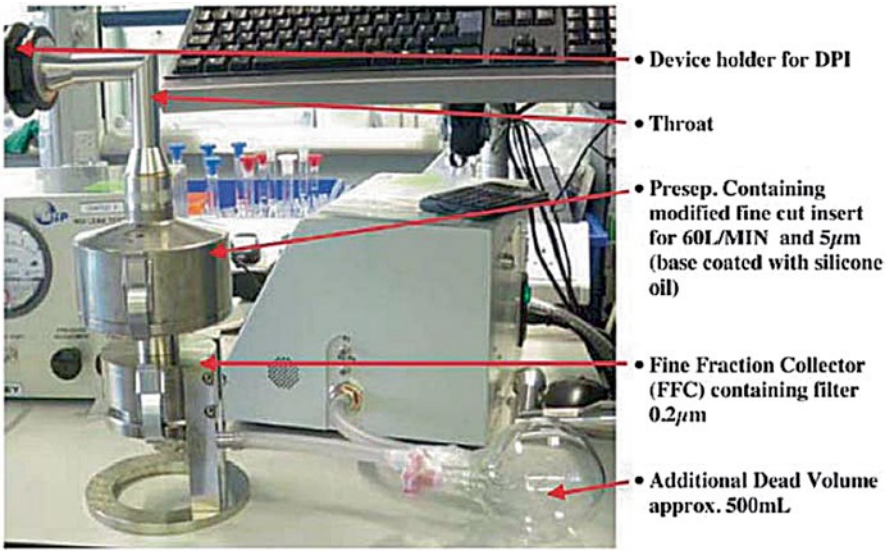

Fig. 10.38 Experimental set-up for the FSI with 500 mL additional dead volume Configuration A investigated by Pantelides et al. (*From* [42]—*used with permission*)

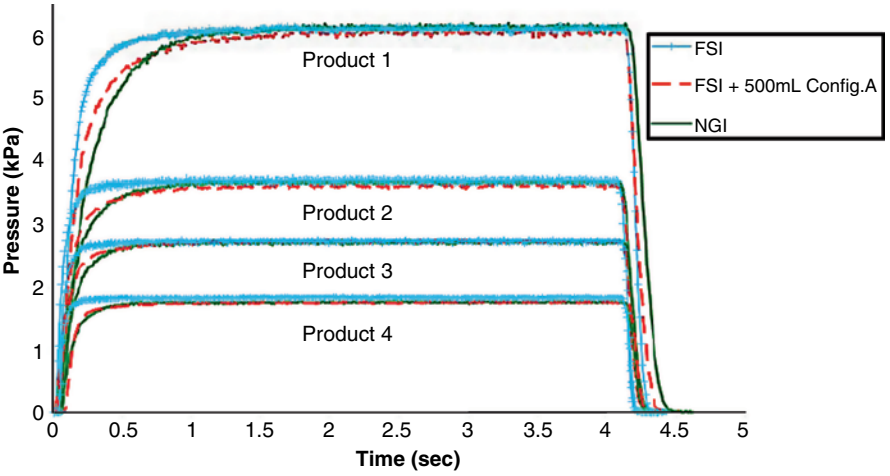

Fig. 10.39 Pressure drop-elapsed time profiles at a nominal flow rate of 60 L/min for DPI products 1–4 (*From* [42]—*used with permission*)

Ph. Eur. induction port [41]) with all of the DPIs. Pressure ramp rate is related to the volume of air which is removed from the impactor before peak pressure drop is attained during the stable flow rate-time portion of the measurement. Importantly, changing the configuration, shape, and size of the extra dead volume added to the FSI made a clear difference to the pressure ramp rate, as illustrated with a series of measurements made with DPI product 1 (Fig. 10.40). Thus Configuration B, that

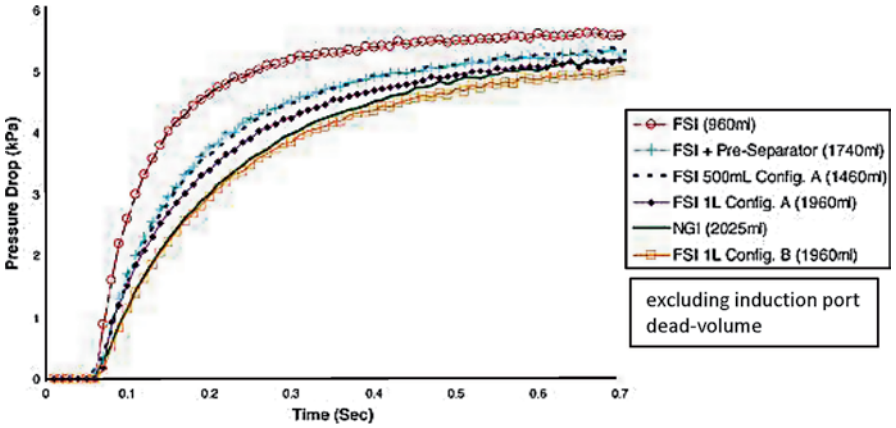

Fig. 10.40 Pressure drop profiles at a nominal flow rate of 60 L/min for DPI product 1 evaluated by Pantelides et al. (*From* [42]—*used with permission*)

allowed a gradual flow expansion on start-up created a FSI-generated pressure drop profile that closely matched that of the NGI. In contrast, when Configuration A that permitted rapid flow expansion was used with the same 1 L volume, the FSI-generated pressure drop profile was observably steeper, reflecting an increased pressure ramp rate, but not as steep as that for the FSI without any added dead volume.

This study showed that if the FSI is equipped with a standard NGI pre-separator (780 mL [41]) before the fine-cut stage, the pressure drop profile was closer to that for the NGI, suggesting that this simple modification to the FSI may be all that is required to achieve comparability for the fluid dynamics for the two systems. However, there was still a significant difference in the pressure drop values (around 1 kPa at about 0.25 s), and this disparity may have been the cause of the significantly higher FPF% shown in Fig. 10.40 for the combined system.

Pantelides et al. completed the investigation by comparing $FPM_{<5.0\mu m}$ per actuation obtained by all the various FSI configurations with reference data (full APSD) obtained for DPI product 1 by the NGI (Fig. 10.41). Increasing the volume of the FSI reduced the magnitude of fine particle mass closer to the value interpolated from the reference APSD. However, dead volume shape and flow resistance of the measurement system [44] likely also had an influence. Thus fine particle mass obtained with the 1-L "Configuration B" added to the FSI was closer to the reference NGI value than the corresponding measure obtained by the FSI when "Configuration A" was used, also adding 1 L to the internal volume of the system. Importantly, such behavior would have been predicted from the relative positions of the pressure drop-elapsed time profiles in Fig. 10.40. These validation measurements added further confirmation that despite the pressure differences mentioned above, the addition of the NGI pre-separator to the FSI improves the correlation between this apparatus and the NGI in terms of fine particle mass.

The small discrepancy in the data shown in Fig. 10.41 between the FSI with pre-separator and NGI was the subject of a follow-on study in which the internal volume of the FSI was augmented to 1,740 mL by the arrangement shown in Fig. 10.42 [45].

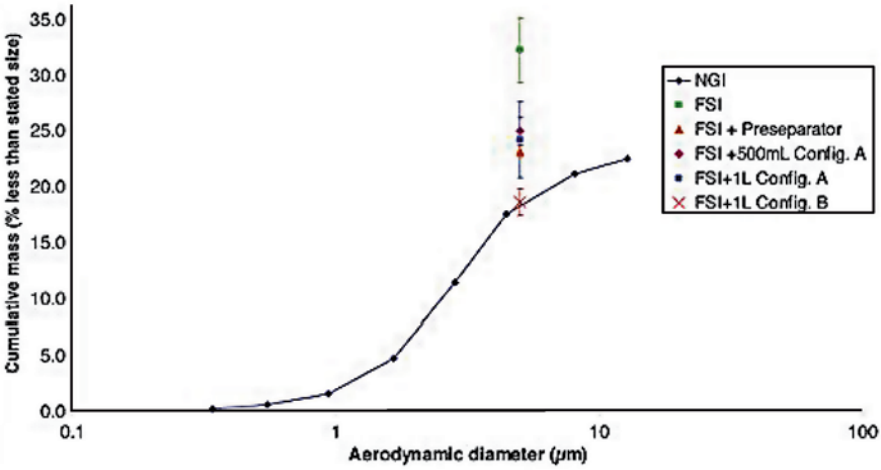

Fig. 10.41 $FPM_{<5.0\mu m}$ for DPI product 1 determined by various FSI configurations in comparison with NGI-measured APSD from measurements of Pantelides et al. (error bars represent ±1 SD for three replicates) (*From* [42]—*used with permission*)

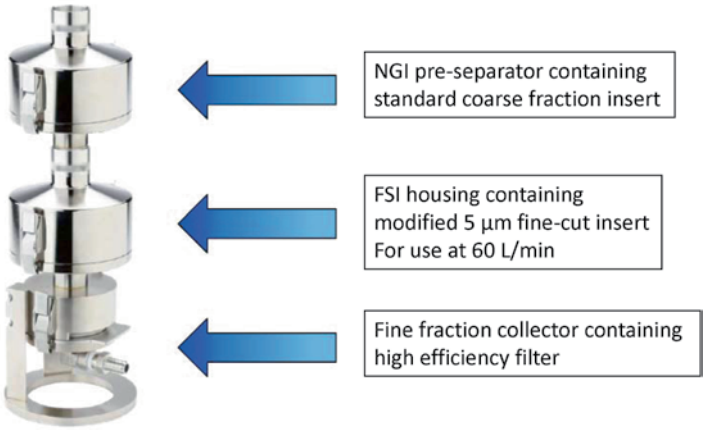

Fig. 10.42 Configuration of FSI for follow-on study by Pantelides et al. matching internal volume more closely to that for the NGI (*From* [45]—*courtesy of D. Russell-Graham*)

The resulting pressure drop-elapsed time profiles for the same DPI product 1 as was evaluated in the previous study are illustrated in Fig. 10.43.

As expected from a comparison of internal dead volumes, the pressure drop-time profile for the volume-enhanced FSI was much closer to that for the NGI. This closer match of dead space resulted in a closer agreement in fine particle mass/actuation between the two systems. Figure 10.44 illustrates the near-to-linear correlation between fine particle mass and air acceleration rate for the FSI, volume-enhanced

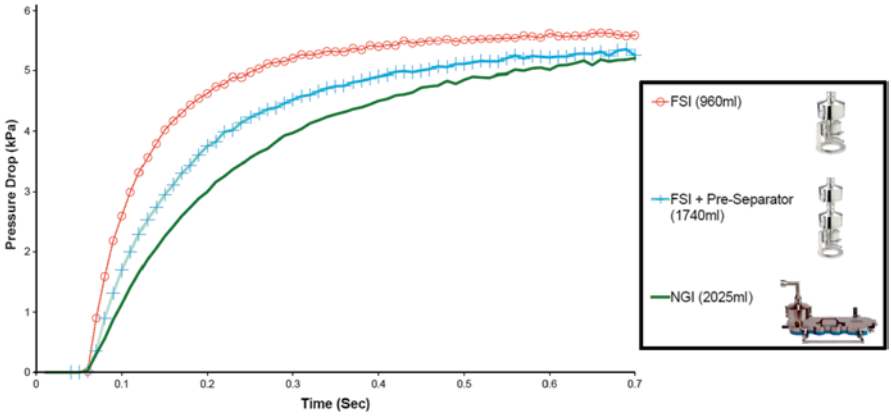

Fig. 10.43 Pressure drop-elapsed time profiles for FSI, FSI with enhanced internal volume and NGI for DPI Product 1 determined by Pantelides et al. at a nominal flow rate of 60 L/min (*From* [45]—*courtesy of D. Russell-Graham*)

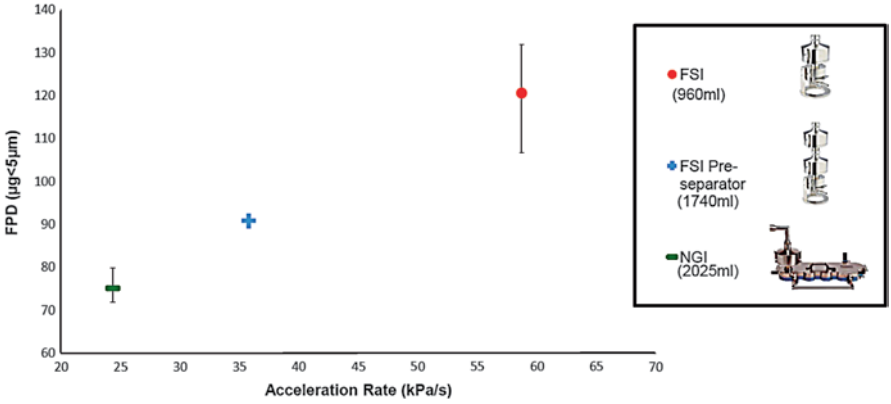

Fig. 10.44 Correlation between $FPM_{<5.0\mu m}$ and air acceleration rate for FSI alone, FSI with enhanced internal volume and NGI for DPI Product 1 determined by Pantelides et al. at a nominal flow rate of 60 L/min (*From* [45]—*courtesy of D. Russell-Graham*)

FSI, and NGI, demonstrating that it is necessary to match internal dead space for the abbreviated CI as closely as practical with that for the corresponding full-resolution impactor for the most accurate work. However, at this early stage in the application of the FSI to the measurement of aerosols from DPIs, it is possible that the effects observed by Pantelides et al. may be DPI type specific. It follows that the addition of dead volume may only be necessary in certain cases following a suitable comparison to a full-resolution impactor.

The basic FSI configuration with 5 µm aerodynamic diameter cut-off between coarse and fine particle fractions has been used by Daniels and Hamilton as part of

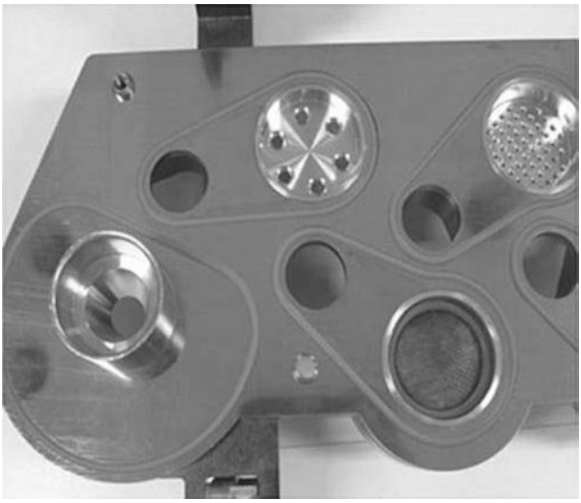

Fig. 10.45 Reduced NGI GSK configuration (*From* [46]—*used with permission*)

a comparison between this abbreviated impactor system and that produced by reducing the NGI (rNGI) to an abbreviated system [46].

This modification was undertaken by eliminating collection stages in the NGI so that following the inlet, the coarse-fine size separation took place at the stage 2 location as normal. However, the filter collection stage containing a bespoke filter was relocated to a position directly above stage 3 (Fig. 10.45), and the remaining stages of the NGI were not used (see Sect. 10.7). API was recovered by rinsing Stages 1 and 2 together (representing the *LPM*) and separately from the recovery of API from the Stage 3 filter (representing the *SPM*, i.e., the fine particle mass <4.46 μm aerodynamic diameter).

A DPI simultaneously delivering two components with different *MMAD* values was used for this study and was tested at a nominal flow rate of 60 L/min with a 4-s "inhalation" time. The FSI was operated with a 5 μm insert. All three systems incorporated the same Copley vacuum pump with TPK flow controller. Similar to the Pfizer group studies, a multichannel Inhalation Profile Recorder (GSK) was used to record the pressure drop-elapsed time profiles via the connection of a pressure transducer to a pressure tap located in the throat of the apparatus-on-test.

Values of *SPM* (here equivalent to $FPM_{<4.51\mu m}$) and *LPM* (equivalent to $FPM_{>4.51\mu m}$ ex NGI and rNGI), each expressed as a percentage of the label-claim dose, from the systems are summarized in Fig. 10.46. SPM for the FSI was observed to be between 5% and 10% greater than the equivalent values obtained when either the standard or reduced NGI systems were used. As expected, the converse was observed for the $CPM_{>5.0\mu m}$.

The pressure drop-elapsed time profiles for the three configurations (Fig. 10.47) were almost identical for both NGI and rNGI, as might be anticipated based on their similar internal dead volumes. However, the air acceleration rate during start-up of flow with the FSI was noticeably faster than for the other systems. Daniels and

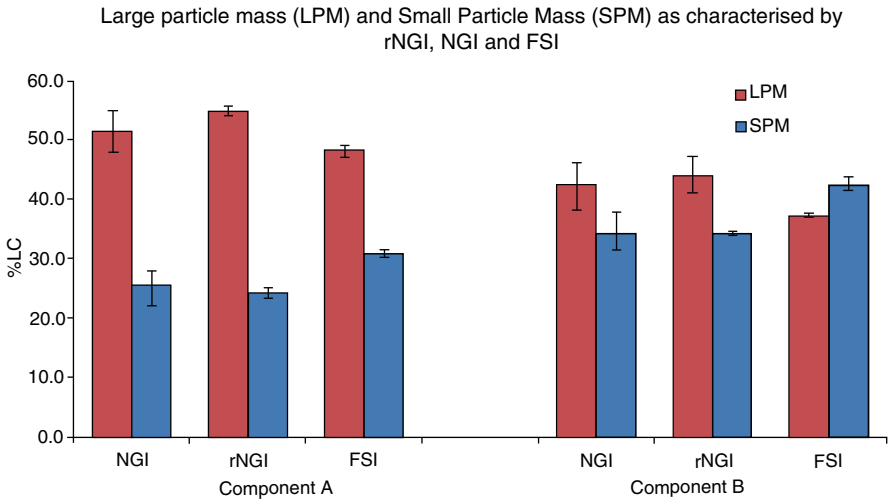

Fig. 10.46 *SPM* (equivalent to $FPM_{<5.0\mu m}$) and *LPM* (equivalent to $FPM_{>5.0\mu m}$) determined for a DPI simultaneously delivering two components with different *MMAD* values evaluated by Daniels and Hamilton at a nominal flow rate of 60 L/min (*From* [46]—*used with permission*)

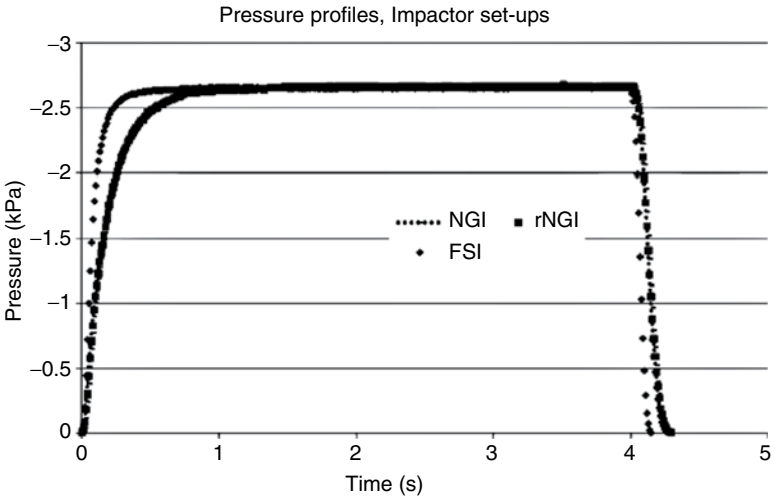

Fig. 10.47 Pressure drop-elapsed time profiles for a DPI simultaneously delivering two components with different *MMAD* values evaluated by Daniels and Hamilton at a nominal flow rate of 60 L/min (*From* [46]—*used with permission*)

Hamilton made the important observation that these differences are likely to be significant in determining the efficiency of the size-fractionation process; and therefore, the ratio of small (fine) to large (coarse) particle mass, because they occur during the critical period of the flow-time profile when powder aerosolization, is

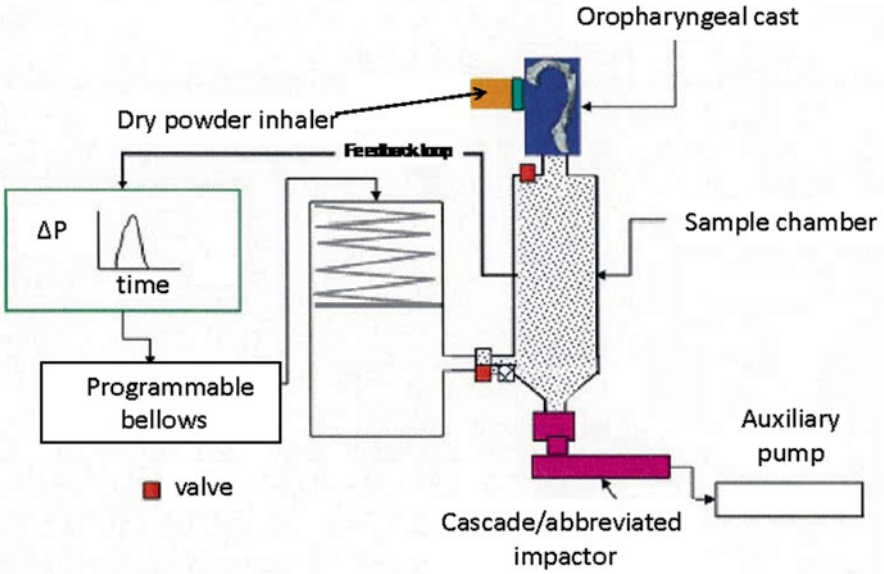

Fig. 10.48 Electronic Lung™ (eLung) set-up for DPI testing by Daniels and Hamilton (*From* [47]—*used with permission*)

most likely to be occurring. This group also noted that the testing time to perform an rNGI measurement and analysis sequence was approximately 2–3 min longer than that to perform similar operations with the FSI.

To confirm the important observations described earlier, in a further study [47], Daniels and Hamilton investigated the significance of the difference in the ramp-up phase of the profiles through replication of two patient representative (asthmatic and COPD) Inhalation profiles using the Electronic Lung™ (eLung) (Fig. 10.48).

In this work, they sampled a proprietary DPI simultaneously delivering two components A and B (Fig. 10.49) having different *MMAD* values, enabling discrimination on the basis of *LPM/SPM* ratio with the boundary still fixed at 5.0 μm. Values of *SPM* and *LPM* for either component (Fig. 10.49) were found to be comparable between the FSI and full-resolution NGI (note their rNGI was not included in this comparison).

This outcome was believed to be a result of eliminating any potential for the flow into the cascade impactor (abbreviated or full resolution) to influence the ramp-up profile of the DPI and therefore its dose emission characteristics. Separation of the flow rate profile controlling dose emission to that of dose characterization confirmed that the data previously reported by this group [46] had arisen as the result of the difference in ramp-up kinetics between the FSI and NGI.

Both the Pfizer and the initial GSK studies demonstrated the importance of matching the internal dead volume of an abbreviated CI with that of the full-resolution CI reference technique for the most accurate results when used in DPI performance evaluations.

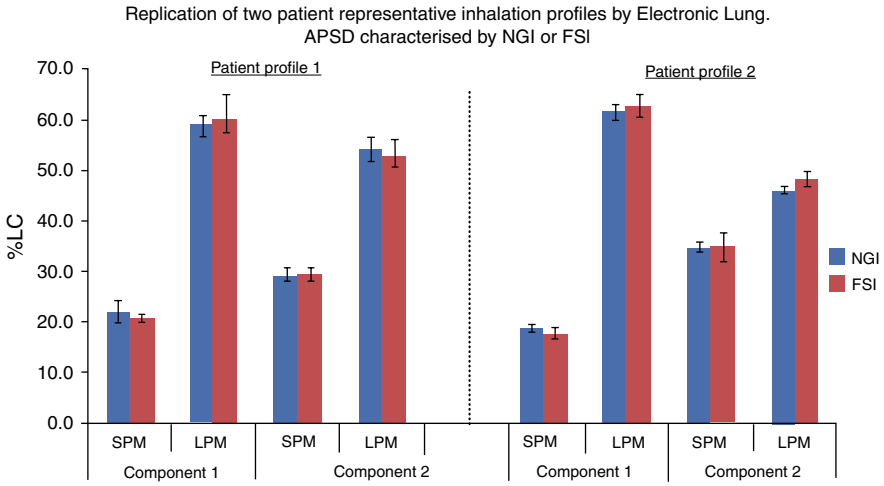

Fig. 10.49 Comparison of NGI and FSI data post replication of human patient profiles by eLung (*From* [47])

Aptar Pharma (Le Vaudreuil, France) also recently reported feasibility studies for the FSI detailing its use for the measurement of another DPI (Prohaler™), featuring their proprietary OBIC™ (open, breathe-in, close) technology [48]. The objectives of their study were to look at several aspects of impaction testing comprising:

1. The performance of the FSI versus the NGI
2. The effect of coating the collection surface of the insert in the FSI
3. The comparison of emitted dose data from the FSI versus a dose unit sampling apparatus (DUSA)—standard equipment recommended by the regulators for the measurement of delivered dose uniformity
4. A comparison of testing parameters for the NGI and FSI
5. Estimation of time and cost advantages of FSI testing versus NGI testing

Comparative tests were carried out at a flow rate of 35 L/min with a 2 L sample volume using the FSI equipped with a 5 µm stage cut-off and an NGI, with three actuations of the device in each case. With three actuations of the DPI the FSI determined slightly higher values of both total emitted dose (equivalent to *TEM*) and fine particle dose <5 µm (equivalent to $FPM_{<5\mu m}$) than did the NGI (Fig. 10.50).

Mean values of *TEM* and $FPM_{<5.0\mu m}$ with a single actuation of the DPI were both around 10% (*TEM*) to 30% ($FPM_{<5.0\mu m}$) higher by FSI compared with the corresponding data from the NGI. However, the 3-dose data for the FSI were in much closer agreement with the corresponding benchmark NGI metrics, being only 1% (*TEM*) and 15% ($FPM_{<5.0\mu m}$) higher than the corresponding NGI values. It was hypothesized that the observed differences were due to increased particle bounce and entrainment when single doses were measured, but collection surface coating

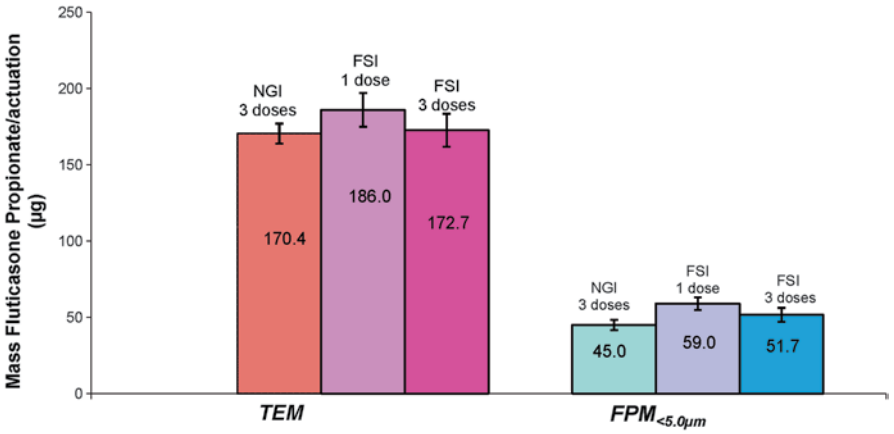

Fig. 10.50 Comparison between NGI and FSI for measures of *TEM* and $FPM_{<5.0\mu m}$ reported by Després-Gnis and Williams (error bars correspond to ±1 SD) (*From* [48]—*courtesy of G. Williams*)

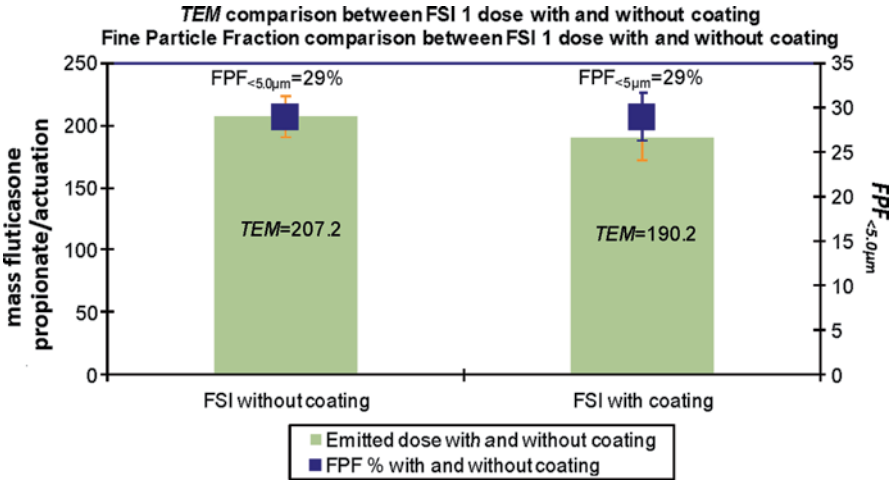

Fig. 10.51 FSI performance with and without stage coating reported by Després-Gnis and Williams (error bars correspond to ±1 SD) (*From* [48]—*courtesy of G. Williams*)

proved unnecessary with a single actuation of the DPI, based on comparative tests showing no statistical difference between *TEM* and $FPF_{<5.0\mu m}$ measured with and without the application of a standard stage coating prepared from a solution of 1% v/v glycerol in ethanol (Fig. 10.51).

Nevertheless, even though these differences were not statistically significant, mean *TEM* with coating (207.2 µg/actuation) was numerically greater than the corresponding value uncoated (190.2 µg/actuation) suggesting that further examination of the stage coating methodology might still be beneficial, possibly resorting

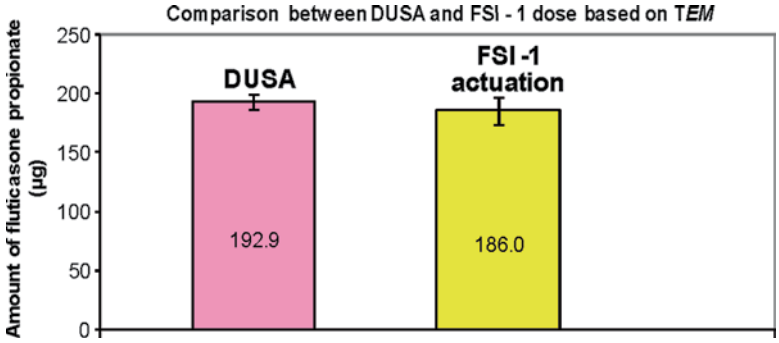

Fig. 10.52 Comparison between FSI and DUSA reported by Després-Gnis and Williams (single dose data) (*From* [48]—*courtesy of G. Williams*)

Table 10.14 Comparison between FSI and NGI in terms of savings in time per measurement, HPLC-based analysis time, and API recovery solvent use (*From* [48]—*courtesy of G. Williams*)

Apparatus	Test duration (min)	API assay duration (min)	Solvent quantity (mL)
NGI	60	140	300
FSI	25	63	200
Gain (%)	**58**	**55**	**33**

to a filter saturated with coating medium, as was done in the follow-on IPAC-RS precision study to eliminate entirely bias from this source [27].

In a follow-on study, a dose uniformity sampling apparatus (DUSA, Copley Scientific Ltd., Nottingham, UK) sampling at 35 L/min with a 4 kPa pressure differential and inhalation volume of 2 L was used to compare with single dose FSI measurements for the same DPI. There was close agreement between the single actuation *TEM* results and those measured with the DUSA (Fig. 10.52).

Taken together, these results suggest that using the FSI with just a single actuation is a suitable approach for *TEM* and $FPM_{<5.0\mu m}$ measurement in support of screening during development work, provided precautions are taken to mitigate bias due to particle bounce and re-entrainment by coating the collection surface of the insert.

The findings of Després-Gnis and Williams support the outcome reported by Stobbs et al. [38], in terms of time savings, suggesting gains in excess of 50% may be possible in both test duration and HPLC analysis time. Reductions in solvent usage were also quantified at 33%, important in terms of the increasing attention being paid to so-called green chemistry initiatives (Table 10.14).

Finally, additional data relating specifically to the test conditions they employed, demonstrated that the sealing integrity of the FSI is comparable to that of the NGI, while the overall pressure drop was considerably lower (Table 10.15). Interstage wall losses were also reduced with the FSI, possibly as the result of needing fewer inhaler actuations with this system. It is important to note, however, that the lower pressure drop of the FSI merits careful consideration in the context of achieving

Table 10.15 Sealing integrity, apparatus air resistance and interstage API loss for the FSI compared with the NGI (*From* [48]—*courtesy of G. Williams*)

(a) Sealing integrity ($\Delta_{\Delta P}$, kPa)

FSI ($n=5$ replicates)		NGI ($n=4$ replicates)	
Mean	0.3	Mean	0.4
SD	0.07	SD	0.04

(b) Equipment air resistance ($cm_{H_2O}^{1/2}\,L/min$)[a]

FSI ($n=3$ replicates)		NGI ($n=3$ replicates)	
Mean	0.12	Mean	0.19
SD	0.00	SD	0.00

(c) Interstage API loss [wall losses] (μg)

FSI: 1 actuation ($n=3$ replicates)		NGI: 3 actuations ($n=3$ replicates)	
Mean	0.6	Mean	1.7
SD	0.33	SD	1.03

n number of replicates

[a]Sealing integrity verified prior to use

comparable start-up kinetics (pressure drop versus elapsed time) for DPI testing in general, reinforcing the advice that such considerations should be a key part of AIM-based method development with this class of OIP.

Rogueda et al., from Novartis Pharma, also presented a comparison of an FSI with insert providing a cut point of 5 μm aerodynamic diameter at 90 L/min with the NGI as full-resolution reference impactor [49]. Their data for various low resistance DPI products used with lactose-blended powders also confirmed that fine particle fraction determined by the FSI could be up to 20% higher $FPF_{<5.0\mu m}$ than equivalent measures using the NGI (see Fig. 10.53 for DPI "system" C) when the pre-separator of both devices were used without coating the interior surfaces with an adhesive agent (i.e., as it would normally be used with the NGI).

Coating the bottom plate of the pre-separator with surfactant in order to reduce particle bounce resulted in a discernible decrease in $FPF_{<5.0\mu m}$ with DPI product "C" (Fig. 10.53), with this value almost comparable to that obtained by the reference NGI (Fig. 10.54). However, the FSI-based data for other products "A" and "B" evaluated were still marginally lower and higher, respectively, than corresponding values determined from the NGI (Fig. 10.54). Nevertheless, these differences compared with equivalent values using the NGI were less than the 10% limit that they set as their acceptance criterion for these measurements.

This group also reported between 35% and 42% savings in time using the FSI compared with the NGI, based on timed measurements with other similar DPIs, corresponding to between 22% and 37% time saved on the experimental work (HPLC analysis excluded).

Confirmatory evidence of the value of the FSI for measuring particles delivered by pMDIs and nebulizers was also provided in early 2009 by Sheng et al. from MAP Pharmaceuticals Inc. (California, USA) [50]. In the first part of their study, two

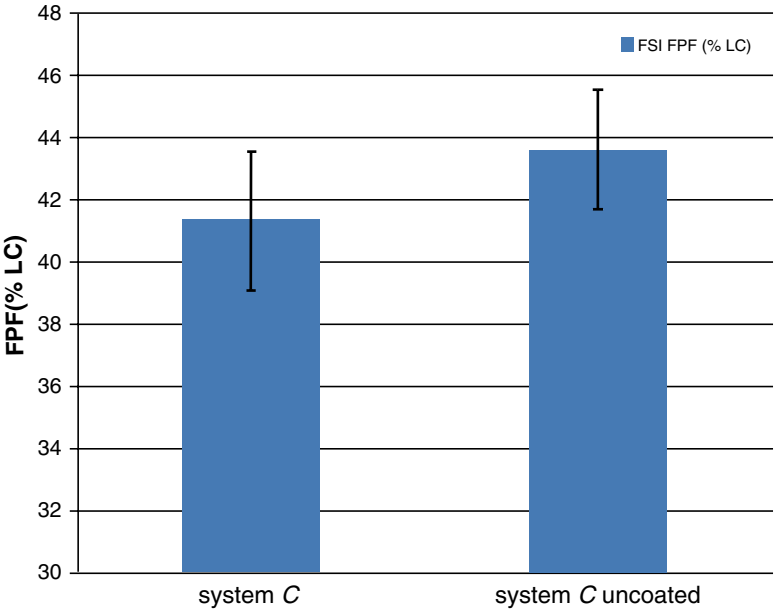

Fig. 10.53 $FPF_{<5.0\mu m}$ measured by FSI with uncoated and surfactant-coated pre-separator bottom plate for DPI product (system) "C"; error bars represent ±1 SD (*From* [49]—*courtesy of P. Rogueda*)

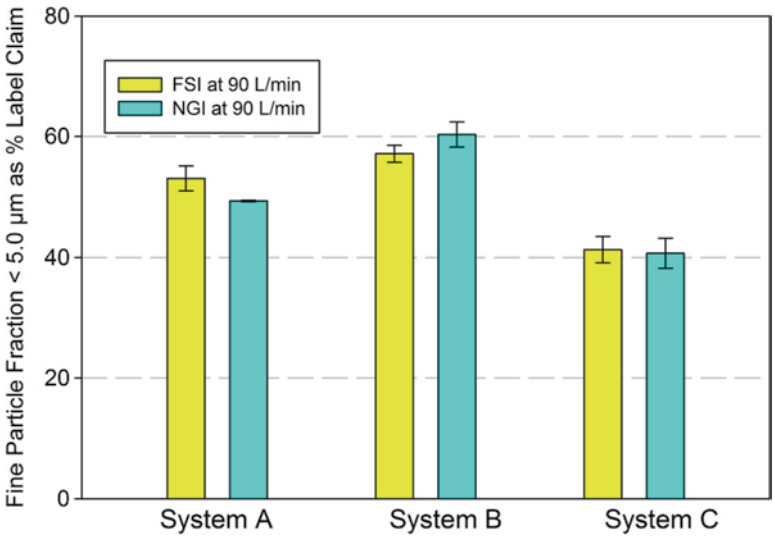

Fig. 10.54 Measurement time comparison between FSI and NGI with coated FSI pre-separator (90 L/min flow rate, 4 L total volume, $n=5$ replicate measurements by one operator); error bars represent ±1 SD (*From* [49]—*courtesy of P. Rogueda*)

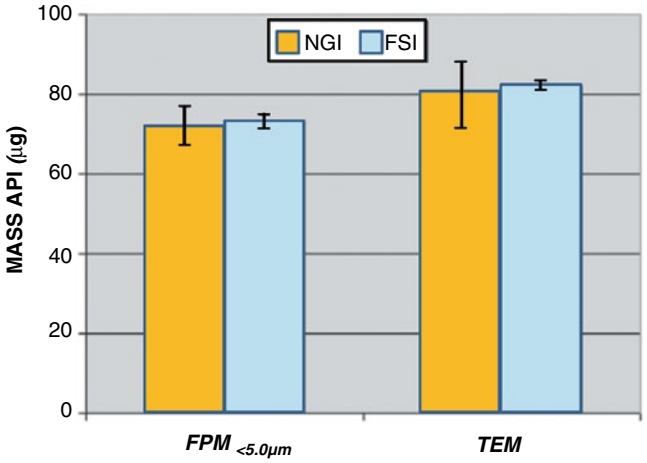

Fig. 10.55 Comparison of MDI formulation using NGI and FSI reported by Sheng et al. based on $FPM_{<5.0\mu m}$ and *TEM*; error bars represent ±1 SD (*From* [50]—*used with permission*)

proprietary budesonide HFA suspension pMDI formulations were measured at a flow rate of 30 L/min, using the FSI, also with 5 µm cut-off for *FPM*, using the NGI as the reference apparatus. The results (Fig. 10.55—one product) were compared in terms of fine particle dose ($FPM_{<5.0\mu m}$) and total emitted mass (*TEM*) using a two-side *t*-test on the basis of the null hypothesis $FPM_{5.0\mu m\text{-}NGI} = FPM_{5.0\mu m\text{-}FSI}$ and $TEM_{NGI} = TEM_{FSI}$. No statistical difference was observable between these two sets of data ($p > 0.05$).

In the second part of their investigation, four proprietary budesonide liquid suspension formulations (A, B, C, and D) containing particles of different morphologies and concentrations were nebulized with an Aeroneb Go® (Aerogen Ltd., Ireland) vibrating membrane system ($n = 3$ replicates at each condition). The aerosol passed through an Aeroneb Go®/NGI induction port mouthpiece adaptor prior to reaching the impactor.

A flow rate of 15 L/min has been recommended for nebulizer testing [51]. However, since at that time, there was no commercially available option to operate the FSI at flow rates <30 L/min (*but see method adopted by Tservistas et al.* [52] *later in this section*), Sheng et al. operated their FSI at this lower limit in this investigation. The FSI yielded similar results for $FPM_{<5.0\mu m}$ and *TEM* to those of NGI for all formulations (Fig. 10.56). Importantly, the values of *TEM* encompassed a wide dosage range of ca. 80 µg, but as with the pMDI-aerosol measurements, the difference between the two measurement techniques for each formulation was not statistically significant for each formulation ($p > 0.05$).

In 2010, Sheng and Watanabe extended the original work to evaluate the FSI as a tool for the rapid screening of pMDI-based formulations in early-stage OIP development [53]. They confirmed agreement ($p > 0.05$) between measures of $FPM_{<5.0\mu m}$ determined by both FSI and NGI during the screening of pMDI formulations (Fig. 10.57).

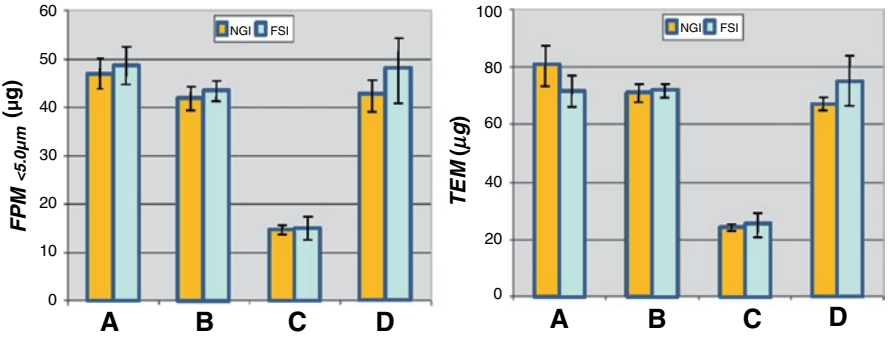

Fig. 10.56 Comparison of four nebulizer-generated budesonide aerosols based on $FPM_{<5.0\mu m}$ and *TEM* reported by Sheng et al. using NGI and FSI systems; error bars represent ±1 SD (*From* [50]—*used with permission*)

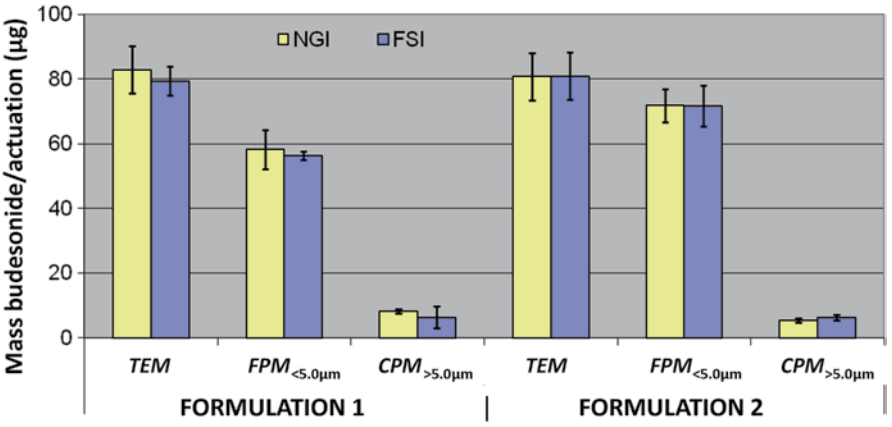

Fig. 10.57 Comparison of *TEM*, $FPM_{<5.0\mu m}$ and $CPM_{>5.0\mu m}$ from two different pMDI formulations measured by Sheng and Watanabe for NGI and FSI operated at 30 L/min; error bars represent ±1 SD ($n=3$ replicates for each impactor) (*From* [53]—*courtesy of G. Sheng*)

In several instances, they also noted slightly lower variability in measurements by their FSI, although further replicate experiments would be needed to confirm this finding.

Interestingly, in a comparison of their pMDI data measured at 30, 45, and 65 L/min [private communication post Workshop], Sheng and Watanabe also included the ACI as a reference impactor. Values of $FPF_{<5.0\mu m}$ by FSI were generally higher than their equivalent from the ACI, with the greatest divergence at the highest flow rate (Fig. 10.58).

In the second part of their study, they compared $FPF_{<5.0\mu m}$ for eight preparations for nebulization containing suspended submicron and super-micron-sized budesonide particles having different morphologies, formulated with and without

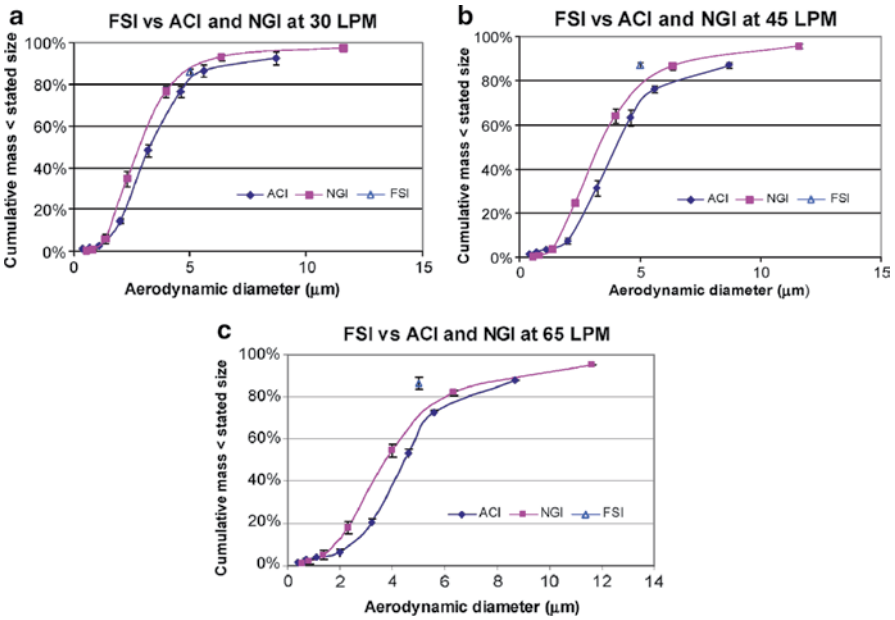

Fig. 10.58 Comparisons of $FPF_{<5.0\mu m}$ reported by Sheng and Watanabe from a pMDI-produced aerosol measured by FSI, NGI, and ACI at different flow rates; error bars represent ±1 SD. (**a**) 30 L/min. (**b**) 45 L/min. (**c**) 65 L/min (*From* [53]—*courtesy of G. Sheng*)

Table 10.16 Nebulizer formulations tested in the study of Sheng and Watanabe; "+" high, "0" medium, "−" low value relative to series average (*From* [53]—*courtesy of G. Sheng*)

Formulation code	Particle morphology based on aspect ratio (−, +)	Surfactant type (0, I, II)/ concentration (+, −)	API concentration (−, 0, +)	Size of particles in formulation
A	−	I/+	+	Submicron
B	−	I/+	+	Submicron
C	−	I/− and II/−	−	Submicron
D	−	I/0 and II/−	0	Submicron
E	−	I/+	+	Submicron
F	+	I/+	+	Micron
G	−	I/+	+	Micron
H	−	I/+	+	Micron
I	+	I/+	+	Micron

surfactant (Table 10.16). Their results (Fig. 10.59), obtained at higher flow rates than recommended (15 L/min) for evaluating this class of inhaler (28–30 L/min), nevertheless demonstrated an excellent correlation ($r^2 \sim 0.97$) between these abbreviated and full-resolution apparatuses.

Sheng and Watanabe also extended their comparison of the FSI to the evaluation of a vibrating membrane nebulizer (Aeroneb® Go, Aerogen Ltd., Galway, Ireland)

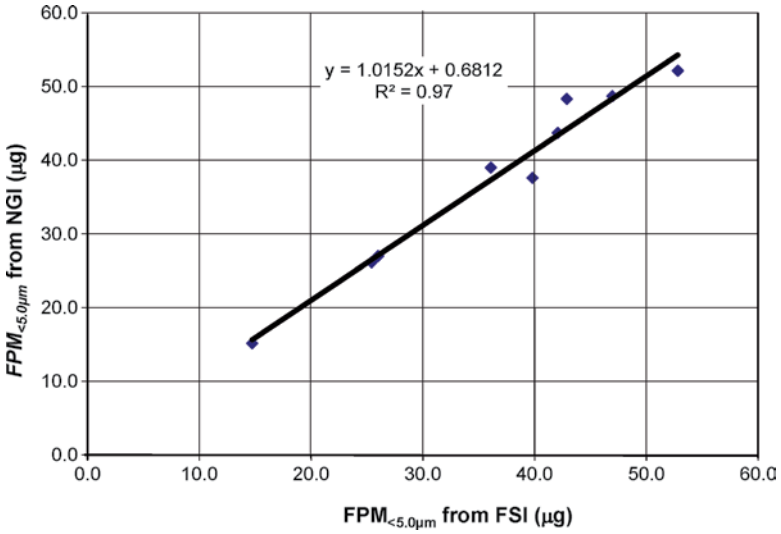

Fig. 10.59 Correlation between $FPM_{<5.0\mu m}$ obtained from NGI and FSI reported by Sheng and Watanabe from 0.5 mL aliquots of different nebulized budesonide preparations (Table 10.16) (*From* [53]—*courtesy of G. Sheng*)

that was operated with a 0.5 mL fill of a proprietary corticosteroid formulation in aqueous suspension for inhalation.

Comparative measurements with an NGI ($n=6$ replicates) and FSI ($n=5$ replicates) undertaken at both 28.3 L/min (Fig. 10.60) and the preferred flow rate of 15 L/min for nebulizer testing (Fig. 10.61) revealed similar values of $FPF_{<5.0\mu m}$, with slightly less variability associated with the FSI data compared with the NGI at the higher flow rate. However, it should be noted that neither the NGI nor the FSI were chilled for this work, as their preliminary studies had shown this precaution to prevent heat transfer-related evaporative loss with the aerosol droplets was not warranted with the Aeroneb® Go system. Furthermore, Dennis et al. had shown in a comparative study with the Aeroneb Go® and a jet nebulizer (MistyMax™, Cardinal Health, USA) that bias in measures of MMAD, GSD, and fine droplet fraction from not chilling the NGI were relatively small (<10% difference between measurements made with this CI at room ambient and chilled to +5 °C) [54]. It is possible, therefore, that NGI chilling may only be needed for the most accurate measurement, perhaps depending upon the formulation concerned [55, 56], and the much lower thermal mass of the FSI is likely to make this precaution even less necessary in routine work.

However, droplet evaporation can be a significant concern when applying the CI measurement technique to the measurement of aerosols produced by jet nebulizers, especially those devices that do not entrain ambient air into the nebulized droplet stream. The considerable heat capacity of the impactor, especially when the NGI is

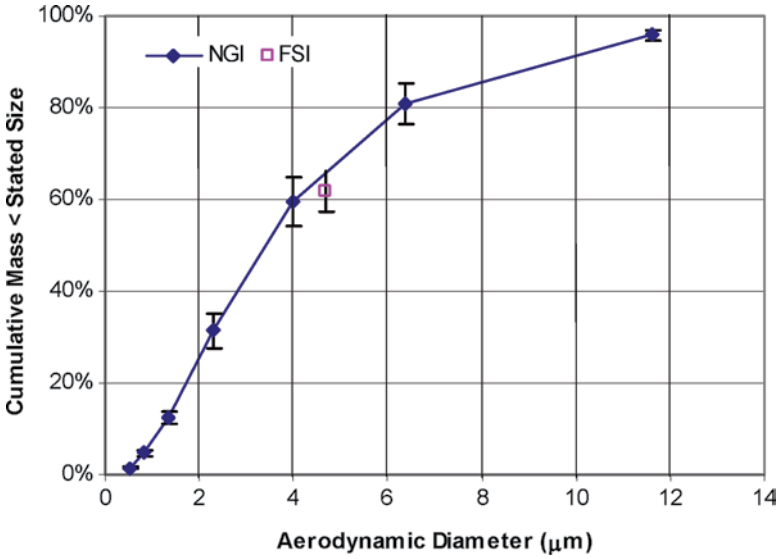

Fig. 10.60 Comparison between FSI and NGI for the assessment of vibrating mesh and jet nebulizer-generated droplets of a 0.5 mL sample of an aqueous suspension product measured at 28.3 L/min by Sheng and Watanabe (*From* [53]—*courtesy of G. Sheng*)

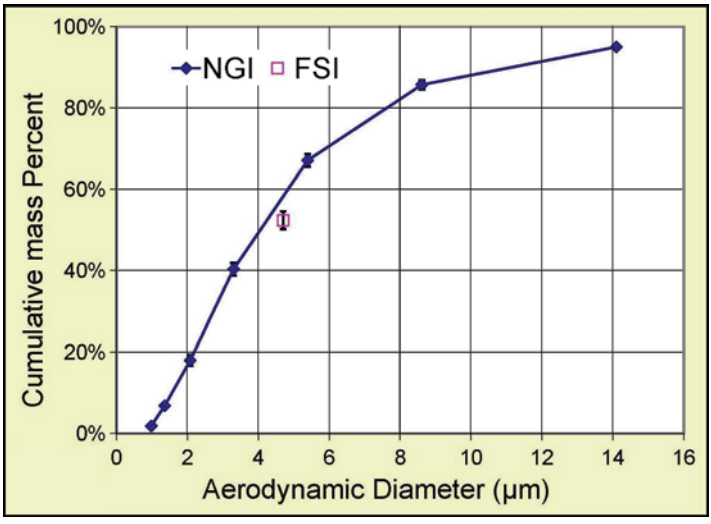

Fig. 10.61 Comparison between FSI and NGI for the assessment of vibrating mesh and jet nebulizer-generated droplets of an aqueous suspension product measured at 15 L/min by Sheng and Watanabe (*From* [53]—*used with permission*)

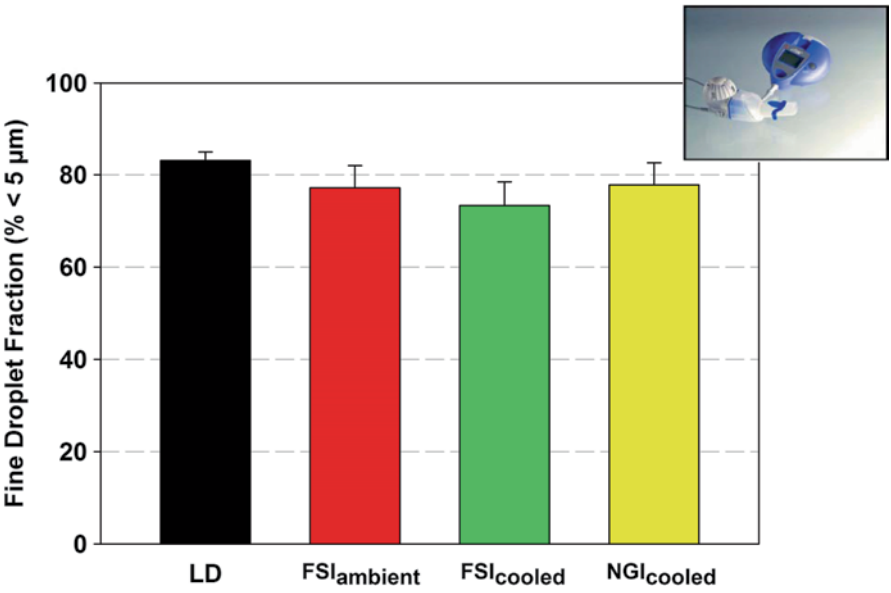

Fig. 10.62 $FPF_{<5.0\mu m}$ (reported as fine droplet fraction, $FDF_{<5.0\mu m}$) by Tservistas et al. for an aqueous aerosol generated by a vibrating membrane nebulizer using FSI, NGI, and laser diffractometry (LD) as measurement methods (*From* [52]—*courtesy of M. Tservistas*)

used, promotes this undesirable effect. The precise mechanism of heat transfer to the aerosol is uncertain; however, in one explanation, water evaporation takes place by heat transfer from the mainly metallic CI as the aerosol passes through the equipment, resulting in undersizing of the formulation [57]. Evaporative changes originating from this cause are routinely avoided by cooling the CI before and/or during measurement [54].

In a feasibility study designed to assess the use of the FSI for nebulizers, Tservistas et al. [52] took a similar approach, comparing fine droplet fraction ($FDF_{<5.0\mu m}$) measured with a cooled FSI (down to 18 °C) from an aqueous formulation delivered by an investigational e-Flow® vibrating mesh nebulizer (PARI GmbH, Starnberg, Germany) with those recorded under ambient conditions at 22 °C (Fig. 10.62). Interestingly, they extended the lower flow rate range of their FSI to 15 L/min by blocking three of the six nozzles on the FSI insert to retain the stage cut-off diameter of 5 µm aerodynamic diameter at 50% of the design flow rate for this AIM apparatus (Fig. 10.63).

Under ambient conditions, the FSI-generated $FDF_{<5.0\mu m}$ values at 15 L/min were substantially equivalent to those produced using a cooled NGI. The cooled FSI produced a lower $FDF_{<5.0\mu m}$, although the difference was relatively small, less than 5 per cent. The highest $FDF_{<5.0\mu m}$ was obtained by laser diffractometry (LD).

These results suggest that the lower thermal capacity of the FSI, a function of its much reduced mass relative to the NGI, is advantageous in terms of accuracy

Fig. 10.63 Modified FSI insert used by Tservistas et al. for nebulizer aerosol measurements at 15 L/min (*From* [52]—*courtesy of M. Tservistas*)

Table 10.17 Comparative times for 6-replicate abbreviated and full-resolution impactor measurements compared with laser diffractometry reported by Tservistas et al. in the context of nebulizer aerosol assessment (*From* [52]—*courtesy of M. Tservistas*)

	Time allocation (h)			
Assessment method	Measurement	API analysis	Data processing	Total
LD	1.5	N/A	1.0	2.5
FSI (cooled)	7.0	6.5	1.0	14.5
FSI (ambient)	5.0	6.5	1.0	12.5
NGI	8.0	18.0	2.0	28.0

associated with nebulizer-generated aqueous droplet size measurements, as the result of less pronounced heat transfer-related evaporative bias.

Comparative data for time savings provided by Tservistas et al. (Table 10.17) add further evidence of approximately 50% gain in productivity with the cooled FSI compared with the NGI.

As might be expected, LD was by far the most rapid technique; however, this measurement method is not directly related to mass of API and is therefore limited to the assessment of solutions, rather than more complex formulations (i.e., suspensions, emulsions, liposomal forms, etc.) that may be encountered with this class of OIP [58].

10.8 Assessing the Performance of AIM Systems Based on the NGI

Since the NGI in its standard design does not have movable stages [14], the development of an abbreviated system based on NGI geometry at first sight seems to be unattractive and possibly a difficult process. However, this CI has a horizontal

configuration that lends itself to semi- or full automation more readily than the vertical stack configuration associated with ACI designs, and the process of abbreviating the full-resolution configuration is not as daunting as might be considered at first sight.

Two distinctly different approaches are feasible; however, there is relatively limited data on either reported thus far in the open literature. The most straightforward method involves the use of deep cups to make certain stages inoperable; particles fail to impact on the collection surface and simply pass to the next stage. In addition, an insert can be fitted to the stage 1 nozzle to reduce jet diameter to give a desirable stage cut point. However, since the internal flow pathway through the NGI is not reduced, the so-called deep-cup approach has the potential drawback that losses to the internal surfaces may increase. Future studies validating this option will therefore need to address this concern.

In the second, more radical approach to the abbreviation of the full-resolution NGI (Fig. 10.64a) first adopted by Svensson and Berg [59], the NGI itself was abbreviated by moving "active" stages followed by the back-up filter so that the flow passed through these components before being returned to the NGI body. Daniels and Hamilton also adopted this arrangement for their reduced NGI (abbreviated to rNGI)-based studies [46], and their data have already been discussed in the previous section in connection with understanding how internal dead space affects start-up flow characteristics in DPI testing with the FSI. Their particular rNGI set-up involved moving the filter collection stage containing a bespoke filter to follow directly before full-resolution NGI stage 3, where separation of fine from coarse subfractions takes place (Fig. 10.45). This change could be made without altering the type of collection cup used or making penetrations through the body of the NGI itself to remove flow from unused stages. Svensson and Berg termed this apparatus the "internal filter" configuration (Fig. 10.64b).

The rNGI approach adopted by Daniels and Hamilton [46] overcomes the need for specialized collection cups, as would be the case if external connections had needed to be made between components to achieve an abbreviated design, as originally proposed by Svensson and Berg in one of their configurations (Fig. 10.64c). Daniels and Hamilton [46] recovered the deposited API by rinsing stages 1 and 2 together (representing the *LPM*) and separately from the recovery of API from the bespoke filter located before stage 3 (representing the *SPM*, i.e., $FPM_{<4.46\mu m}$). The comparative data for their particular DPI obtained with this rNGI configuration compared favorably with measurements by full NGI. However, the comparison of data from either of the two NGI configurations and an FSI was less good (Fig. 10.46). After their follow-up study using the eLung™ to replicate patient inhalation profiles (Fig. 10.48), this relatively poor agreement was attributed to the possibility that the original FSI configuration in its simpler set-up (constant Q of 60 L/min with a 4-s "inhalation" time) may have affected the ramp-up profile of the DPI.

The ability to move the cut size between large and small particle fractions by insertion of the filter stage in different stage positions in the rNGI, so that it is close to the MMAD of the OIP of interest, is a significant advantage for product QC applications. Svensson and Berg evaluated three different stage positions of the filter in

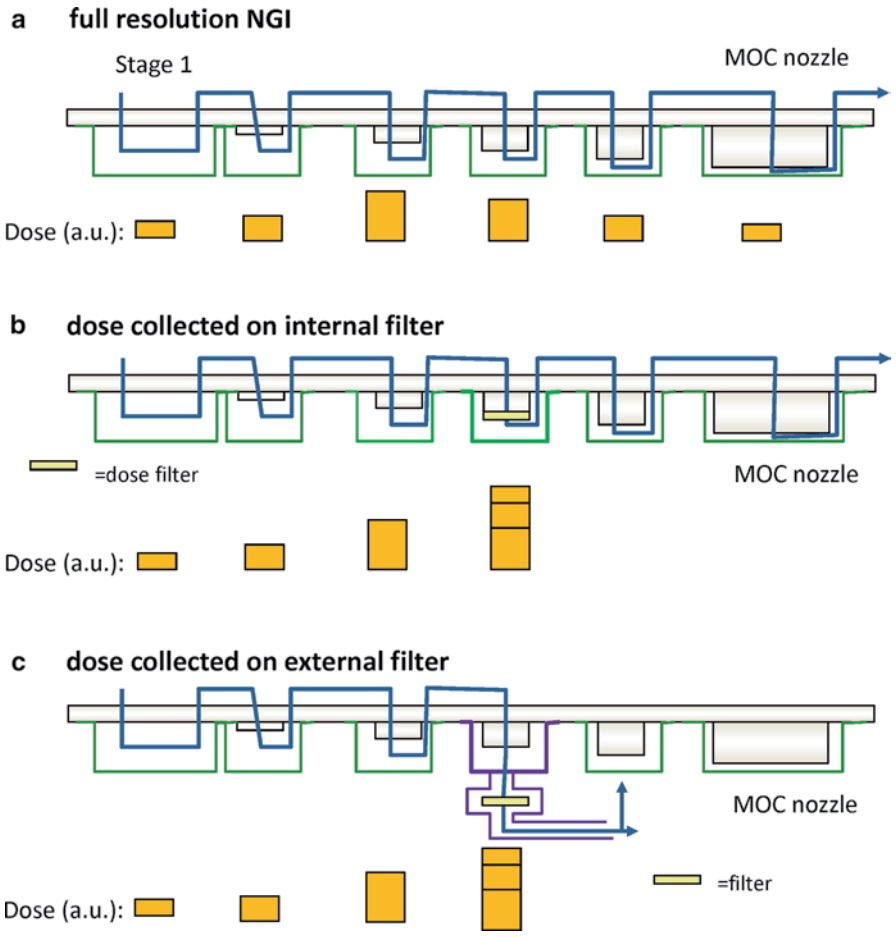

Fig. 10.64 Three concepts developed by Svensson and Berg for creating abbreviated versions of the NGI (rNGI) (*From* [59]—*courtesy of M. Svensson*)

their investigations of the rNGI [59]. Their "internal filter" or "nozzle-filter" design (Fig. 10.64b), already mentioned in connection with the evaluation undertaken by Daniels and Hamilton (Fig. 10.45), was developed and introduced immediately after stage of interest in the seal body to be able to capture the *SPM*. It should be noted that the remaining stages (after the filter) to the micro-orifice collector (MOC) were still present in the seal body during the measurements with this abbreviated configuration. This arrangement guarantees an identical flow-time profile if a filter with sufficiently low air flow resistance is used, which is important in the context of DPI testing.

In the alternative so-called external filter or outlet filter design (Fig. 10.64c), Svensson and Berg reconfigured their rNGI so that flow exiting the abbreviated

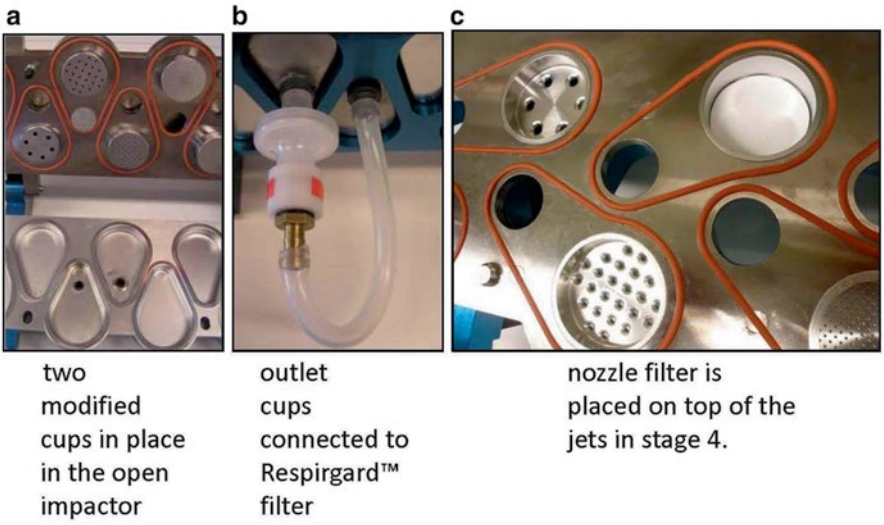

Fig. 10.65 Modified NGI by Svensson and Berg showing "O"-cup option (**a** and **b**) and internal filter option (**c**) for abbreviated testing of OIPs (*From* [59]—*courtesy of M. Svensson*)

section of the apparatus was directed through an externally mounted filter and then redirected into the NGI again after passage through the filter.

Both configurations can also be seen in Fig. 10.65; the modified outlet stage cups (necessary for the external filter approach) are shown in (a), the external and internal filter options are depicted in (b) and (c), respectively.

The main aim of their study was to judge whether these so-called filter methods can be regarded equivalent to the standard impactor method in which all stages are individually analyzed. Therefore, parallel experiments using full NGI set-up were performed and used for equivalence testing versus the proposed filter methods. Three different DPIs with three different formulations and two different pMDI products (CFC and HFA propellant) were used in this study. The comparison of the two methods was performed by comparing a total of 91 mean values from the full NGI and the corresponding filter method (Fig. 10.66).

Every mean value comprised data from either two or three impactor tests (full NGI) and 5–10 filter samples for the filter method, so that in total, around 650 individual tests were conducted. Except for the pMDI, each DPI were tested at two different flows corresponding to 2 and 4 kPa differential pressure over the device, spanning a flow range from 40 to 77 L/min. A strong linear relationship was obtained between the filter measure and the full NGI measures of *FPM* obtained at the same selected size limits. The correlation coefficients (r^2) were >0.95 for nozzle filter and >0.98 for the outlet cup method. The slopes for the fitted lines were close to the line of identity, varying from 0.89 to 1.03. However, the authors noted that the linear relationship, determined from the slope and associated r^2 value, was weaker for

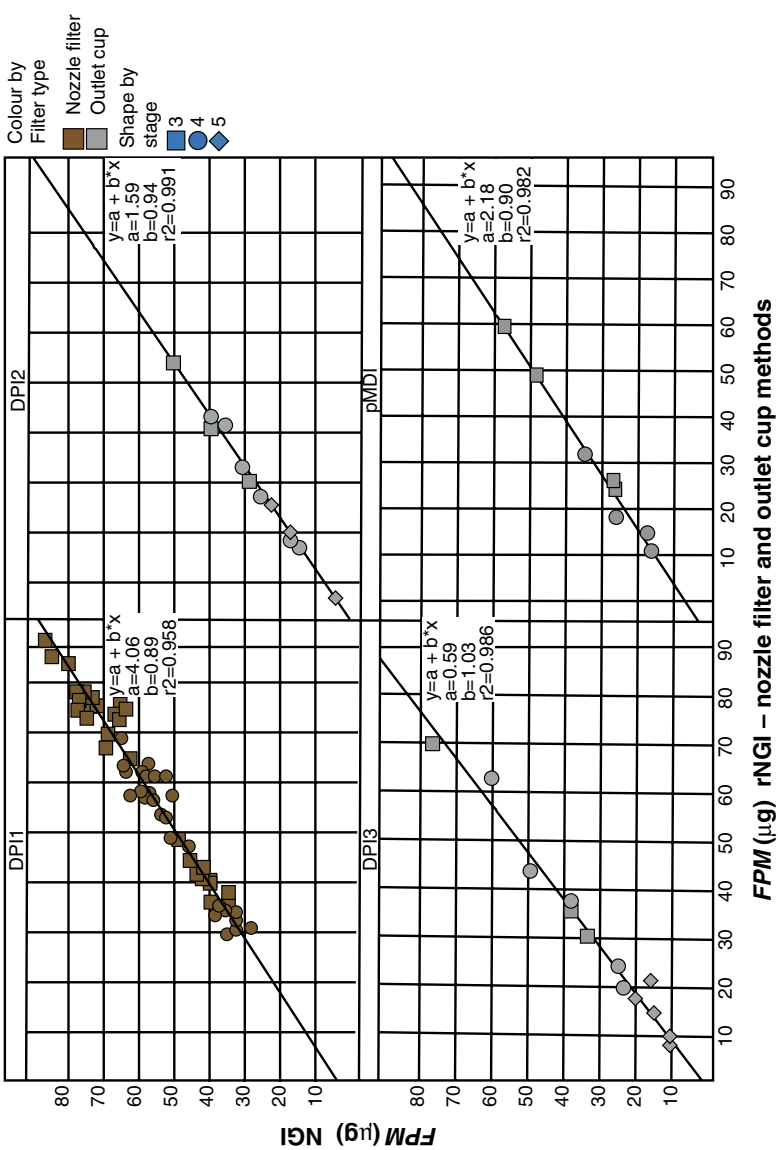

Fig. 10.66 Full-resolution versus abbreviated NGI measures of *FPM* reported by Svensson and Berg for various pMDI and DPI products; data from each inhaler category are shown in the separate panels, and the different stages are indicated by *shape* and *colors* on the markers corresponding to the filter type used (*From* [59]—*courtesy of M. Svensson*)

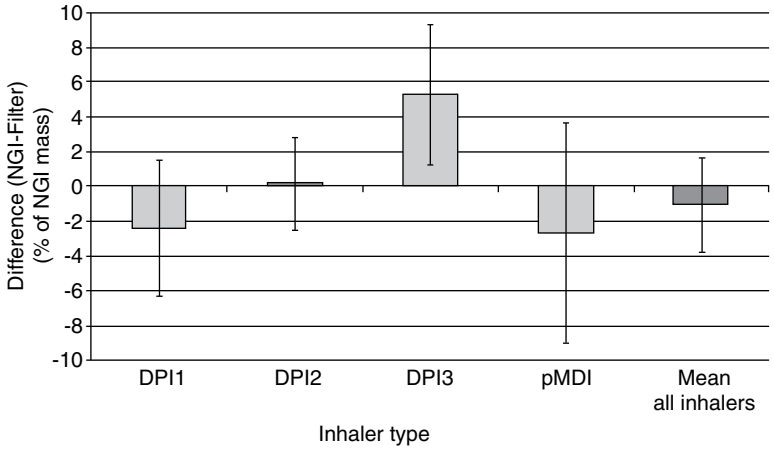

Fig. 10.67 Differences in *FPM* between the full NGI and the filter method for the inhaler types used in the study reported by Svensson and Berg; error bars are 95% confidence intervals (*From* [59]—*courtesy of M. Svensson*)

DPI-1 compared to the other inhaler types, and they provided the following rationale from their findings:

1. The nozzle-filter methodology is a less mature methodology in their laboratory, whereas the outlet "O"-cup has been established and used in development studies for several years.
2. DPI-1 as a device and the three formulations used in this device were both concepts in early development phase at the time when the work was undertaken, so the dosing properties may be more variable than the other inhalers that are products that are in late stage development.

Importantly, they did not observe that any particular stage was better (or worse) suited to be used in these filter methodologies (see marker shape in Fig. 10.66) and that no outliers were obtained in the data set.

Svensson and Berg went on to calculate the mean differences (presented in percentage terms of the found mass in the NGI test) between the NGI and the filter methods for each of the inhaler types (Fig. 10.67). Both negative and positive differences were observed, ranging from +5% to −2.5%. DPI-3 displayed significant difference between NGI and filter method, but when all 91 mean values were regarded as one data set, the difference became minimal (around 1%) and importantly, no significant difference was obtained between the two methods (standard NGI versus Filter concepts).

From a practical perspective, Svensson and Berg made the judgment that the nozzle-filter-abbreviated approach is about two times faster than the external filter method [59]. Moreover, since the external filter method, in its current design, includes a disposable plastic fixture, the nozzle filter is preferable from

an environmental perspective. The authors concluded that the filter method is also very feasible for determination of the fine particle dose uniformity (FPDU) of a product; a parameter that is very difficult and laborious to retrieve from full NGI measurements. They also observed that it is necessary to size separate the dose below the first size-fractionating stage in two parts in order to achieve greater sensitivity in terms of changes in ASPD and dose passing beyond the impactor inlet. As a next step toward realization of two size fractions (and samples) in the abbreviated NGI platform, experiments are currently in progress using a modified NGI in which the stages have been physically interchanged in combination with the nozzle-filter approach. This approach should enable capture of the LPM and SPM in a cup and a filter, respectively, thereby resulting in an elegant abbreviated methodology to implement.

10.9 Short Stack ACI Systems Created by Rearranging Location of Back-Up Filter

In 2012, Horodnik et al. demonstrated an important alternative arrangement to the reduced ACI configurations previously described [60], as their approach avoided the removal of stages, therefore preserving the internal dead space of the full-resolution ACI. In their particular configuration, they relocated the back-up filter stage immediately downstream of the second impaction stage. The equipment was operated at 60 L/min and active measuring components therefore consisted of stages 1, 0, and filter.

The normal length spring-loaded clamps supplied with the full-resolution ACI could be used to ensure a tight seal between stages of their configuration, as an additional benefit [60]. The physical appearance of their abbreviated ACI was therefore comparable with that of the full-resolution system (Fig. 10.68).

Horodonik et al. went on to use this arrangement to evaluate a new DPI blend delivery system containing mometasone furoate intended for use with patients undergoing mechanical ventilation. The entry to the CI therefore comprised a spacer designed for use in such an environment with its distal end consisting of a short length of 22 mm diameter tubing representing part of a ventilator circuit, rather than the Ph. Eur./USP induction port. The focus of their study was on the proof of concept for a new in vitro method to evaluate how their DPI might perform in the clinic. They therefore did not present comparative data with the full-resolution ACI. However values of $FPM_{<\text{ca.6.5}\mu\text{m}}$ ($n = 5$ replicates at each condition) were consistent over a wide range of values of recovered mass of this particular API from the filter stage (Fig. 10.69).

This simple-to-configure arrangement may avoid both the need to take measures to match the flow rate-time profile in DPI testing, already discussed. Horodonik et al. retained the same number of stages in their short stack ACI by locating redundant stages below the filter collection stage, so that the internal dead space was the same as that for a full-resolution ACI. However, although suitable

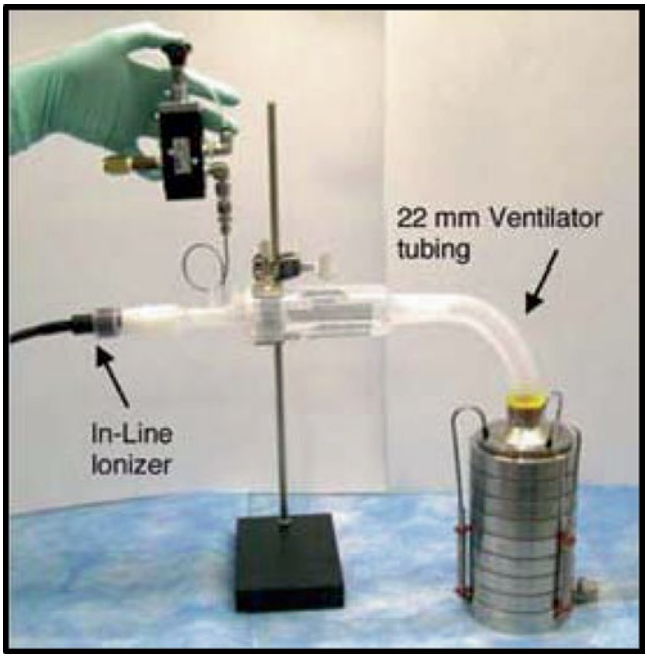

Fig. 10.68 "Short stack" arrangement of Horodnik et al. [60] in which they reconfigured a full-resolution ACI such that the back-up filter is located immediately below stage 1, and the other stages are retained (*From* [60]—*used with permission*)

for DPI testing where the total dead space in the measurement system is important, such an arrangement may not be effective if used in connection with the evaluation of pMDIs containing low-volatile cosolvent. Under such circumstances, it would be more appropriate to locate one or more redundant stages (i.e., not containing a collection surface) before the size-fractionating stage, as was done by Mitchell et al. [20], to ensure that cosolvent evaporation in the reduced system matched that of the full-resolution CI.

10.10 AIM-Based Measurement Equipment: Learning from Validation Studies, Current Status, and Future Needs

In December 2010 a workshop was organized by EPAG to act as a forum for the discussion of ways to develop AIM-based apparatus toward maturity, given the large amount of experimental data presented in the preceding sections of this chapter in support of their adoption [61]. In the panel discussion that followed,

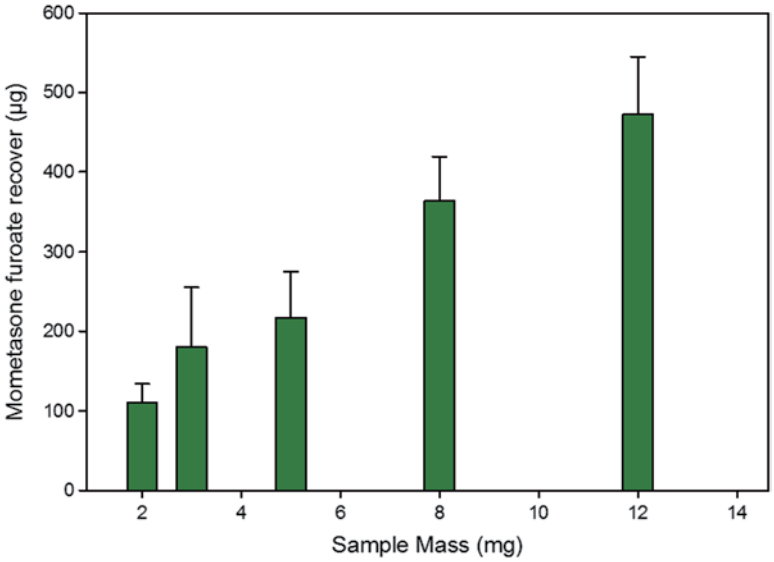

Fig. 10.69 $FPM_{<ca.6.5\mu m}$ of mometasone furoate [$n=5$ replicates at each condition (mean ± SD)] delivered to the short stack ACI over a range of sample weights which, with a 12 mg sample load (15% blend mometasone furoate), will deliver approximately 500 µg to the filter stage (*From* [60]—*used with permission*)

the current status of the measurement technology was established and following issues were identified [62]:

1. Measurements made by AIM-based equipment for pMDIs and nebulizers provide measures of fine particle fraction that are in substantial agreement with the equivalent metric from the corresponding full-resolution impactor (either the ACI or NGI).
2. Measures of *FPF* by FSI were frequently higher than the corresponding full-resolution data for DPI testing. In contrast with the evaluation of pMDIs and nebulizers, where the impactor is operated at a fixed flow rate throughout the determination, the DPI test is more complex in that the flow rate at initiation of the measurement is zero and rapidly rises to a stable value as the pressure field within the DPI and measurement system stabilizes. Two possible causes were identified that need further investigation:

    a. The start-up kinetics of both abbreviated and full-resolution impactor systems appear to be important, since the compendial method necessitates initiating flow from the DPI at the start of measurement, so that the flow through the system is developing during the initial few hundred milliseconds of the determination.
    b. Differences in sharpness of cut for the insert in the FSI compared with both NGI and perhaps more so with the ACI whose stage collection efficiency curves are noticeably less steep than those of the NGI may also be responsible

for small upward shifts in fine particle fraction observed at 5 µm aerodynamic diameter with the FSI.

Further work is needed to understand the relative importance of both causes, as well as to determine how much of the divergence between abbreviated and full-resolution DPI-based measurements is formulation based and therefore productspecific.

3. The Twin Impinger (Apparatus A in monograph 2.9.18 of the European Pharmacopoeia) may become a suitable candidate AIM apparatus. It already has only a single cut-point size of 6.4 µm at 60 L/min [5]. Being an impingement device, the potential for bias from bounce and re-entrainment are eliminated by virtue of collecting the particles in the impingement fluid, as well as having the intrinsic advantage that recovery of active pharmaceutical ingredient from the impingement fluid can be achieved without further work-up in some cases. Modifications to achieve a slight reduction in the cut point to 5 µm at a defined flow rate in the range within which MDI and DPI testing, respectively, takes place (30–100 L/min) appear to be feasible.

   A better alternative might be to develop a reduced (say 2 or 3-stage) version of the MSLI (Fig. 10.70), which also achieves avoidance of particle bounce and

Fig. 10.70 Multistage liquid impinger: a candidate for abbreviation? (*Courtesy of Copley Scientific Ltd.*)

re-entrainment and in which the aerodynamically critical parts are manufactured from metal [63]. Both the Twin Impinger (Fig. 10.2) and MSLI systems benefit from having no interstage losses, but the MSLI has the distinct advantage, particularly for work with DPIs, of being calibrated from 30 to 100 L/min [12]. However, the possibility of using a reduced stack version of the MSLI throughout this flow rate range will be limited, without a range of flow rate dependent stages being designed and manufactured to give the desired cut-off diameter at the intended test flow rate (as in the case of the FSI).

4. The desire to develop AIM-based apparatuses should also consider designs that are potentially automatable. However, at this stage, more work is needed in understanding the role that AIM has to play in the life-cycle management of OIPs before the scope for partial or full automation will become clear. In the near future, semiautomated fixtures may have more prospects of being adopted, given the substantial financial investment required to automate AIM-based systems, despite their relative simplicity compared with their full-resolution counterparts.
5. There was a consensus that AIM-based measurements are unlikely to be allowed by themselves in regulatory submissions, given the need to have full-resolution aerodynamic particle size distribution data in order to interpret safety and efficacy data from the clinical batches. However, once relationships are established and appropriately validated, AIM-based measurements could be considered especially in a product QC environment. It is important to note that the full-resolution CI would always be available to support the process in the event that an out-of-specification investigation is needed. A role may also exist for an AIM-based approach in the speeding up of early development formulation screening, but a convincing case will likely need to be made on a company-by-company basis, given the reduction in the data relating to aerosol aerodynamic size that results with an AIM-based methodology.
6. These observations and suggestions for future work are still current, although at a recent workshop organized by the US Pharmacopeia, at which AIM was discussed together with EDA there was more understanding concerning the importance of matching dead volume of the abbreviated system to that for the full-resolution reference CI, especially in the evaluation of DPIs [64].
7. The large body of data that has been presented in this chapter illustrates the degree of commitment from stakeholders to understand both the limitations as well as the perhaps more obvious advantages that AIM-based CI measurements have to offer in the assessment of aerosols from all types of OIP. Table 10.18 summarizes the salient points in connection with the extension of good cascade impactor practice (GCIP—see Chap. 4) to include AIM-based approaches.

At the present time, there are no hard-and-fast rules for choosing the most appropriate full-resolution CI with which to match data from an AIM-based method. This situation has arisen because there is still insufficient experience with all of the various options available for AIM-based measurements. Nevertheless, given the apparent importance of matching internal dead space between AIM and full-resolution apparatuses where volatile species are present or to match start-up kinetics for DPI testing.

Table 10.18 Points to consider (PtC) when implementing an AIM-based CI method; "√" important; "≈" unimportant

PtC	Description	OIP class applicability		
		MDI	DPI	Nebulizer/SMI
1	Select appropriate full-resolution CI as benchmark method (Table 10.19)	√		
2	Eliminate particle bounce and re-entrainment	√		≈
3	Match pressure drop rise time of AIM system to benchmark CI[a]	√		
4	Chill AIM and benchmark CI	≈		√
5	Refer to benchmark CI data as first step in resolving questionable AIM data	√		

[a]In the case of DPI testing, adding a first impaction stage to match the full-resolution impactor will not by itself be sufficient to mirror the volume and flow resistance of the full impactor. However, in the case of the ACI, it would be a practical alternative to retain the redundant stages in the abbreviated impactor, but locate them beneath the filter stage (e.g., in the stage order: 0, 2, 5, Filter, 1, 2, 3, 5, 7) to achieve this goal

Table 10.19 Matching an AIM-based CI to a full-resolution benchmark CI

AIM system	Suggested full-resolution CI
FSA, T-FSA variants	Andersen 8-stage nonviable impactor (ACI)
FPD	Andersen 8-stage viable impactor (ACVI)
rNGI variants	Next Generation Pharmaceutical Impactor (NGI)
FSI	No obvious matching full-resolution CI, therefore use with any CI and evaluate need to match dead space for OIP being tested. Using NGI as reference full-resolution CI with FSI could result in some components (e.g., inlet and pre-separator housing) being shared, allowing reduction in cost for additional equipment. Furthermore, familiarity of test recovery procedures for these components is very similar between FSI and NGI. Validation work with appropriate benchmark CI needed with other systems
Other systems including abbreviated MSLI	

Table 10.19 provides guidance concerning this matter. The interested reader is urged to keep up-to-date with the continually developing literature concerning good AIM practices, as newer approaches to resolving compatibility concerns are published.

References

1. European Pharmaceutical Aerosol Group (2010) Workshop on AIM-Based Techniques, Edinburgh, UK. http://www.epag.co.uk/Library/Default2.asp. Accessed 12 Jan 2012
2. International Pharmaceutical Consortium on Regulation and Science (IPAC-RS) (2008) IPAC-RS conference "Bringing value to the patient in a changing world", Rockville, MD, USA. http://www.ipacrs.com/ipac2008.html. Accessed 12 Jan 2012
3. International Pharmaceutical Consortium on Regulation and Science (IPAC-RS) (2010) IPAC-RS conference "Bringing value to the patient in a changing world", Rockville, MD, USA. http://www.ipacrs.com/2011%20Conference.html. Accessed 12 Jan 2012

4. European Directorate for the Quality of Medicines and Healthcare (EDQM) (2002) Preparations for inhalation: aerodynamic assessment of fine particles. Section 2.9.18 – European Pharmacopeia – Apparatus B in versions up to 4th edition, Council of Europe, Strasbourg, France
5. Hallworth GW, Westmoreland DG (1987) The Twin Impinger: a simple device for assessing the delivery of drugs from metered dose pressurized aerosol inhalers. J Pharm Pharmacol 39(12):966–972
6. May KR (1966) Multi-stage liquid impinger. Bact Rev 30:559–570
7. Miller N, Marple VA, Schultz RK, Poon WS (1992) Assessment of the Twin Impinger for size measurement of metered dose inhaler sprays. Pharm Res 9(9):1123–1127
8. Onyechi JO, Martin GP, Marriott C, Murphy L (1994) Deposition of dry powder aerosols in cascade impactors at different flow rates. J Aerosol Med 7(2):181–184
9. Watson JP, Lewis RA (1995) Generic salbutamol metered dose inhalers. Thorax 50(5):590–592
10. Mendes PJ, Pinto JF, Sousa JMM (2007) A non-dimensional functional relationship for the fine particle fraction produced by dry powder inhalers. J Aerosol Sci 38(6):612–624
11. Tougas TP, Christopher D, Mitchell JP, Strickland H, Wyka B, Van Oort M, Lyapustina S (2009) Improved quality control metrics for cascade impaction measurements of orally inhaled drug products (OIPs). AAPS PharmSciTech 10(4):1276–1285
12. Asking L, Olsson B (1997) Calibration at different flow rates of a multistage liquid impinger. Aerosol Sci Technol 27(1):39–49
13. Marple VA, Rubow KL, Olson BA (2001) Inertial, gravitational, centrifugal, and thermal collection techniques. In: Baron PA, Willeke K (eds) Aerosol measurement: principles, techniques and applications, 2nd edn. Wiley Interscience, New York, pp 229–260
14. Marple VA, Roberts DL, Romay FJ, Miller NC, Truman KG, Van Oort M, Olsson B, Holroyd MJ, Mitchell JP, Hochrainer D (2003) Next generation pharmaceutical impactor. Part I: Design. J Aerosol Med 16(3):283–299
15. Van Oort M, Downey B (1996) Cascade impaction of MDIs and DPIs: Induction port, inlet cone, and pre-separator lid designs recommended for inclusion in the general test chapter Aerosols <601> Pharm Forum 22(2):2204–2210
16. Van Oort M, Roberts W (1996) Variable stage-variable volume strategy for cascade impaction. In: Dalby RN, Byron PR, Farr SJ (eds) Respiratory drug delivery-V. Interpharm, Buffalo Grove, IL, pp 418–421
17. Poochikian G, Bertha CM (2002) Regulatory view on current issues pertaining to inhalation drug products. In: Dalby RN, Byron PR, Peart J, Farr SJ (eds) Respiratory drug delivery-VIII. Davis Horwood International, Raleigh, NC, pp 159–164
18. Bowles N, Cahill E, Haeberlin B, Jones C, Mett I, Mitchell J, Müller-Walz R, Musa R, Nichols S, Parkins D, Petterssen G, Preissmann A, Purewal T, Schmelzer C (2007) Application of quality-by-design to inhalation products. In: Dalby RN, Byron PR, Peart J, Suman JD (eds) Respiratory drug delivery–Europe 2007. Davis Healthcare, River Grove, IL, pp 61–69
19. Mitchell JP, Nagel MW, Avvakoumova V, MacKay H, Ali R (2009) The abbreviated impactor measurement (AIM) concept: Part 1—influence of particle bounce and re-entrainment—evaluation with a "dry" pressurized metered dose inhaler (pMDI)-based formulation. AAPS PharmSciTech 10(1):243–251
20. Mitchell JP, Nagel MW, Avvakoumova V, MacKay H, Ali R (2009) The abbreviated impactor measurement (AIM) concept: Part 2—influence of evaporation of a volatile component—evaluation with a "droplet producing" pressurized metered dose inhaler (pMDI)-based formulation containing ethanol as co-solvent. AAPS PharmSciTech 10(1):252–257
21. Mitchell JP, Copley M (2010) Accelerated inhaled product testing. Pharma Mag Jan–Feb: 14–17. http://www.pharma-mag.com/pharma/index.html. Accessed 12 Jan 2012
22. United States Federal Drug Administration (FDA) (1998) Draft guidance: metered dose inhaler (MDI) and dry powder inhaler (DPI) drug products chemistry, manufacturing and controls documentation. United States Federal Drug Administration, Rockville, MD, USA. Docket 98D-0997, http://www.fda.gov/downloads/Drugs/GuidanceComplianceRegulatoryInformation/Guidances/ucm070573.pdf. Accessed 22 Aug 2011

23. Graham SJ, Lawrence RC, Ormsby ED, Pike RK (1995) Particle size distribution of single and multiple sprays of salbutamol metered-dose inhalers (pMDIs). Pharm Res 12(9):1380–1384
24. Kamiya A, Sakagami M, Hindle M, Byron P (2004) Aerodynamic sizing of metered dose inhalers: an evaluation of the Andersen and next generation pharmaceutical impactors and their USP methods. J Pharm Sci 93(7):1828–1837
25. Kamiya A, Sakagami M, Hindle M, Byron PR (2003) Particle sizing with the next generation impactor: a study of Vanceril™ metered dose inhaler. Proc 14th ISAM Congress, Baltimore, MD, USA, J Aerosol Med 16(2):216 (abstract)
26. Mitchell JP, Nagel MW, Doyle C, Ali RS, Avvakoumova V, Christopher D, Quiroz J, Strickland H, Tougas T, Lyapustina S (2010) Relative precision of inhaler aerodynamic particle size distribution (APSD) metrics by full resolution and abbreviated Andersen Cascade Impactors (ACIs): Part 1. AAPS PharmSciTech 11(2):843–851
27. Mitchell JP, Nagel MW, Doyle C, Ali RS, Avvakoumova V, Christopher D, Quiroz J, Strickland H, Tougas T, Lyapustina S (2010) Relative precision of inhaler aerodynamic particle size distribution (APSD) metrics by full resolution and abbreviated Andersen Cascade Impactors (ACIs): Part 2–Investigation of bias in extra-fine mass fraction with AIM-HRT impactor. AAPS PharmSciTech 11(3):1115–1118
28. Keegan GM, Lewis DA (2012) Rapid prototype screening with the Copley fast screening Andersen (FSA). In: Dalby RN, Byron PR, Peart J, Suman JD, Young PM (eds) Respiratory drug delivery 2012. Davis HealthCare, River Grove, IL, pp 469–472
29. Keegan GM, Lewis DA (2012) Formulation-dependent effects on aerodynamic particle size measurements using the fast screening Andersen (FSA). In: Dalby RN, Byron PR, Peart J, Suman JD, Young PM (eds) Respiratory drug delivery 2012. Davis HealthCare, River Grove, IL, pp 465–468
30. Andersen A (1966) A sampler for respiratory health assessment. Am Ind Hyg Assoc J 27(2):160–165
31. Yao MS, Mainelis G (2007) Analysis of portable impactor performance for enumeration of viable bioaerosols. J Occup Environ Hyg 4(7):514–524
32. Chambers FE, Smurthwaite M (2012) Comparative performance evaluation of the Westech fine particle dose (FPD) impactor. In: Dalby RN, Byron PR, Peart J, Suman JD, Young PM (eds) Respiratory drug delivery-2012. Davis HealthCare, River Grove, IL, pp 553–557
33. Guo C, Ngo D, Ahadi S, Doub WH (2011) Evaluation of an abbreviated impactor for fine particle fraction (FPF) determination of inhalation drugs. AAPS Annual Meeting, Washington, DC
34. Roberts DL, Romay F (2009) Design of the fast screening impactor based on the NGI preseparator. Drug delivery to the lungs-20, The Aerosol Society, Edinburgh, UK, 20:206–209. http://ddl-conference.org.uk/index.php?q=previous_conferences. Accessed 4 Aug 2012
35. Marple VA, Olson BA, Santhanakrishnan K, Mitchell JP, Murray SC, Hudson-Curtis BL (2003) Next generation pharmaceutical impactor (a new impactor for pharmaceutical inhaler testing). Part II: Archival calibration. J Aerosol Med 16(3):301–324
36. Marple VA, Olson BA, Santhanakrishnan K, Mitchell JP, Murray SC, Hudson-Curtis BL (2004) Next generation pharmaceutical impactor: a new impactor for pharmaceutical inhaler testing. Part III. Extension of archival calibration to 15 L/min. J Aerosol Med 17(4):335–343
37. MSP Corporation (2009) Fast Screening Impactor™ for quantifying "large" and "small" particles emitted by inhalable drug devices: user guide. St. Paul, MN, USA. FSI-0185-6002, Revision A, available at: www.mspcorp.com. Accessed 14 Jan 2012
38. Stobbs B, McAuley E, Bogard H, Monsallier E (2009) Evaluation of the fast screening impactor for determining dine particle fraction of dry powder inhalers. Drug delivery to the lungs-20, The Aerosol Society, Edinburgh, UK, 20:158–161. http://ddl-conference.org.uk/index.php?q=previous_conferences. Accessed 4 Aug 2012
39. Copley M, Mitchell J, McAuley E, Russell-Graham D (2010) Implementing the AIM concept. Inhalation 4(1):7–11
40. Russell-Graham D, Cooper A, Stobbs B, McAulay E, Bogard H, Heath V, Monsallier E (2010) Further evaluation of the fast-screening impactor for determining fine particle fraction of dry

powder inhalers. Drug delivery to the lungs-21, The Aerosol Society, Edinburgh, UK, 21:374–377. http://ddl-conference.org.uk/index.php?q=previous_conferences. Accessed 4 Aug 2012
41. Copley M, Smurthwaite M, Roberts DL, Mitchell JP (2005) Revised internal volumes to those provided by Mitchell JP and Nagel MW in "Cascade impactors for the size characterization of aerosols from medical inhalers: their uses and limitations". J Aerosol Med 18(3):364–366
42. Pantelides PN, Bogard H, Russell-Graham D, Cooper AD, Pitcairn GR (2011) Investigation into the use of the fast screening impactor as an abbreviated impactor measurement (AIM) tool for dry powder inhalers. In: Dalby RN, Byron PR, Peart J, Suman JD, Young PM (eds) Respiratory drug delivery–Europe 2011. Davis Healthcare, River Grove, IL, pp 391–395
43. Burnell PKP, Small T, Doig S, Johal B, Jenkins R, Gibson GJ (2001) Ex-vivo product performance of Diskus™ and Turbuhaler™ inhalers using inhalation profiles from patients with severe chronic obstructive pulmonary disease. Respir Med 95(5):324–330
44. Roberts DL, Chiruta M (2007) Transient impactor behavior during the testing of dry-powder inhalers via compendial methods. Drug delivery to the lungs-18, The Aerosol Society, Edinburgh, UK, 18:202–205
45. Pantelides PN, Bogard H, Russell-Graham D, Cooper AD, Pitcairn GR (2011) An evaluation of a fast screening impactor (FSI) set-up for abbreviated impactor measurement: quality control (AIM-QC) of dry powder inhalers. UK Academy of Pharmaceutical Sciences (APSGB) Inhalation 2011 meeting, University of Bath, UK, July (abstract)
46. Daniels GE, Hamilton M (2011) Assessment of early screening methodology using the reduced next generation and fast screening impactor systems. In: Dalby RN, Byron PR, Peart J, Suman JD, Young PM (eds) Respiratory drug delivery–Europe 2011. Davis Healthcare, River Grove, IL, pp 327–330
47. Hamilton M, Daniels G (2011) Assessment of early screening methodology using the Next Generation and Fast Screen Impactor systems. Drug delivery to the lungs-22, The Aerosol Society, Edinburgh, UK, 22:355–358. http://ddl-conference.org.uk/index.php?q=previous_conferences. Accessed 4 Aug 2012
48. Després-Gnis F, Williams G (2010) Comparison of next generation impactor and fast-screening impactor for determining fine particle fraction of dry powder inhalers. Drug delivery to the lungs-21, The Aerosol Society, Edinburgh, UK, 21:386–389. http://ddl-conference.org.uk/index.php?q=previous_conferences. Accessed 4 Aug 2012
49. Rogueda P, Morrical B, Chew YD (2010) Comparison of NGI and the fast screening impactor (FSI) for suitability for analytical drug development. Drug delivery to the lungs-21, The Aerosol Society, Edinburgh, UK, 21:394–397. http://ddl-conference.org.uk/index.php?q=previous_conferences. Accessed 4 Aug 2012
50. Sheng G, Zhang J, Simmons R, Watanabe W (2010) Fast screening impactor (FSI) as a prescreening tool for MDIs and nebulizers. In: Dalby RN, Byron PR, Peart J, Suman JD, Farr SJ, Young PM (eds) Respiratory drug delivery-2010. Davis Healthcare, River Grove, IL, pp 637–640
51. European Directorate for the Quality of Medicines and Healthcare (EDQM) (2012) Preparations for nebulisation: characterisation, general chapter 2.9.44, Council of Europe, Strasbourg, France
52. Tservistas M, Uhlig M, Mitchell J (2010) Assessment of abbreviated impactor measurement (AIM) methods for nebulizer characterization. Drug delivery to the lungs-21, The Aerosol Society, Edinburgh, UK, 21:378–381. http://ddl-conference.org.uk/index.php?q=previous_conferences. Accessed 4 Aug 2012
53. Sheng G, Watanabe W (2010) Feasibility of fast screening impactor as a screening tool. Drug delivery to the lungs-21, The Aerosol Society, Edinburgh, UK, 21:390–393. http://ddl-conference.org.uk/index.php?q=previous_conferences. Accessed 4 Aug 2012
54. Dennis J, Berg E, Sandell D, Ali A, Lamb P, Tservistas M, Karlsson M, Mitchell J (2008) Cooling the NGI: an approach to size a nebulised aerosol more accurately. Pharm Europa Sci Notes 1:27–30
55. Fowdar N, Hammond M, Solomon D (2010) A comparison of the effect of continuous cooling of an NGI on a solution and suspension based nebulized product. Drug delivery to the lungs-21,

The Aerosol Society, Edinburgh, UK, 21:275–279. http://ddl-conference.org.uk/index.php?q=previous_conferences. Accessed 4 Aug 2012
56. Williams K (2010) The influence of ambient relative humidity during cooled NGI Testing. Drug delivery to the lungs-21, The Aerosol Society, Edinburgh, UK, 21:292–294. http://ddl-conference.org.uk/index.php?q=previous_conferences. Accessed 4 Aug 2012
57. Finlay WH, Stapleton K (1999) Undersizing of droplets from a vented nebulizer caused by aerosol heating during transit through an Andersen impactor. J Aerosol Sci 30(1):105–109
58. Mitchell JP, Bauer R, Lyapustina S, Tougas T, Glaab V (2011) Non-impactor-based methods for sizing of aerosols emitted from orally inhaled and nasal drug products (OINDPs). AAPS PharmSciTech 12(3):965–988
59. Svensson M, Berg E (2010) Measuring the fine particle dose using inter-stage filters in the NGI – an overview of two methods. Drug delivery to the lungs-21, The Aerosol Society, Edinburgh, UK, 21:382–385. http://ddl-conference.org.uk/index.php?q=previous_confernces. Accessed 4 Aug 2012
60. Horodnik W, Garber N, Ewing G, Donovan B (2012) The *in vitro* delivery of a dry powder blend using pressurized air and a pMDI designed spacer and actuator combination product (AeroChamber MV) into a ventilator circuit tubing and "short stack" Andersen cascade impactor (ACI) for particle size characterization. In: Dalby RN, Byron PR, Peart J, Suman JD, Young PM (eds) Respiratory drug delivery 2012. Davis HealthCare, River Grove, IL, pp 581–584
61. Mitchell JP, Nichols SC (2011) Drug delivery to the lungs 21 – European Pharmaceutical Aerosol Group Abbreviated Impactor Measurement workshop summary. Therapeut Deliv 2(3):301–305. http://ddl-conference.org.uk/index.php?q=previous_conferences. Accessed 4 Aug 2012
62. Mitchell JP, Nichols SC (2011) European Pharmaceutical Aerosol Group (EPAG): Abbreviated Impactor Measurement (AIM) workshop – December 8th 2010. In: Dalby RN, Byron PR, Peart J, Suman JD, Young PM (eds) Respiratory drug delivery–Europe 2011. Davis Healthcare, River Grove, IL, pp 469–472
63. Bell JH, Brown K, Glasby J (1973) Variation in delivery of isoprenaline from various pressurized inhalers. J Pharm Pharmacol 25(S):32P–36P
64. United States Pharmacopeia (2011) A co-sponsored workshop by USP and AAPS on aerosols–inhalation and nasal drug products, Rockville, MD, USA, December 12–13. http://www.usp.org/meetings/asMeetingIntl/aerosols.html. Accessed 18 Jan 2012